Minnesota River Surface Tile Inlet Research

Modeling Component

by

Bruce N. Wilson
Elizabeth Burt
Paul Oduro
Mike Headrick
AbdelKarim AbuLaban
J. William Brown
Erin Brooks

Biosystems and Agricultural Engineering Department
University of Minnesota
St. Paul, Minnesota

Final Report
Legislative Commission on Minnesota Resources

October, 1997

95 7(h)

Table of Contents

Minnesota River Surface Tile Inlet Research: Modeling Component

B. Wilson, E. Burt, P. Oduro, M. Headrick, A. AbuLaban, J.Brown, E. Brooks

Introduction

Surface tile inlets are frequently used in the Minnesota River Basin to remove ponded water from agricultural fields. These inlets allow a more timely planting of crops and reduce flood damages to crop from major rainfall events. However, surface tile inlets also provide a direct pathway for surface water to reach drainage ditches, streams, or rivers. In addition, sediment and other pollutants, which otherwise may be trapped in the field, are discharged into these channels. The flow and transport of contaminants by surface tile inlets are important environmental concerns, especially for the extensive agricultural drainage systems of the Minnesota River Basin.

The objective of this study is to develop and evaluate a simulation model for watersheds with surface tile inlets. The model needs to simulate hydrologic and sedimentologic processes, including the influences of best management practices for the land and for the inlets themselves. An evaluation of the predictive accuracy of the model is an important step in its development. The report first describes the simulation model developed for the project. The accuracy of the model is then evaluated using data collected in the Minnesota River Basin. The simulation model is used to assess the impact of alternative tillage operations and the effectiveness of grass buffers as possible management practices.

Simulation Model

DROPLETS Model

A suite of stand-alone routines are used to assess the impact of surface tile inlets. The long-term goal is to link these routines into a single, comprehensive model. The routines are collectively referred to as the DROPLETS (**D**rainage **R**esponse **O**f **P**othole **L**andscapes and the **E**rosion and **T**ransport of **S**ediment) Model. The key components of DROPLETS are: (1) the Water Erosion and Prediction Project (WEPP) model developed by the Agricultural Research Service (Nearing et al., 1989) to simulate the hydrologic and sedimentologic response of the upland watershed of the surface inlet, (2) interface routines to extract information from WEPP output files, (3) the BASIN routine to simulate the trapping of sediment at the inlet caused by ponded water, (4) the GRASSF routine to simulate the trapping of sediment by a vegetative filter, (5) the routine to simulate the hydraulic response of a series of surface tile inlets, and (6) the routine to simulate the flow from subsurface tile lines. The last routine is limited by estimates of percolation and evapotranspiration rates. Although these values are computed in the WEPP model, obtaining this information from the output is difficult. The best long-term solution is to

compute these values independently of the WEPP model.

In the DROPLETS model, the *response units* (RUs) are the basic landscape units to compute runoff/sediment delivery to depression, streams, lakes, etc. *Elemental watersheds (EWs)* are formed by combining one or more RUs. Elemental watershed are defined to account for RUs that cannot be treated independently or to allow complex watersheds to be evaluated more efficiently. An important example of the former use is the response of a series of surface tile inlets as shown in Figure 1. The response of this system cannot be determined by evaluating each depression separately. The ponded depth of water in a lower depression has an impact on the discharge from the other depressions.

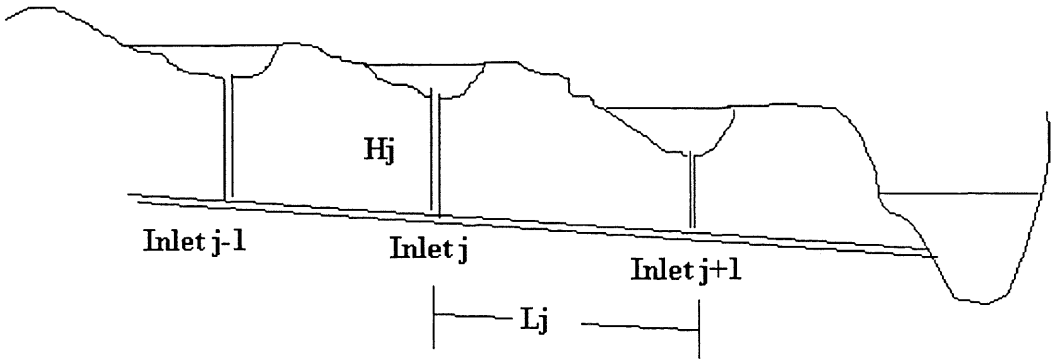

Figure 1. Elemental Watershed Defined by Series of Surface Tile Inlets.

A typical application of DROPLETS would be performed in the following steps:

* Determine values for RUs,
* Determine response for EWs,
* Route values in channels, rivers, and streams, and
* Combine values at confluence points.

Simulation of the Response Units - WEPP

The WEPP model is used to simulate the hydrologic and sedimentologic response of the watershed for the surface tile inlet. The WEPP model is capable of simulating weather variables, snow accumulation and melt, infiltration, overland flow hydraulics, plant growth, residue decomposition, and soil erosion and deposition. A brief overview of the computational algorithms is given here. Additional details are given in the model evaluation section and in the user manual (Nick et al., 1995).

The WEPP model uses a stochastic weather generator to predict mean daily precipitation, daily maximum and minimum temperature, mean daily solar radiation and mean daily wind direction and speed. A standard two-state, first-order Markov Chain is used to determine whether a particular day has precipitation. The precipitation is considered to be a rainfall event, unless the average daily air temperature is below freezing. If the average daily air temperature is below freezing, the precipitation is assumed to be snowfall. The depth of precipitation is computed from a skewed normal distribution. Rainfall duration is

determined from an exponential distribution. Daily maximum and minimum temperatures and solar radiation are computed using normal distributions. The weather generator is also capable of determining the time-distribution of rainfall depths within a storm.

The WEPP model includes routines to account for snowmelt and frost depth. The snowmelt routine uses air temperature, solar radiation, vapor transfer and precipitation to determine daily snowmelt depth. Frost depth is computed using unidirectional heat flow equations. The WEPP model also includes a routine to account for snowdrifting processes.

Infiltration in the WEPP model is determined using the Green-Ampt-Mein-Larson model. Green-Ampt-Mein-Larson infiltration model has two stages: infiltration prior to surface ponding and infiltration after surface ponding. A critical parameter is the effective conductivity. An innovation of the WEPP model is the dynamic prediction of this value as function of soil, residue, and plant conditions.

Relatively simple routines are used in the WEPP model to determine overland flow hydraulics. Broad sheet flow is assumed to estimate the peak flow rate and runoff duration; however, the flow is divided among equally spaced rills to estimate soil detachment and transport. Steady state conditions are assumed to determine erosion processes. The peak flow rate is used to determine steady flow conditions. Rectangular cross-sections are used to compute depth of flow, velocity, and shear stress in rills.

The WEPP model determines the soil moisture in the root zone by using a water balance for the profile. Important processes include evaporation, plant transpiration, and percolation. The water balance algorithm uses the daily precipitation, temperature, and solar radiation from the weather generator; the infiltration volume from the infiltration component; and the daily leaf area index, root depth, and residue cover from the plant growth component.

Plant growth and residue decomposition are also computed in the WEPP model. The plant growth component determines those plant variables that influence runoff and erosion processes. Plant variables include vegetative biomass, root growth and leaf area index. The decomposition of surface and subsurface residue and root mass is also computed in the WEPP model.

The WEPP model allows soil parameters to vary with time and tillage practices. Dynamic soil parameters include random roughness, oriented roughness, bulk density, wetting-front suction, saturated conductivity, interrill and rill erodibility and critical shear stress. Saturated conductivity, for example, is adjusted for soil sealing and crusting, macropore volume, soil freezing, and soil canopy.

Soil erosion in the WEPP model is divided into interrill and rill areas. Interrill erosion is assumed to be proportional to the square of rainfall intensity. Potential rill erosion is determined from the excess bed shear. Adjustments in the potential detachment are made using the sediment load and transport capacity of the flow. Sediment deposition is

possible if the sediment load exceeds the transport capacity. Sediment transport capacity is a function of downslope position.

Sedimentation With Ponded Water - The BASIN Model

The potential trapping of sediment with ponded water at the inlet is predicted using the modified BASIN model. This model is based on a mass balance for an infinitesimal layer using advection-diffusion processes. Although it has a relatively simple structure, it still accounts for most of the physical processes affecting sedimentation including turbulent diffusion and bed scour. The processes are important in modeling the impact of management practices that retain water on the surface. A brief user's guide for BASIN is given in Appendix C.

In the BASIN model, the retaining volume is divided into a series of chambers of equal volume, analogous to a series of reactors in chemical engineering literature. This concept is illustrated in Figure 2, where a detention pond cross-section is shown following the original development by Wilson and Barfield (1985). Sediment mixing, settling, and resuspension are considered by subdividing the chamber into rectangular shaped layers. The mass balance for an infinitesimal layer can be derived as

$$\frac{\partial C}{\partial t} = \frac{Q_{i-1} v_f}{EV_i} \left[C_p - C \right] + \omega_s \frac{\partial C}{\partial z} + \frac{\partial C}{\partial z} \left(\epsilon_s \frac{\partial C}{\partial z} \right) \tag{1}$$

The symbols Q_{i-1}, EV_i, and v_f represent discharge into the reactor chamber, effective reactor volume, and the ratio of the velocity to the mean velocity, respectively, C, ω_s, and ϵ_s are the sediment concentration, settling velocity and turbulent diffusion coefficient, respectively. The first term on the right-hand side represents the advection rate of sediment into the reactor chambers. The second and third terms are used to predict the rate of sediment settling and the rate of turbulent diffusion, respectively.

For numerical solution and for specification of boundary conditions, Equation 1 is more conveniently written as

$$\frac{\partial C}{\partial t} = \frac{Q_{i-1} v_f}{EV_i} \left[C_p - C \right] - \frac{\partial F}{\partial z} \tag{2}$$

where

$$F = - \omega_s C - \epsilon_s \frac{\partial C}{\partial z} \tag{3}$$

where F represents the net flux rate of sediment due to turbulence and settling.

At the pond's bed, the net rate of scour or mass transfer rate at the boundary can be written as

$$F_b = S_f - \omega_s C \tag{4}$$

where F_b is the net flux rate at the pond's bed (i.e., net scour rate), S_f is the detachment rate per unit area, and other terms are as previously defined. In BASIN, the detachment rate from the pond's bed is predicted by modifying Einstein's (1950) bed load theory. The rate

of particle detachment is then governed by the instantaneous lift force, the weight of the particle, and the number of particles available for detachment. The rather lengthy description of this algorithm is given by Wilson et al. (1984).

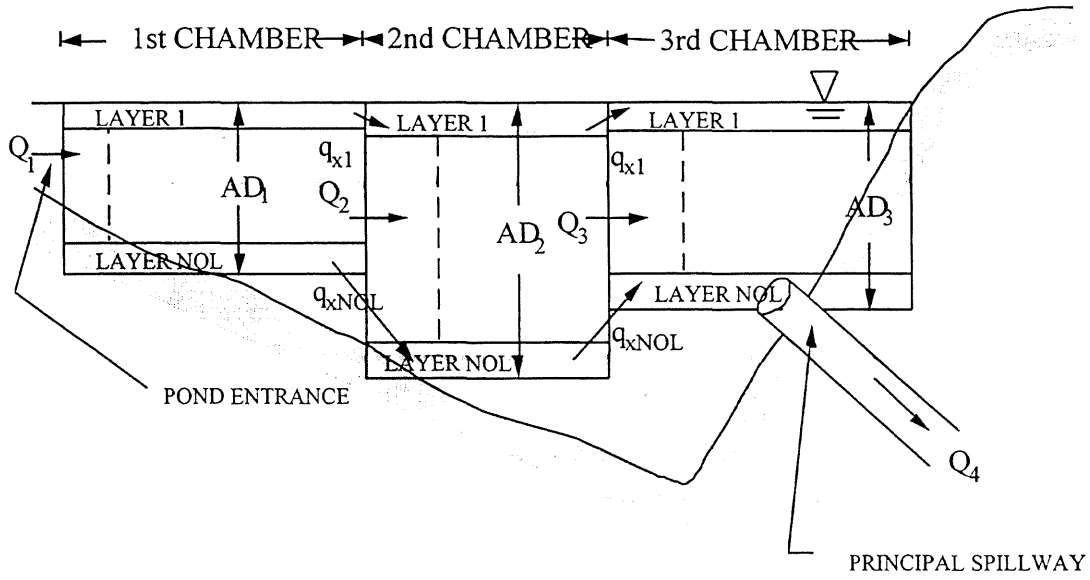

Figure 2. Cross-sectional View of a Hypothetical Pond.

The numerical solution to Equation 2 is obtained by modifying the hybrid difference scheme given by Dhamotharan et al. (1981). The solution can then be formulated in the following matrix solution

$$\mathbf{A}\ \mathbf{C} = \mathbf{B} \tag{5}$$

where **A** is a n x n tridiagonal matrix with known coefficients, **C** is a column vector of unknown concentration values at each node point for the current time step, and **B** is a column vector of known quantities from advection between reactors and from previous time step values. Equation 5 can be solved for **C** by using simple numerical techniques as given by Wilson et al. (1984).

As shown in Figure 2, the maximum distance that a particle must fall to become trapped varies between the inlet and outlet of the pond. In BASIN, this variation in depth is modeled using a volume-weighted depth for each reactor chamber. In Figure 2, the volume-weighted depth is represented by symbols AD_1, AD_2, and AD_3. The volume-weighted depth varies with the changing water level in the pond.

The accuracy of BASIN was compared to observed results gathered on two different pilot scale ponds. A total of 12 sediment laden runs were evaluated. The pond model did an excellent job of predicting the shape of the effluent sedimentgraphs. Relative to the peak influent concentration, the peak effluent concentration was predicted with reasonable accuracy. In general, the pond model tended to overpredict the effluent concentration for high influent concentration runs. The model was sensitive to possible errors in the particle size distribution.

Sedimentation With Vegetative Filter - The GRASSF Model

A modified GRASSF code is used to simulate the sedimentation effectiveness of a vegetative buffer strip. GRASSF was developed from studies investigating the ability of an erect media to trap sediment. The initial tests used metal pegs, but were later extended to grasses. Laboratory studies were used to develop predictive equations for bed load transport (Tollner et al., 1982) and for suspended load transport (Tollner et al., 1976). The application of these equations have been further modified by Hayes et al. (1979), Barfield and Hayes (1980) and Wilson et al. (1982). A brief user's guide for GRASSF is given in Appendix B.

Based on experimental results from the studies cited above, it was found that the sediment deposition pattern in vegetative filters resembled the profile shown in Figure 3. As sediment laden flow impinges on the filter, a reduction in its velocity causes the transport capacity to be lowered, which allows sediment deposition to occur. In GRASSF, it is assumed that the bed load material is deposited in the sediment wedge and that the suspended load is trapped in the remaining portion of the filter.

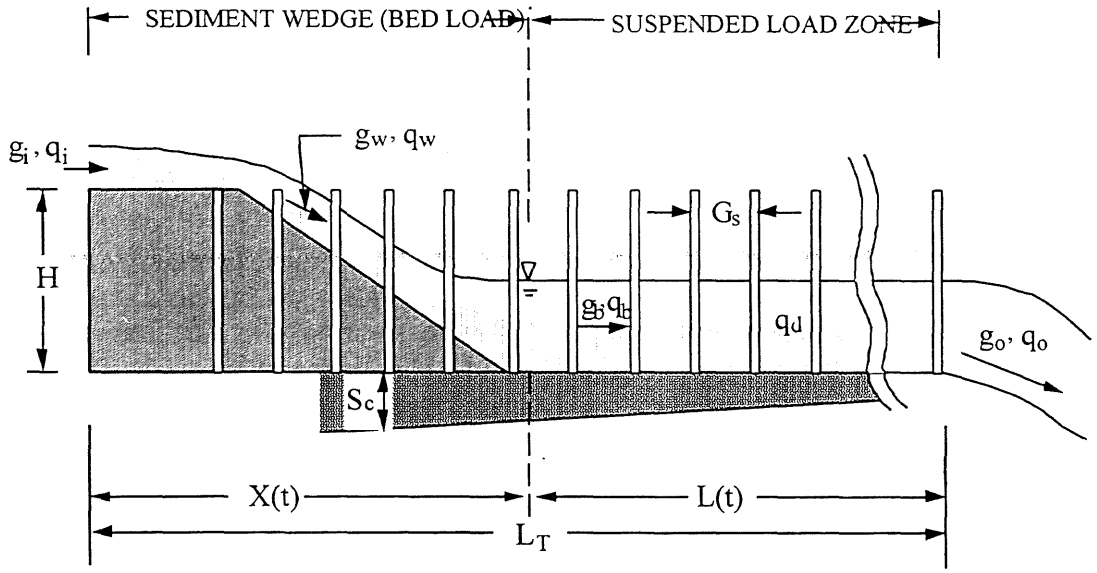

Figure 3. Schematic of a Vegetative Filter.

Einstein's bed load dimensionless parameters were calibrated using observed data in laboratory tests and are used to calculate the transport capacity of bed material in the filter (Tollner et al., 1982). Based on these studies, bed load transport in a grass filter is predicted as,

$$g_b = K \frac{(R_s S)^{3.57}}{d_p^{2.07}} \tag{6}$$

where

$$K = \frac{40367\ SG}{(\ SG\ -\ 1\ )^{3.07}} \tag{7}$$

In the above expression, g_b is the bed load transport rate [N/m/s], R_s is the spacing hydraulic radius [m], and d_p is the diameter of the particle [m]. The characteristic hydraulic dimension in Equation 6 is the spacing hydraulic radius (R_s) and is defined by an analogy between the spacing of grass elements and a rectangular channel of the same width.

As shown by Figure 3, the suspended load zone extends from the base of the deposition wedge to the outlet of the filter. In contrast to the bed load dimensionless parameters used in the sediment wedge, the suspended load zone is analyzed using the Reynolds' number (measure of turbulence) and the dimensionless fall number (measure of settling characteristics). Tollner et al. (1976) predicted the trap efficiency of the suspended load zone as

$$T_s = \exp\left[- 0.00105 \frac{R_e^{0.82}}{N_f^{0.91}} \right] \tag{8}$$

where

$$N_f = \frac{L\ \omega_s}{V\ h} \quad \text{and} \quad R_e = \frac{V\ R_s}{\nu} \tag{9}$$

where T_s is the trap efficiency of suspended sediment, N_f is the particle fall number, R_e is the Reynolds' number, L is the length of the suspended sediment zone, ω_s is the settling velocity of the particle, V is the flow velocity, y is the flow depth, ν is the kinematic viscosity, and R_s is the spacing hydraulic radius.

In GRASSF, the trap efficiency of suspended sediment is calculated for three different classes of particle diameters: coarse-sized particles (greater than 37 μ), medium sized particles (between 37 μ and 0.4 μ), and fine-sized particles (less than 0.4 μ).

The trap efficiency of sediment in the suspended zone is adjusted for cumulation of sediment on the bed and for infiltration losses. The cumulation of sediment on the filter bed reduces trap efficiency because the stools and grass indentations are filled. The infiltration losses increase trap efficiency because sediment particles are carried to the filter's bed with the downward movement of the transporting fluid.

GRASSF was tested on observed data collected by Hayes (1979) on five vegetative strips located on the University of Kentucky experimental farm. Inflow hydrographs and sedimentgraphs were obtained by spraying an inclined platform containing spoil material. This procedure yielded a nonhomogeneous particle size distribution and an unsteady inflow sedimentgraph. The ability of GRASSF to predict effluent concentration is very good.

Interface Routines

The two routines were developed to obtain the necessary output from the WEPP model and convert it into a useable form. The conceptualized representation of this process is shown in Figure 4 where the output from the interface routines are inputs into BASIN and GRASSF models.

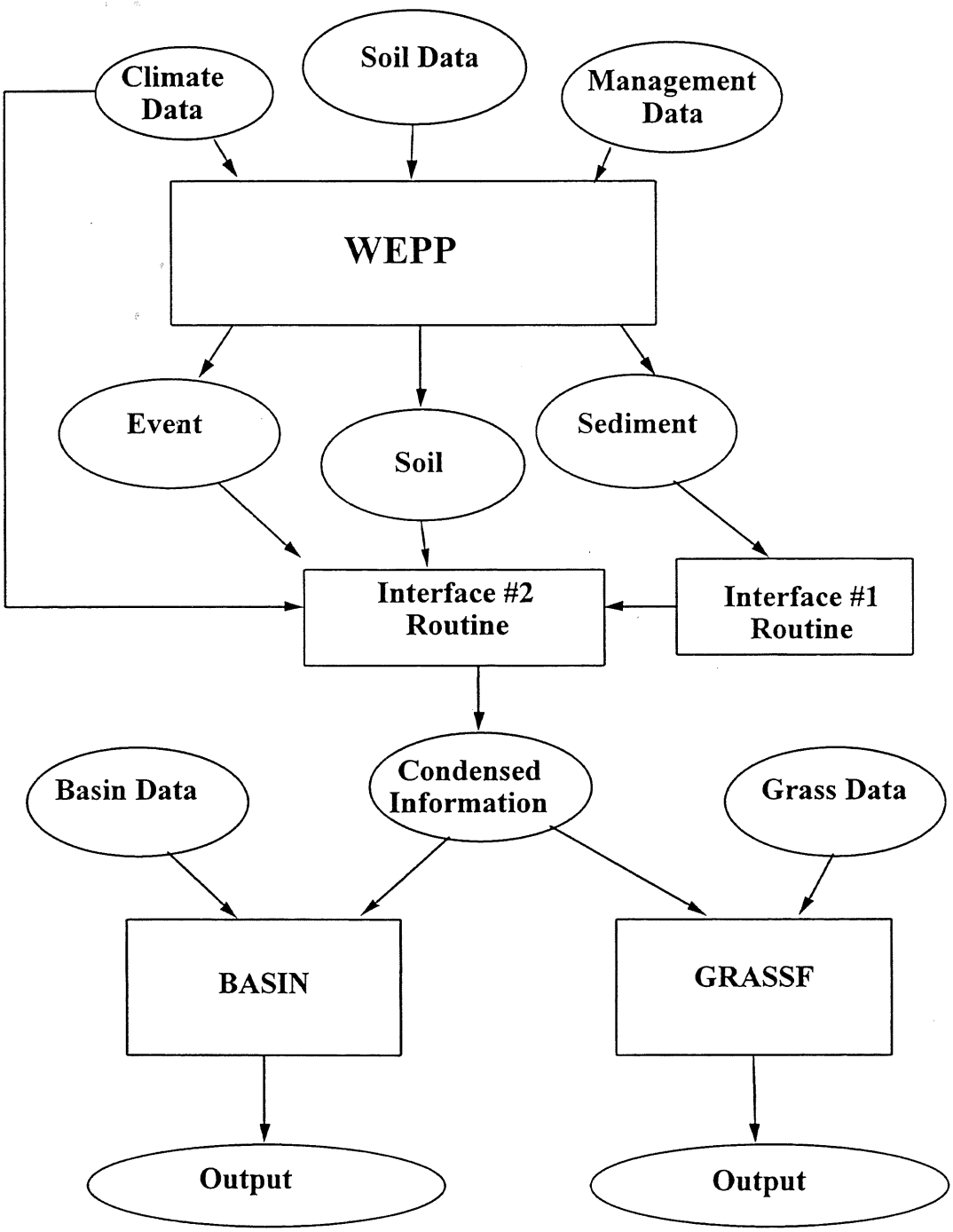

Figure 4. Use of Interface Routines.

The output from WEPP is provided in two formats: a numeric tabular format and a summary format that includes a mix of numbers, tables, and text. The INTERFACE

routines sort the data and reduces data from the climatic input file and eight WEPP output files into one file. The INTERFACE1 routine reduces a summary file from WEPP that contains the sediment yield and particle size information, along with text, to a tabular form file. This file will be used by INTERFACE2 to create the final input file for the other DROPLETS routines. The interface routines are executed by the program called SPA97. A brief user's guide to SPA97 is given in Appendix A.

The INTERFACE2 routine is used to combine all of the tabular output to a single useable file. The routine reads information from the WEPP output soil and event directories, the input climate directory, and the output from INTERFACE1. The routine reduces the data to include only those events where there was runoff and sediment from the hillslope. The routine determines if the runoff is due to rainfall or snowmelt. For this project, no snowmelt events were included in the reduced file. The resulting file is in a comma delimited format that allows it to be loaded into a spreadsheet as well as into the BASIN and GRASSF models.

The interface routines also generates coefficients used to obtain the runoff hydrograph and the sediment graph. The hydrograph ordinates are estimated using Haan's Method (Barfield et al., 1981) or assuming a constant inflow rate. The later option is selected for short time to peak rainfall intensities. The sediment yield and particle size distribution for each runoff event are determined by the WEPP model. The sedimentgraph is estimated assuming that the concentration is proportional to the flow rate (Barfield et al., 1981).

Hydraulic Response of Surface Tile Inlets

Watershed Area and Geometric and Pipe Characteristics

It is common for drainage systems in the Minnesota River Basin to have a series of surface tile inlets as previously shown in Figure 1. The corresponding top view for three surface depressions is shown in Figure 5. DROPLETS requires information on the geometric characteristics and watershed area for each of the depressions and the pipe characteristics for each of the inlets. The user has two basic options for defining these parameters: (1) internally compute them using the statistical characteristics of depressional watersheds and (2) enter them directly. The internally computed parameters are based on the approach previously developed by Haan and Johnson (1968) and used by Moore and Larson (1979). This approach will be given first. The work of Haan and Johnson is based on measurements taken from the East Fork Harden Creek watershed located in central Iowa and Emmet County in northern Iowa, which is located directly south of Martin County, Minnesota.

The first step in **internally computing** the depression characteristics is to estimate the *surface area* for each depression. Haan and Johnson (1967) conducted a detailed study of the location and number for the East Fork Harden Creek watershed in Iowa. They concluded that the location and number are essentially randomly distributed. The distribution of surface area was found to be well represented by the Weibull distribution (also called the Extreme Value Type III distribution). Values of this distribution are

usually bounded on the left by zero. Since a surface area of zero is meaningless, the values are bounded on the left by α. The probability density function of the three-parameter Weibull distribution is of the following form

$$f(A-\alpha) = \frac{\gamma}{\beta}\left(\frac{A-\alpha}{\beta}\right)^{\gamma-1} \exp\left[-\left(\frac{A-\alpha}{\beta}\right)^{\gamma}\right] \text{ for } A-\alpha \geq 0 \quad (10)$$

where $f(A-\alpha)$ is the probability density function for the random variable $(A-\alpha)$, A is the surface area in acres, and α, β and γ are parameters that are fitted to the data set. For the combined data set of East Fork Harden Creek and Emmet County, Haan and Johnson (1967) estimated $\alpha = 0.037$ acres, $\beta = 1.038$ acres, and $\gamma = 0.746$.

The cumulative distribution of depression is defined as

$$F(A-\alpha) = \int_0^{(A-\alpha)/\beta} \gamma\, y^{\gamma-1} \exp[-y^{\gamma}]\, dy \quad (11)$$

where $y = (A-\alpha)/\beta$. Since $d[\exp(-y^{\gamma})] = -\exp(-y^{\gamma})(\gamma y^{\gamma-1})dy$, we can integrate directly as

$$F(A-\alpha) = 1 - \exp\left[-\left(\frac{A-\alpha}{\beta}\right)^{\gamma}\right] \quad (12)$$

This relationship can be rearranged to solve for *surface area*, A, as

$$A = \alpha + \beta[-\ln(1 - F(A-\alpha))]^{1/\gamma} \quad (13)$$

Randomly distributed population can be obtained by generating random number between zero and one for $F(A-\alpha)$. This value can then be placed into the above equation to determine the corresponding surface area in acres.

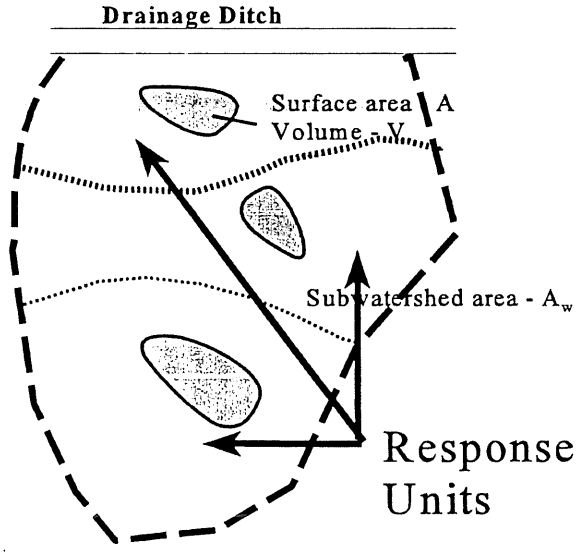

Figure 5. Top View of Series of Depressions.

Haan and Johnson (1967) also related the *subwatershed area* to the surface area of the depression using the following relationship

$$A_w = \kappa_w A^{\eta_w} \tag{14}$$

where A_w is the subwatershed area in acres draining into the depression and A is the surface area of the depression. By using approximately 230 depressions in Emmet County, Haan and Johnson (1967) obtained the regression values of $\kappa_w = 14.4$, $\eta_w = 0.46$ and $R^2 = 0.45$.

For a given total watershed area, the number of depressions and the surface area and the subwatershed area for each depression can now be estimated. First, a random number between zero and one is obtained. The surface area of the depression can then obtained by using Equation 13 and the subwatershed area by using Equation 14. This process is repeated until the cumulative area is equal to the total drainage area.

Haan and Johnson (1967) also examined the relationship between *depression volume* and surface area and the relationship between depression volume and *water depth*. The following general relationships were obtained

$$V = \kappa_a A^{\eta_a} \tag{15}$$

and

$$V = \kappa_h h^{\eta_h} \tag{16}$$

and by rearranging Equation 16, we also obtain

$$h = (1/\kappa_h)^{1/\eta_h} V^{1/\eta_h} = \kappa_v V^{\eta_v} \tag{17}$$

where V is the depression volume in acre-feet, A is the surface area of the depression in acres, and h is the water depth in feet. The parameter values and pertinent statistics obtained by Haan and Johnson (1967) are given in Table 1.

Table 1. Regression Parameters of Geometric Characteristics of Depressions.

Relationship	Statistics	Harden Creek	Emmet County
# of Depressions	n	70	230
Volume/Area	κ_a	0.34	0.27
	η_a	1.44	1.36
	R^2	0.92	0.71
Volume/Depth	κ_h	0.49	0.41
	η_h	2.42	2.31
	R^2	0.80	0.89
	κ_v	1.34	1.47
	η_v	0.41	0.43

There is an inherent relationship between the coefficients of Equations 15 and 16. Since dV = A dh, we obtain from Equation 4

$$\frac{dV}{dh} = A = \eta_h (\kappa_h) h^{\eta_h - 1} \tag{18}$$

and

$$h = \left(\frac{A}{\eta_h \kappa_h} \right)^{\frac{1}{\eta_h - 1}} \tag{19}$$

By using this relationship between depth and surface area, the volume defined by Equation 16 can be written as function of surface area as

$$V = \kappa_h \left(\frac{A}{\eta_h \kappa_h} \right)^{\frac{\eta_h}{\eta_h - 1}} \tag{20}$$

By comparing the coefficients of this equation with those of Equation 15, one conclude that

$$\eta_a = \frac{\eta_h}{\eta_h - 1} \quad \text{and} \quad \kappa_a = \frac{\kappa_h}{(\eta_h \kappa_h)^{\eta_a}} \tag{21}$$

The above relationships result in estimates of $\eta_a = 1.76$ and $\kappa_a = 0.45$ for Emmet County and $\eta_a = 1.70$ and $\kappa_a = 0.36$ for East Fork Harden Creek. Differences between these estimates and the regression parameters in Table 1 are not surprising because of the imperfect fit of the regression equations.

The *distance* between the center of depressions can be estimated by assuming that the depressions are square. The distance is then approximately

$$L_j = 0.5 * (\sqrt{43560\ A_{w,j}} + \sqrt{43560\ A_{w,j+1}}) \tag{22}$$

where L_j is the distance in feet between depressions j+1 and j and $A_{w,j}$ and $A_{w,j+1}$ are the respective watershed areas in acres. The distance from the last depression to the drainage ditch is computed as

$$L_n = 0.5 * \sqrt{43560\ A_{w,n}} \tag{23}$$

The *diameter* of the drainage system and the inlet can be estimated using the drainage coefficient. The drainage coefficient is defined as the required rate of water removal to prevent excessive crop damage and is usually specified in inches per day. The total flow rate in units of in-acre/h (≈ cfs) is

$$Q_d = A_d \frac{DC}{24} \tag{24}$$

where Q_d is the flow rate in the tile line in cfs, A_d is the cumulative drainage area, and DC is the drainage coefficient in in/day. If Manning's equation is used to estimate the flow velocity in drainage lines, the flow rate is also defined as

$$Q_d = \frac{1.49}{Mn_t} \left(\frac{\pi D^2}{4} \right) \left(\frac{D}{4} \right)^{2/3} S_t^{1/2} \tag{25}$$

where Mn_t is the Manning's n for the tile line, S_t is the slope of the tile line, and D is the diameter in feet. From Equation 24 and 25, the diameter in feet is computed as

$$D = \left(A_d \frac{DC}{24} \frac{Mn_t \, 4^{5/3}}{1.49 \, \pi \sqrt{S_t}} \right)^{3/8} = \left(0.0897 \frac{A_d (DC)(Mn)}{\sqrt{S_t}} \right)^{3/8} \quad (26)$$

The *elevation of the rim of the depression* can be computed from the elevation at the top of the drainage ditch, the length between depressions defined by Equations 22 and 23, and the average land slope. The elevation to the rim is then computed as

$$E_{tj} = S_l L_t + E_d \quad (27)$$

where E_{tj} is the elevation to the depression rim, L_t is the cumulative length from the drainage ditch, and E_d is the elevation at the top of the ditch.

The *elevation of the depression bottom* can be estimated as

$$E_{pj} = E_{tj} - h_{max,j} \quad (28)$$

where E_{pj} is the elevation at the bottom of the depression and $h_{max,j}$ is the depression depth. The depression depth is computed from Equation 17 where the volume is computed for the surface area computed by Equation 15.

The model also allows the user to **enter specific values** for each depression. The data file is organized using the following sequence of parameters for each depression.

ID A_{wj} D_j L_j E_{tj} $h_{max,j}$ Mn_{cj} $T_{o,j}$ κ_{hj} η_{hj} FileName

where ID is depression number, T_{oj} and Mn_{cj} are the top width, corresponding to a depth of one foot, and Manning's n of the outlet of the overflow channel from depression j and other terms are as previously defined. The "FileName" is the name of the data file that contains stage versus surface area values. These values are only used if κ_{hj} is negative.

If stage versus surface area values are entered, the cumulative volume for each stage is computed using the following equation

$$V(h) = \int_0^h A \, dh = V_{t,i} + \int_{h_i}^h A \, dh \quad (29)$$

Volume for a given flow depth or flow depth for given volume is determined by linear interpolation.

Hydraulic Response of a Series of Inlets

For the depression, four types of flows are possible: (1) weir flow, (2) orifice flow, (3) pipe flow, and (4) overland/channel flow. Overland/channel flow occurs when water overtops the depression and flows to a downstream depression or channel. The total flow is the lesser of the flow rate predicted for weir, orifice, or pipe conditions plus the

overland/channel flow.

Weir flow is estimated as

$$Q_{wj} = C_w L_w h_j^{3/2} = C_w (\pi SD_j) h_j^{3/2} \tag{30}$$

where Q_{wj} is the weir flow rate for a water depth of h_j, C_w is the weir coefficient and SD_j is the diameter of the surface tile inlet.

Orifice flow is estimated as

$$Q_{oj} = C_o A_o \sqrt{2gh_j} = C_o \left(\frac{\pi SD_j^2}{4} \right) \sqrt{2gh_j} \tag{31}$$

where Q_{oj} is the orifice flow rate, C_o is the orifice coefficient and other terms are as previously defined.

Pipe flow is estimated using Manning's equation for full pipe flow. In general, the flow rate in the tile line is defined as

$$Q_{tj} = \frac{1.49}{Mn_t} \left(\frac{\pi D_j^2}{4} \right) \left(\frac{D_j}{4} \right)^{2/3} S_{tj}^{1/2} \tag{32}$$

where Q_{tj} is the flow rate in the tile line at inlet j and S_{tj} is the hydraulic slope. The hydraulic slope can be estimated using the hydraulic head for two adjacient depressions, or

$$S_t^{1/2} = \sqrt{\frac{H_j^{k-1} - H_{j+1}^{k-1}}{L_j}} \quad \text{if } H_j > H_{j+1} \tag{33a}$$

or

$$S_t^{1/2} = -\sqrt{\frac{H_{j+1}^{k-1} - H_j^{k-1}}{L_j}} \quad \text{if } H_j < H_{j+1} \tag{33b}$$

A negative hydraulic slope indicates the flow is from the downslope depression to the upslope depression.

Since Q_{tj} is the flow in the tile line, the flow from the inlet itself is calculated as

$$Q_{pj} = Q_{tj} - Q_{tj-1} - Q_{Lj} \tag{34}$$

where Q_{tj-1} is the flow rate upslope of inlet j and Q_{lj} is the flow rate at inlet j from subsurface tile lines.

When the water surface elevation in the depression exceeds the elevation at the top of the rim ($h_j > h_{max,j}$), water flows downslope to a lower depression or to a drainage channel. This flow rate is estimated by assuming uniform flow in a parabolic channel. The top width of a parabolic channel can be written as (Barfield et al., 1981)

$$T_j = T_{s,j}\left(\frac{h_{o,j}}{h_{s,j}}\right)^{1/2} \tag{35a}$$

where T_j is the top width corresponding to the uniform flow depth in the channel ($h_{o,j}$). Procedures to estimate $h_{o,j}$ are given later in this section. $T_{s,j}$ is the top width corresponding to a standard flow depth $h_{s,j}$. To simplify input information, $h_{s,j}$ is taken as one foot. The symbol of $h_{s,j}$ will be replaced by one foot to simplify algebraic manipulations.

Cross-sectional area for parabolic channel is defined as (Barfield et al., 1981)

$$A_{c,j} = \frac{2}{3} T_j h_{o,j} = \frac{4}{3} T_{s,j} h_{o,j}^{3/2} \tag{35b}$$

and the hydraulic radius is defined as (Barfield et al., 1981)

$$R_{c,j} = \frac{T_j^2 h_{o,j}}{(3/2)T_j^2 + 4h_{o,j}^2} = \frac{T_s^2 h_{o,j}^2}{(3/2)T_s^2 h_{o,j} + 4h_{o,j}^2} \approx \frac{2}{3} h_{o,j} \tag{35c}$$

where $A_{c,j}$ is the cross sectional area of flow for the channel flow depth in the channel of h_o and $R_{c,j}$ is the hydraulic radius for the channel. The above approximation is valid for a large top width relative to the flow depth. The units in Equation 35c appear inconsistent because h_s has not been carried along in the computations.

The velocity in the parabolic channel can be estimated from Manning's equation for uniform flow as

$$V_{c,j} = \frac{1.49}{Mn_{c,j}} R_{c,j}^{2/3} S_1^{1/2} \tag{36}$$

where the subscript refers to properties in the channel between depressions.

Bernoulli's equation is applied to two points in the surface discharges system: 1 - a point located at the water surface in the depression and 2 - a point where the flow is at uniform condition. Bernoulli's equation can then be written as

$$\frac{\alpha V_1^2}{2g} + h_1 + z_1 = \frac{\alpha V_2^2}{2g} + h_{o,j} + z_2 + h_f \tag{37a}$$

where α is approximately one. At point 1, $h_1 + z_1 = H_j$, and $V_1 \approx 0$. At point 2, we assume $h_f = E_{t,j} - z_2$. Bernoulli's equation can then be evaluated as

$$h_{o,j} + \frac{\left(\frac{1.49}{Mn_{c,j}} (0.67 h_{o,j})^{2/3} S_1^{1/2}\right)^2}{2g} = H_j - E_{t,j} \tag{37b}$$

or rearranged as

$$h_{o,j} + h_{o,j}^{4/3}\left(\frac{1.14 S_1}{Mn_{c,j}^2 2g}\right) = H_j - E_{t,j} \tag{37c}$$

which can be solved using a trial-and-error technique.

After $h_{o,j}$ is determined, the outflow rate through the surface channel can be computed from Manning's equation as

$$Q_{s,j} = \frac{1.49}{Mn_{c,j}} \left(\frac{T_s^2 h_{o,j}^2}{(3/2) T_s^2 h_{o,j} + 4 h_{o,j}^2} \right)^{2/3} S_l^{1/2} \frac{4 T_{s,j} h_{o,j}^{3/2}}{3} \tag{38}$$

Hydrologic Routing

The outflow hydrographs for each depression are determined by solving the conservation of mass for a constant density fluid, or

$$I - O = \frac{dV}{dt} \tag{39a}$$

which can be numerically approximated as

$$\frac{I_{k+1} + I_k}{2} \Delta t - \frac{O_{k+1} + O_k}{2} \Delta t = V_{k+1} - V_k \tag{39b}$$

and rearranged as

$$V_{k+1} = V_k + \frac{I_{k+1} + I_k}{2} \Delta t - O_k \frac{\Delta t}{2} - O_{k+1} \frac{\Delta t}{2} \tag{39c}$$

The inflow is runoff from the watershed and possible flow from an upslope depression, or

$$I_{k+1} = I_{k+1}^w + I_{k+1}^d \tag{40a}$$

where the first term is the inflow from the watershed and the second term is inflow from the previous depression. Likewise, the outflow can be divided into components as

$$O_{k+1} = O_{k+1}^s + O_{k+1}^o \tag{40b}$$

where the first term is the outflow through the surface inlet and the second is the outflow from overtopping.

For a given time, k+1, the following iterative steps are used to obtain the outflow rate.

(1) For each j depression, estimate the inflow rate $I_{j,k+1}$ from WEPP output files and possible overflow from the upslope depression . Set $O_{old} = O_k$. Compute the following constant for the time step:

$$Cnst_j = V_{j,k} + \frac{I_{j,k+1} + I_{j,k}}{2} \Delta t - O_{j,k} \frac{\Delta t}{2} \tag{41a}$$

(2) Estimate the new outflow rate as

$$O_{j,k+1} = O_{j,k} + \frac{O_{j,k} - O_{j,k-1}}{2} \tag{41b}$$

(3) For each depression, estimate the volume at the end of the time step as

$$V_{j,k+1} = Cnst_j - O_{j,k+1}\frac{\Delta t}{2} \quad (41c)$$

(4) Estimate the flow depth for this volume using either the power function previously given by Equation 17

$$h_{j,k+1} = \kappa_v V_{j,k+1}^{\eta_v} \quad (41d)$$

or by linear interpolation if the user has entered stage-area values.

(5) Compute the outflow rate $O_{j,k+1}$ for $h_{j,k+1}$ using the procedures described in the previous section.

(6) If ABS($O_{j,k+1}$ - O_{old}) < OTOL then quit; otherwise $O_{old} = O_{j,k+1}$ and repeat Steps #3 through #6.

Subsurface Drainage Component

Introduction

Two different approaches are used to simulate subsurface flow in tile lines. One approach is based on the relationships obtained by Kirkham and coauthors using potential flow theory. This approach is recommended if detailed information is available about the drainage system. The other approach is based on a known drainage coefficient. This approach is recommended if limited information is available. Both approaches are based on steady-state conditions. Unsteady flow is simulated by varying the water table height using a water balance. The flow rates are adjusted to account for downline pressure.

The theoretical approach of Kirkham and coauthors' are developed first. Relationships for the drainage coefficient method are then developed. Adjustment for downline pressure is presented. Dynamic flow rates are determined by using the conservation of mass for the subsurface soil profile. Separate subsections are used to develop these equations for the Kirkham Method and the Drainage Coefficient Method.

Kirkham's Subsurface Flow Equations

In 1958, Kirham analyzed the drainage to circular tile using potential flow theory. This solution is valid for steady-state conditions and a homogenous soil. A sketch of his flow system and the definition of important parameters are shown in Figure 6.

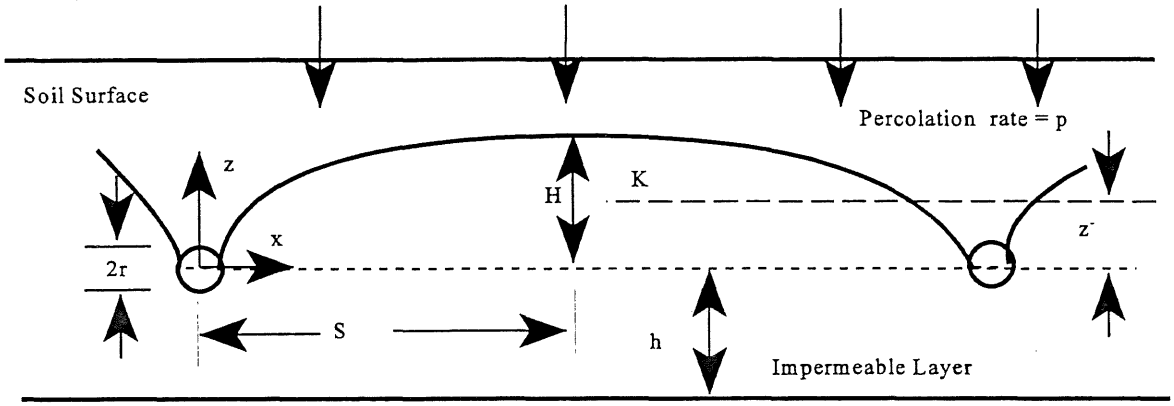

Figure 6. Definition Sketch for Flow to Tile Lines for Homogenous Soil.

Kirham's (1958) solution for the height above the centerline of the drain as a function of x can be written as

$$z = \frac{2Sp}{K}\hat{F} \tag{42a}$$

where terms are as defined in Figure 6 and $\hat{F}$ is a function of x, r, S and h as shown below.

$$\hat{F} = \frac{1}{\pi}\left(\ln\left(\frac{\sin(\pi x/2S)}{\sin(\pi r/2S)}\right) + \sum_{i=1}^{\infty} \frac{\left[\cos\left(\frac{i\pi r}{S}\right) - \cos\left(\frac{i\pi x}{S}\right)\right]\left[\coth\left(\frac{i\pi h}{S}\right) - 1\right]}{i} \right) \tag{42b}$$

The maximum height is obtained at x = S, or

$$H = \frac{2Sp}{K}F \tag{43a}$$

where H is the maximum height of the water table above the drains and other terms are as defined in the above figure. The function F is defined as

$$F = \frac{1}{\pi}\left(\ln\left(\frac{2S}{\pi r}\right) + \sum_{i=1}^{\infty} \frac{\left[\cos\left(\frac{i\pi r}{S}\right) - \cos(i\pi)\right]\left[\coth\left(\frac{i\pi h}{S}\right) - 1\right]}{i} \right) \tag{43b}$$

where $\sin(\pi r/2S)$ is closely approximated by $\pi r/2S$ for small r/2S.

To evaluate the number of terms necessary to approximate the summation term in the definition of F, F was solved for zero terms, 5 terms, 10 terms, 20 terms, and 100 terms. The percent error obtained, using 100 terms as the true solution, was computed for various values of 2S/h and h/2r. The results are shown in Figure 7. The percent error is clearly small for 20 or more terms. Twenty terms are used to solve Equations 42b and 43b.

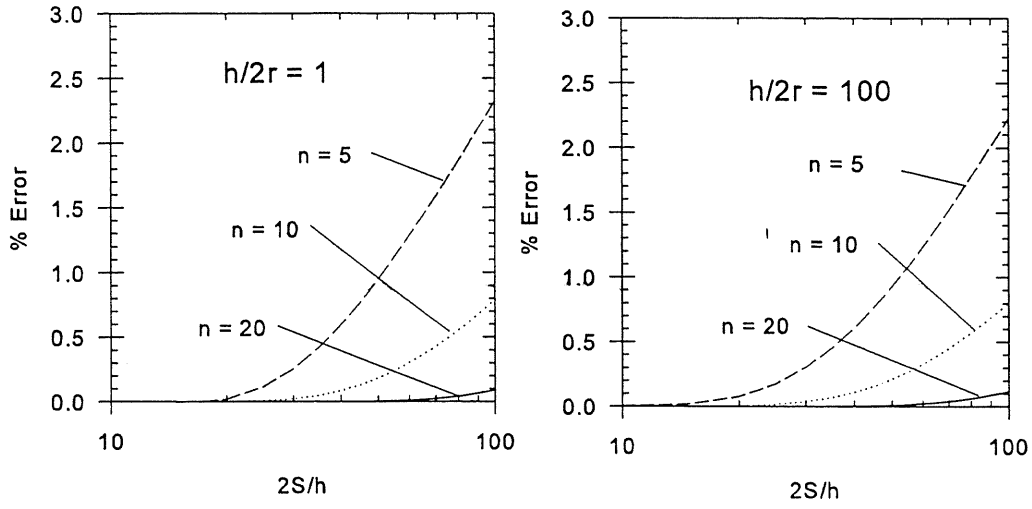

Figure 7. Error in Using Finite Number of Terms in Kirkham's Geometry Parameter.

In 1964, Kirkham further refined his solution by multiplying the right-hand side of the equation by 1/(1 - p/K). The equations are then modified as

$$z = \frac{2Sp}{K}\hat{F}\left(\frac{K}{K-p}\right) = 2S\hat{F}\left(\frac{p}{K-p}\right) \tag{44a}$$

and the water table height at x=S can be obtained as

$$H = 2SF\left(\frac{p}{K-p}\right) \tag{44b}$$

If F is known, the discharge per unit area can be obtained directly as

$$p = \frac{KH}{2SF+H} = K\frac{H}{2SF+H} \tag{44c}$$

or for discharge per unit length as

$$q_d = pS = \frac{KHS}{2SF+H} \tag{44d}$$

It is clear from the above equations that p is always less than K. This is, of course, expected because the percolation rate is maximum at complete saturation. If the flow from the other side of the drain line is identical, then the total flow from the tile line is twice the values given by the above equation.

Tokoz and Kirkham (1971) modified the potential flow solution to include flow in soils with different conductivities. Only a two-layered soil will be considered here. A schematic illustrating the key variables is shown in Figure 8.

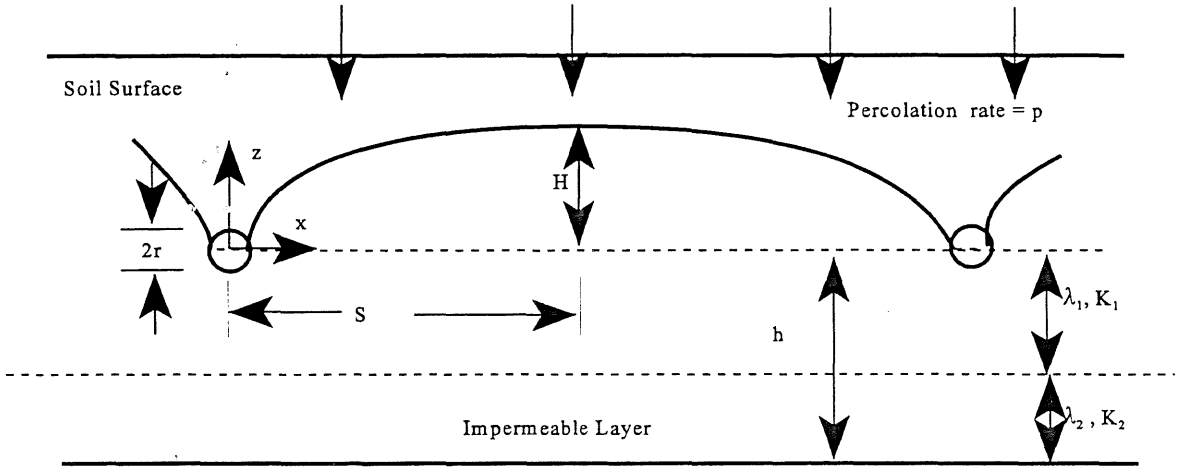

Figure 8. Definition Sketch for Flow to Tile Lines for Layered Soil.

By using potential flow theory, the water table height at x=S is defined as

$$H = 2S\left(\frac{p}{K_1 - p}\right) G \tag{45a}$$

where K_1 is the saturated conductivity in the top layer, S, p, and H are as previously defined and G is defined as

$$G = \frac{1}{\pi}\left(\ln\left(\frac{1}{\sin(\pi r/2S)}\right) + \sum_{i=1}^{\infty} \Omega_i \frac{\left[\cos\left(\frac{i\pi r}{S}\right) - \cos(i\pi)\right]\left[\coth\left(\frac{i\pi\lambda_1}{S}\right) - 1\right]}{i} \right) \tag{45b}$$

where Ω_i is a function of the conductivity in the lower layer. It is defined as

$$\Omega_i = 1 - \left(\frac{e^{i\pi\lambda_1/S}}{\sinh(i\pi\lambda_1/S)}\right) \frac{1}{\frac{K_1}{K_2}\coth\left(i\pi\frac{h-\lambda_1}{S}\right) + \coth\left(\frac{i\pi\lambda_1}{S}\right)} \tag{45c}$$

The value of G is only dependent of the drainage system geometry and conductivities, that is, it is independent of time.

A generalized result of potential flow theory to determine the discharge per unit area can be written as

$$p = \frac{K_1 H}{2SJ_K + H} \tag{46a}$$

and the discharge per unit length as

$$q_d = pS = \frac{K_1 H S}{2SJ_K + H} \tag{46b}$$

and the total discharge as

$$\hat{Q}_d = p A_d = A_d \left(\frac{K_1 H}{2SJ_K + H}\right) \tag{46c}$$

where A_d is the area under tile drains. The value of H corresponding to a given flow rate is simply

$$H = 2S \frac{J_K \hat{Q}_d}{K_1 A_d - \hat{Q}_d} \tag{46d}$$

where J_K is a time independent parameter defined for homogenous soil as

$$J_K = F = \frac{1}{\pi}\left(\ln\left(\frac{2S}{\pi r}\right) + \sum_{i=1}^{\infty} \frac{\left[\cos\left(\frac{i\pi r}{S}\right) - \cos(i\pi)\right]\left[\coth\left(\frac{i\pi h}{S}\right) - 1\right]}{i} \right) \tag{47a}$$

and for layered soil as

$$J_K = G = \frac{1}{\pi}\left(\ln\left(\frac{1}{\sin(\pi r/2S)}\right) + \sum_{i=1}^{\infty} \Omega_i \frac{\left[\cos\left(\frac{i\pi r}{S}\right) - \cos(i\pi)\right]\left[\coth\left(\frac{i\pi\lambda_1}{S}\right) - 1\right]}{i} \right) \tag{47b}$$

where Ω_i is defined by Equation 45c.

For each depression, the user enters the following information to compute flow rates using the above equations:

ID, L_m', Slope, S, L_ℓ, Z_t, D_t, λ_1, K_1, λ_2, K_2, ϕ_d, FILENAME

where ID, Z_t, D_t, ϕ_d, and FILENAME are as previously defined and L_m' is the length of the main line (one-half of total), Slope is the slope of the main line, S is the spacing between laterals, L_ℓ is the length of the laterals, λ_1 and K_1 are the thickness and saturated conductivity of the top layer and λ_2 and K_2 are the thickness and saturated conductivity of the second layer. For $K_2 \leq 0$, Kirkham's non-layered solution will be used.

Drainage Coefficient Method

Detailed information about the subsurface drainage system will be unknown for many sites. For these sites, subsurface flow can be simulated by using the drainage coefficient method. The maximum discharge of the subsurface drainage system is defined as

$$\hat{Q}_{dm} = D_c E_f A_f A_w \tag{48}$$

where $\hat{Q}_{dm}$ is the maximum flow rate from the system, D_c is the drainage coefficient (L/T), E_f is the effectiveness of the drainage system (i.e, if the system is performing optimally for crop productivity, $E_f = 1$), A_w is the watershed area (L^2), and A_f is the fraction of the watershed with subsurface drainage.

Let's define the water table height corresponding to the maximum flow rate as

$$H_m = Z_t - z_c \tag{49}$$

where Z_t is the representative depth to the tile lines and z_c is the depth of the water

table from the surface corresponding to maximum discharge, which is initially defined as 0.25 ft. For a value of H greater than H_m, the flow rate is estimated as

$$\hat{Q}_d = \hat{Q}_{dm} \qquad \text{for } H \geq H_m \tag{50}$$

To determine the flow rate for a water table height, H, less than H_m, the theoretical solution of Kirkham's for a homogenous soil (Equation 44d) will be used. The ratio of two flow rates for water table height of H and H_m can be written as

$$\frac{\hat{Q}_d}{\hat{Q}_{dm}} = \frac{p\, E_f\, A_f\, A_w}{p_m\, E_f\, A_f\, A_w} = \frac{KH/(2SF+H)}{KH_m/(2SF+H_m)} = \frac{H\,(2SF+H_m)}{H_m\,(2SF+H)} \qquad \text{for } 0 < H < H_m \tag{51a}$$

We can solve for 2SF using the discharge and water table height for maximum flow, or

$$2SF = \frac{p_m}{(K - p_m)\, H_m} = \frac{D_c E_f}{(K - D_c E_f)\, H_m} \tag{51b}$$

and therefore obtain the following relationship for flow rate corresponding to a water table height

$$\hat{Q}_d = \hat{Q}_{dm}\ \frac{H\,[D_c E_f + (K - D_c E_f) H_m^2]}{H_m\,[D_c E_f + (K - D_c E_f) H_m H]} \qquad \text{for } 0 < H < H_m, \text{ and } K > D_c E_f \tag{52}$$

For the drainage coefficient method, each depressional area requires the following input information:

ID, D_c, Z_t, F_e, F_a, D_t, K_s, ϕ_d, FILENAME

where ID is the identification number of the response unit, Z_t is the depth from the soil surface to the tile line, D_c is the drainage coefficient, F_e is the factor to represent the effectiveness of the drainage system, F_a is the fraction of the watershed that has subsurface drainage, D_t is the tile diameter, K_s is the saturated conductivity, ϕ_d is the drainable porosity and FILENAME is the name of the file that contains daily ET and percolation values.

As discussed later, a value of S is needed to estimate the average water table height. To estimate S for the simple drainage coefficient method, Kirkham's solution for a homogenous soil will again be used. By neglecting the summation terms, F is defined as

$$F = \frac{1}{\pi} \ln\left(\frac{2S}{\pi r}\right) \tag{53a}$$

The above approximation is accurate for small h/S. From Kirkham's equation,

$$H_m = 2SF\left(\frac{p_m}{K - p_m}\right) = \left(\frac{2S \ln(2S/\pi r)}{\pi}\right)\left(\frac{p_m}{K - p_m}\right) \tag{53b}$$

or

$$S \ln\left(\frac{2S}{\pi r}\right) = \frac{\pi H_m (K - D_c E_f)}{2 D_c E_f} = \zeta \tag{54}$$

where ζ is a defined from known input or computed values. The only unknown in the above equation is S. To solve for S without using a trial-and-error approach, an approximate solution can be obtained by using the Taylor series expansions for ln(1+x) and ln(1-x),

$$\ln\left(\frac{1+x}{1-x}\right) = 2\left(x + \frac{x^3}{3} + \frac{x^5}{5} + \ldots.\right) \tag{55a}$$

which converges for $|x| < 1$. For our case,

$$\frac{1+x}{1-x} = \frac{2S}{\pi r} \quad \text{and therefore} \quad x = \frac{(2S/\pi r) - 1}{(2S/\pi r) + 1} \tag{55b}$$

where x is less than one. By neglecting third order terms, we obtain

$$S \ln\left(\frac{2S}{\pi r}\right) \approx 2S_o \frac{2S_o - \pi r}{2S_o + \pi r} = \zeta \tag{55c}$$

where S_o is used to indicate an approximate spacing value. We can rearrange the above equation to solve for S_o as

$$4S_o^2 - 2(\pi r + \zeta)S_o - \pi r \zeta = 0 \tag{55d}$$

Since third-order terms are neglected, $S > S_o$. By using the quadratic equation, S_o can be solved as

$$8 S_o = 2(\pi r + \zeta) \pm \sqrt{4(\pi r + \zeta)^2 + 16 \pi r} \tag{55e}$$

Since the square root term is always greater than the first term on the right-hand side, the positive square root is the only physically meaningful solution. We therefore obtain

$$S_o = \frac{1}{4}\left[\pi r + \zeta + \sqrt{\pi r(\pi r + 2\zeta + 4) + \zeta^2}\right] \tag{56}$$

The above equation is an approximation obtained by neglecting higher order terms. A second-order Newton method can be used to obtain a more precise estimate. This approach is based on a Taylor series expansion of the following form

$$f(x) = f(x_o) + (x - x_o) f'(x_o) + \frac{(x - x_o)^2}{2} f''(x_o) + \ldots \tag{57a}$$

where f(x) here is

$$f(x) = f(S) = S \ln\left(\frac{2S}{\pi r}\right) - \zeta \tag{57b}$$

where S is the unknown, and x_o is estimated from the truncated series S_o. We are interested in finding S such that f(S)=0. By neglecting third-order terms, this value of S can be obtained by using the quadratic equation as

$$S' - S_o = \frac{-f'(S_o) \pm \sqrt{[f'(S_o)]^2 - 2f''(S_o)f(S_o)}}{f''(S_o)} \tag{57c}$$

where S' is used to indicate an approximate estimate. Since $S' > S_o$, the left-hand side of the equation is positive, and therefore, the positive square root is the only feasible solution. We then obtain

$$S' = S_o - \frac{f'(S_o)}{f''(S_o)} + \sqrt{\left(\frac{f'(S_o)}{f''(S_o)}\right)^2 - 2\frac{f(S_o)}{f''(S_o)}} \tag{57d}$$

The first derivative can be evaluated directly as

$$f' = \ln(2S_o/\pi r) + S_o \frac{2/\pi r}{2S_o/\pi r} = \ln(2S_o/\pi r) + 1 \tag{57e}$$

and the second derivative as

$$f'' = \frac{2/\pi r}{2S_o/\pi r} = \frac{1}{S_o} \tag{57f}$$

By using these relationships, S' can be evaluated as

$$S' = S_o - S_o[1 + \ln(2S_o/\pi r)] + S_o\sqrt{[1 + \ln(2S_o/\pi r)]^2 - 2\ln(2S_o/\pi r) + 2\zeta/S_o} \tag{57g}$$

or

$$S' = S_o\left(\sqrt{[\ln(2S_o/\pi r)]^2 + 2\zeta/S_o + 1} - \ln(2S_o/\pi r)\right) \tag{58}$$

To evaluate the accuracy of S', a value of r = 0.5 ft was assumed. For a given S, the value of ζ was computed from known values of S and r. The estimated values of S_o and S' were then computed for the known r and ζ. The percent error was computed. The results are shown in Figure 9. Equation 58 becomes less accurate as the tile spacing increases. The percent error is, however, still less than 5% for spacings of 250 feet. This is clearly within the accuracy necessary to approximate the spacing in the drainage coefficient method.

Modifications for Downline Pressure

Kirkham's equations, and extensions used with the Drainage Coefficient Method, were derived assuming that the potential in the tile lines corresponds to atmospheric air pressure. For some drainage systems, especially for extreme runoff events, there can be a pressure head as the result of downline conditions.

The impact of downline pressure will be considered by reducing the effective head for tile discharge. This crude approach is similar to that taken by Deboer and Johnson (1975) and Moore and Larson (1980). A schematic illustrating important terms is shown in Figure 10. In Figure 10, H_p is the pressure head in the tile line and H' is the effective head of flow to the line. Flow rate will be determined as a function of the effective head.

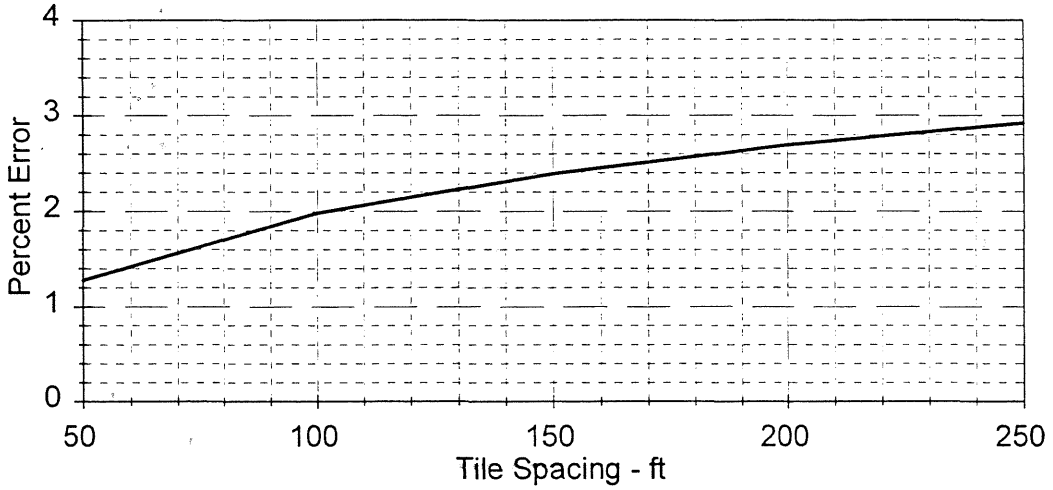

Figure 9. Percent Error in Using Equation 58 to Compute S.

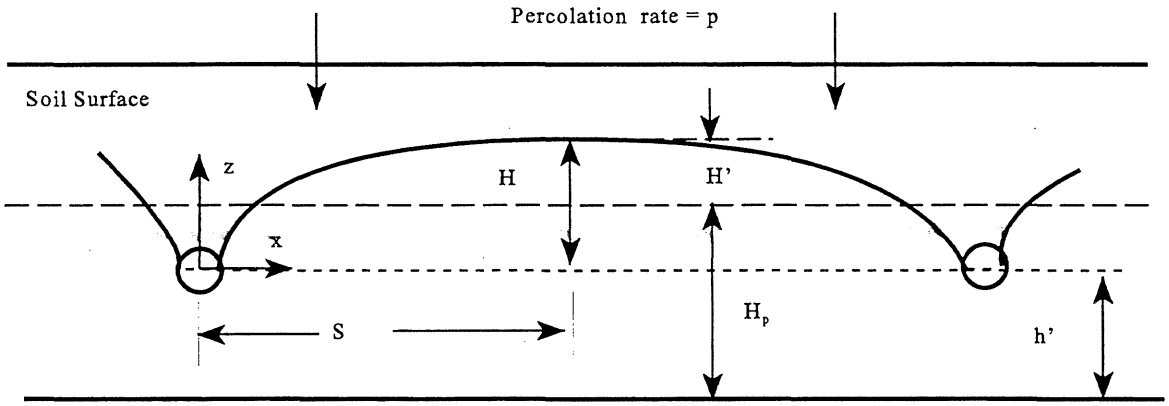

Figure 10. Definition Schematic of Tile Flow with Downline Pressure.

If the datum is taken as the tile depth at the surface tile inlet, the value of h' can be estimated as

$$h' = el_{bot} - Z_i + 0.5L_m s_t \tag{59}$$

where el_{bot} is the elevation at the bottom of the depression, Z_i is the depth below the bottom to the junction of subsurface tile, 0.5 L_m is one-half of the distance of the lateral, and s_t is the slope of the tile line. Although the logic could be extended to individual lateral lines, the adjustment by downline pressure will be evaluated for a single point located at the midpoint of the line.

For *Kirkham's Method*, the discharge per unit area using the effective head is computed as

$$p' = K_1 \frac{H'}{2SJ_K + H'} \tag{60a}$$

where

$$H' = H + h' - H_p \tag{60b}$$

The ratio of the discharge with and without downline pressure can easily be obtained by taking the ratio of their predictive equations. We then obtain

$$Q_d = C_p \hat{Q}_d \tag{61}$$

where C_p is defined as

$$C_p = 1 \quad \text{for } H_p < h \tag{62a}$$

$$C_p = \frac{(H + h' - H_p)/H}{(2SJ_K + (H + h' - H_p))/(2SJ_K + H)} \quad \text{for } h' < H_p < H \tag{62b}$$

$$C_p = 0 \quad \text{for } H < H_p \tag{62c}$$

If $H < H_p$, the flow from the tile line is into the soil. The proposed approach is too imprecise to include this process.

For the *Drainage Coefficient Method*, the tile flow rate is defined as

$$\hat{Q}_d = \hat{Q}_{dm} \frac{(H + h' - H_p)\,[D_c E_f + (K - D_c E_f) H_m^2]}{H_m\,[D_c E_f + (K - D_c E_f) H_m (H + h' - H_p)]} \quad \text{for } 0 < H < H_m, \text{ and } K > D_c E_f \tag{63}$$

and therefore C_p is defined as

$$C_p = \frac{(H + h' - H_p)\,[D_c E_f + H_m (K - D_c E_f)(H + h' - H_p)]}{H\,[D_c E_f + H_m (K - D_c E_f) H]} \quad \text{for } h' < H_p < H \tag{64a}$$

For $H > H_m$, we define C_p as

$$C_p = \frac{H_m + h' - H_p}{H_m} \tag{64b}$$

General Formulation of Mass Balance Relationships

For mass balance computations, it is useful to determine the average height of the water table above the drain. The average height is defined mathematically as

$$\bar{z} = \frac{\int_0^S z(x)\,dx}{S} \tag{65}$$

where z(x) is the water table height. To simplify computations, this value is estimated using Kirkham's solution for a homogenous soil. In addition, the terms that are not a function of x are lumped into constants as shown below:

$$z(x) = k_1 \left(\ln[k_2 \sin(\pi x/2S)] + k_3 + \sum_{i=1}^{\infty} (-k_4 \cos(i\pi x/S)) \right) \tag{66}$$

where k_1 through k_4 are combinations of terms that are not a function of x. The second and third terms on the right-hand side can be integrated directly. The first term, however, requires a numerical solution.

As previously shown, tile flow is defined relative to the water table height at x=S (i.e., H); whereas, the mass balance uses the average depth, $\bar{z}$. The ratio of average depth and maximum depth is therefore an useful parameter. It is defined as

$$\xi = \frac{\bar{z}}{H} \tag{67}$$

Since the term 2Sp/(K-p) is in the numerator and denominator, it cancels and ξ can be evaluated as

$$\xi = \frac{\left(\frac{1}{S-r}\right) \sum_{j=1}^{m} \hat{F}(x)\, \Delta x}{\hat{F}(x=H)} \tag{68}$$

where m is the number of intervals for the numerical approximation of $\bar{z}$.

Since the curvature of the water table is steeper near the drain, it is desireable to have small intervals in the region. The function will evaluated using equally spaced values for a logarithmic scale. The logarithmic spacing is defined as

$$\Delta x_L = \frac{\ln(S) - \ln(r)}{m} \tag{69a}$$

The endpoint of the jth interval for the log scale is defined as

$$x_{L,j} = x_{L,j-1} + \Delta x_L \tag{69b}$$

where for the first interval, $x_{L,j-1} = \ln(r)$. The midpoint and spacing for the arithmic scale are then defined as

$$\bar{x}_j = \exp\left(x_{L,j} - \frac{\Delta x_L}{2}\right) \tag{69c}$$

$$\Delta x_j = \exp(x_{L,j}) - \exp(x_{L,j-1}) \tag{69d}$$

The percent error is shown in Figure 11 for m = 10, 20, 50, and 100, assuming m=500 correspond to the true solution. The values are computed for h/2r = 1 and 2S/h = 20. The error for m=20 is less than 5% and therefore represents a reasonable approximation to the true solution.

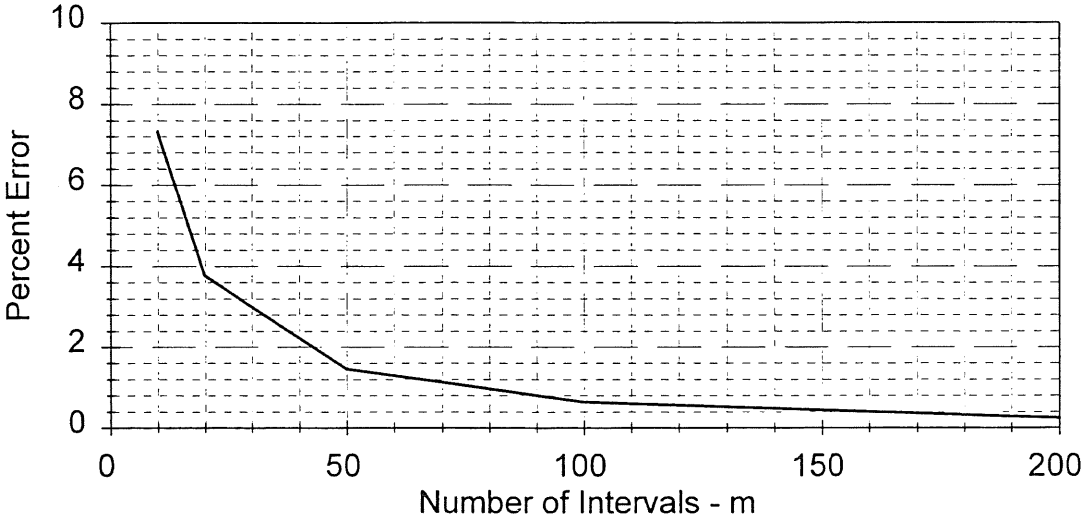

Figure 11. Percent Error in Estimating ξ for Using m Discrete Intervals.

A schematic showing important terms in the mass balance is shown in Figure 12. The conservation of mass for the *saturated region* can be written as

$$pA_d - ETA_d - Q_d - Q_b - Q_{DS} = \frac{d(\phi_d \bar{z} A_d)}{dt} \tag{70}$$

where p is the percolation rate, L is an effective length of the tile, 2S is the spacing between tile lines, Q_d is the discharge rate in tile lines (L^3/T), Q_b is the base flow rate to nearby streams, Q_{DS} is the deep seepage flow rate, ϕ_d is the drainable porosity, A_d is the subsurface drained area defined as 2SL, and $\bar{z}$ is the mean water table height above the centerline of the drain.

We will assume that $Q_b + Q_{DS}$ is negligible compared to Q_d. We simplify using $\bar{z} = \xi H$ and $\phi_{da} = \phi_d A_d$ to obtain

$$Q_{perc} - Q_{ET} - Q_d = \phi_{da} \frac{d(\xi H)}{dt} \tag{71}$$

A numerical approximation to Equation 70 for a daily time step can be written as

$$\Delta V_{perc} - \Delta V_{ET} - \left(\frac{Q_{d,s} + Q_{d,e}}{2} \right) \Delta t = \phi_{da} \, \xi \, (H_e - H_s) \tag{72a}$$

where ΔV_{perc} and ΔV_{ET} are the daily percolation and evaporation volume The subscripts s and e refer to the values at the start and end of the day, respectively. By lumping the known terms together, we further simplify as

$$\phi_{da} \, \xi \, H_e + \frac{C_p \hat{Q}_{d,e} \Delta t}{2} = \chi = \Delta V_{perc} - \Delta V_{ET} - \frac{Q_{d,s} \Delta t}{2} + \phi_{da} \xi H_s \tag{72b}$$

where χ are the known terms from WEPP simulations or from values obtained from the previous time step. To simplify computations, the adjustment for downline

pressure will be based on the previous time step value.

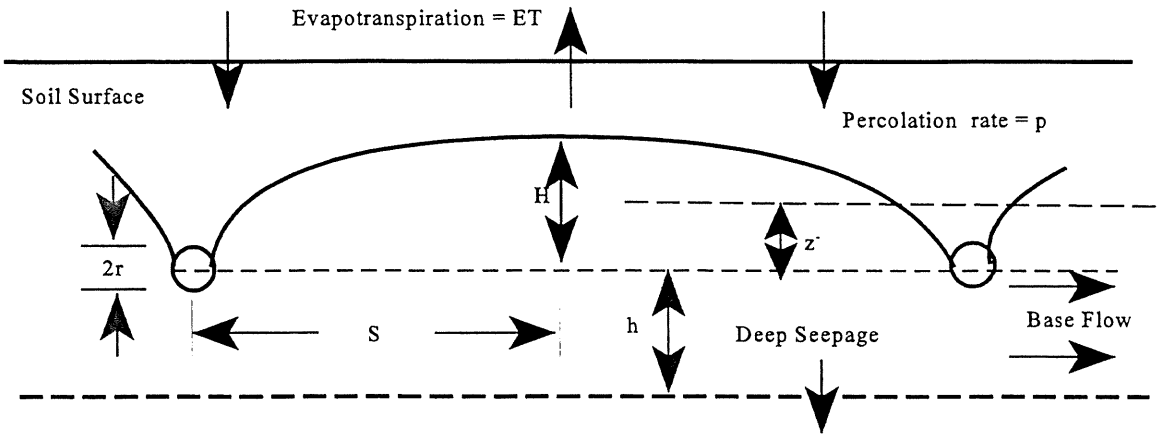

Figure 12. Definition Schematic for Mass Balance Formulation.

Solution Using Kirkham Method

For the Kirkham Method, we have the following relationship between discharge and H,

$$H_e = 2S \frac{J_K \hat{Q}_{d,e}}{K_1 A_d - \hat{Q}_{d,e}} = l_s \frac{J_K \hat{Q}_{d,e}}{K_1 A_d - \hat{Q}_{d,e}} \tag{73}$$

where l_s will be used to indicate lateral spacing between tile lines.

By substituting this relationship into the conservation of mass, we obtain,

$$l_s \phi_{da} \xi \hat{Q}_{d,e} J_K + K_1 A_d C_p \hat{Q}_{d,e} \frac{\Delta t}{2} - C_p \hat{Q}_{d,e}^2 \frac{\Delta t}{2} = \chi K_1 A_d - \chi \hat{Q}_{d,e} \tag{74a}$$

or

$$\hat{Q}_{d,e}^2 C_p \frac{\Delta t}{2} - (\chi + l_s \phi_{da} \xi J_K + K_1 A_d C_p \frac{\Delta t}{2}) \hat{Q}_{d,e} + \chi K_1 A_d = 0 \tag{74b}$$

which can be solved using the quadratic equation as

$$\hat{Q}_{d,e} = \frac{b \pm \sqrt{b^2 - 2 C_p \Delta t K_1 A_d \chi}}{C_p \Delta t} \tag{74c}$$

where

$$b = \chi + l_s \phi_{da} \xi J_K + K_1 A_d C_p \frac{\Delta t}{2} \tag{75}$$

For the special case when $\chi = 0$, the outflow is zero and therefore the negative square root term is the proper solution, or

$$\hat{Q}_{d,e} = \frac{b - \sqrt{b^2 - 2C_p \Delta t K_1 A_d \chi}}{C_p \Delta t} \tag{76}$$

The value of H_e can then be computed by Equation 73.

A summary of the computational steps for the Kirkham Method is given below.

(1) For each depression compute h' and ξ using Equations 59 and 68, respectively. Compute $\phi_{da} = \phi_d A_d$.

(2) Select initial H and H_p and compute initial flow rates using Equations 46c and 61 with adjustment for downline pressure given by Equation 62.

(3) Determine the percolation and evapotranspiration values for the time step and compute χ defined by Equation 72b.

(4) For $0 < H_s$ and $H_p < H_s + h'$, flow rate at the end of the time step, without adjusting for downline pressure, is computed using Equation 76 and the water table height at the end of the time step is computed by Equation 73.

(5) For $H_s < 0$ and $H_s + h' < H_p$, outflow rate at the end of the time step is computed as

$$\hat{Q}_{d,e} = 0 \quad \text{and} \quad H_e = \frac{\chi}{\phi_{da} \xi} \tag{77}$$

(6) The outflow rate is adjusted for downline pressure and the computational steps of Steps #3 through #6 are repeated for each time step.

Solution Using the Drainage Coefficient Method

For drainage coefficient method, we have the following relationship between tile flow and H

$$\hat{Q}_d = \hat{Q}_{dm} \frac{H\,[D_c E_f + (K - D_c E_f) H_m^2]}{H_m\,[D_c E_f + (K - D_c E_f) H_m H]} = C_{dc} \left(\frac{H}{\alpha + \beta H} \right) \tag{78}$$

where

$$C_{dc} = \hat{Q}_{dm} \frac{\alpha + \beta H_m}{H_m} \tag{79a}$$

and

$$\alpha = D_c E_f \quad \text{and} \quad \beta = D_c E_f H_m \tag{79b}$$

The above equation can be rearranged for use in the mass balance as

$$H_e = \frac{\alpha \hat{Q}_{d,e}}{C_{dc} - \beta \hat{Q}_{d,e}} \tag{80}$$

By substituting this relationship into the conservation of mass, we obtain,

$$\phi_{da}\,\xi\,\alpha\,\hat{Q}_{d,e} + C_{dc}\,C_p\,\hat{Q}_{d,e}\,\frac{\Delta t}{2} - \beta\,C_p\,\hat{Q}_{d,e}^2\,\frac{\Delta t}{2} = C_{dc}\,\chi - \beta\,\chi\,\hat{Q}_{d,e} \tag{81a}$$

or

$$\hat{Q}_{d,e}^2\,\frac{C_p\,\beta\,\Delta t}{2} - (\beta\chi + \phi_{da}\,\xi\,\alpha + C_{dc}\,C_p\,\frac{\Delta t}{2})\,\hat{Q}_{d,e} + C_{dc}\,\chi = 0 \tag{81b}$$

which can be solved using the quadratic equation as

$$\hat{Q}_{d,e} = \frac{b - \sqrt{b^2 - 2\,C_p\,\beta\,\chi\,\Delta t\,C_{dc}}}{C_p\,\beta\,\Delta t} \tag{82}$$

where

$$b = \beta\chi + \phi_{da}\,\xi\,\alpha + C_{dc}\,C_p\,\frac{\Delta t}{2} \tag{83}$$

Once again the negative square root term is needed to obtain the proper solution for the case when $\chi = 0$.

A summary of the computational steps for the Drainage Coefficient Method is given below.

(1) Estimate the midpoint distance between tile lines using Equation 58, which requires an initial estimate of the distance given by Equation 56. Determine H_m using Equation 49. Estimate the length of the lateral line using

$$L_m = \frac{\sqrt{A_w\,A_f}}{2} \tag{84}$$

(2) For each depression compute h' and ξ using Equations 59 and 68, respectively. Compute $\phi_{da} = \phi_d\,A_d$.

(3) Select initial H and H_p and compute initial flow rates using Equations 52 and 61 with adjustment for downline pressure given by Equation 64.

(4) Determine the percolation and evapotranspiration values for the time step and compute χ defined by Equation 72b.

(5) For $0 < H_s$ and $H_p < H_s + h'$, flow rate at the end of the time step, without adjusting for downline pressure, is computed using Equation 82 and the water table height at the end of the time step is computed by Equation 80.

(6) For $H_s < 0$ and $H_s + h' < H_p$, outflow rate at the end of the time step is computed as

$$\hat{Q}_{d,e} = 0 \quad \text{and} \quad H_e = \frac{\chi}{\phi_{da}\,\xi} \tag{77}$$

(7) The outflow rate is adjusted for downline pressure and the computational steps of Steps #3 through #6 are repeated for each time step.

Evaluation of Modeling Routines

Introduction

The evaluation of models is typically done by comparing predicted values to those observed in a laboratory or field experiment. It should be recognized, however, that there is uncertainty associated with observed data, which ideally should be represented by probability distributions (Haan et al, 1993). In addition, it is difficult to determine whether differences between predicted and observed values are the result of an inadequate model or the result of inappropriate estimation of input parameters. The methodology used to estimate the parameters is therefore an important component of model evaluation. The sensitivity of the model to input parameters plays an important role in selecting proper values and in determining the impact of possible errors in these values. Despite these limitations, some form of critical evaluation procedure is required to maintain the integrity of modeling and to ensure that the increasing use of models does not result in misinformation (Addiscott et al, 1995).

The project evaluated the accuracy of the WEPP model for Minnesota conditions. The evaluation includes the analysis of predicted and observed meteorological, snowmelt, runoff, and erosion data.

Climate variables

Introduction

The accuracy of the weather prediction algorithms of the WEPP model is evaluated for different sites in Minnesota. Observed maximum, minimum, and dew-point temperatures and precipitation characteristics are compared to those predicted by the WEPP model. Since precipitation is the driving force for runoff and soil loss, accurate simulation of this variable is particularly important. An important factor in selecting test locations is the minimum period of record to determine representative statistics of the observed data. For this study the minimum period of record is 25 years.

Daily weather variables for Minnesota were obtained via the Internet from the National Climatic Data Center (NCDC) in Asheville, North Carolina. The daily weather data from the NCDC, typically collected from airports across the state, include maximum and minimum temperature, maximum and minimum relative humidity, precipitation, percent sun, and average wind speed and direction. Hourly precipitation values for Minneapolis, St. Cloud, International Falls, Rochester, and Duluth were obtained from Midwest Climate Center in Champaign, Illinois. The fifteen-minute precipitation data was obtained from Hydrosphere Incorporated, Colorado Springs, Colorado.

Meteorological stations in Minnesota that had at least 25 years of 15-minute or hourly precipitation data were considered as possible test sites. From these stations, test sites

were randomly chosen from different geographic regions of Minnesota. Figure 13 shows the location of the test sites used to evaluate the meteorological algorithms of the WEPP model.

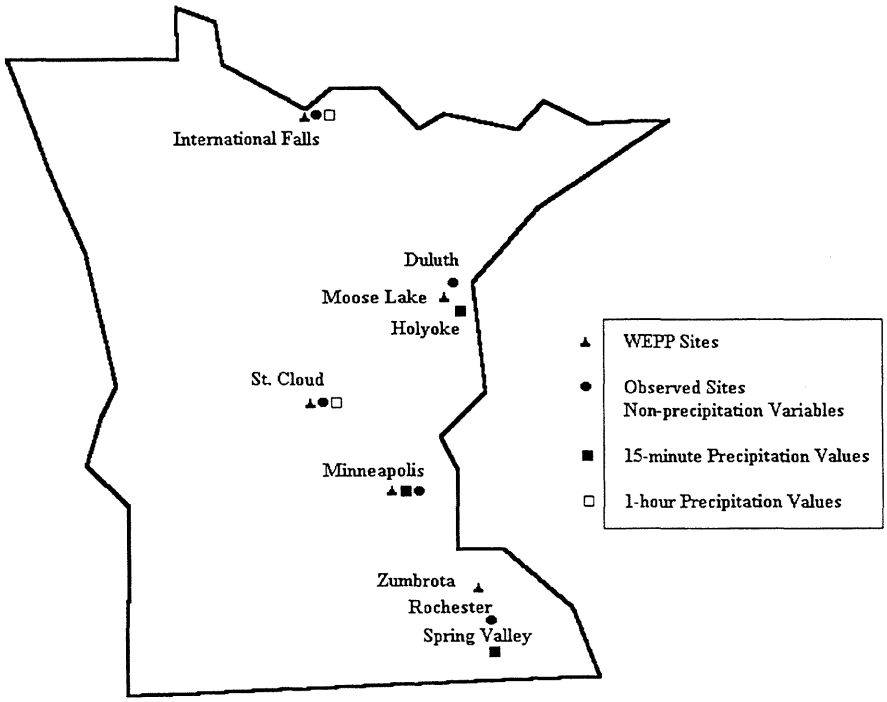

Figure 13. Locations of Meteorological Stations Used to Evaluate Climate Variables.

For each observed data location, a WEPP weather generator location was also selected. The user of WEPP may choose this site by name or by using the location of the nearest site for a given latitude and longitude. Below is a list of the observed sites and their corresponding WEPP locations.

Table 2. Observed Sites and Their Corresponding WEPP Locations.

Observed Data Location	Corresponding WEPP Location
Minneapolis	Minneapolis
Duluth	Moose Lake
Rochester	Zumbrota
St. Cloud	St. Cloud
International Falls	International Falls

The daily weather set of WEPP model was simulated using a record length of 990 years. Although 30 years is used by the National Weather Service to define average or normal conditions, Baffuat et al. (1996) showed that 30 years of data are not enough to obtain stable WEPP estimate of average soil loss. They concluded that one should choose a minimum period of 200 years.

Non-Precipitation Weather Variables

In the WEPP model, Monte Carlo simulation techniques are used to simulate maximum, minimum, and dew-point temperatures by assuming that these variables are normally distributed. For each day, a random standard normal deviate is obtained for each variable. The daily temperature values are obtained as

$$T = \bar{T} + s_T \nu B \tag{85}$$

where T is the temperature (maximum, minimum, or dew point), $\bar{T}$ is the mean monthly temperature, s_T is the standard deviation, ν is a random standard normal deviate, and B is parameters that allows the standard deviation to change with the precipitation state of the previous day.

Predicted and observed average daily maximum, minimum, and dew-point temperatures for Minneapolis, Minnesota are shown in Figures 14, 15, and 16. The predicted and observed means and standard deviations of annual temperature values are given in Table 3. Also shown in these figures are the predicted and observed temperatures one standard deviation greater than and less than the mean. The use of the monthly mean temperatures in Equation 85 is clearly shown by the horizontal line segments between the start and end dates of each monthly period.

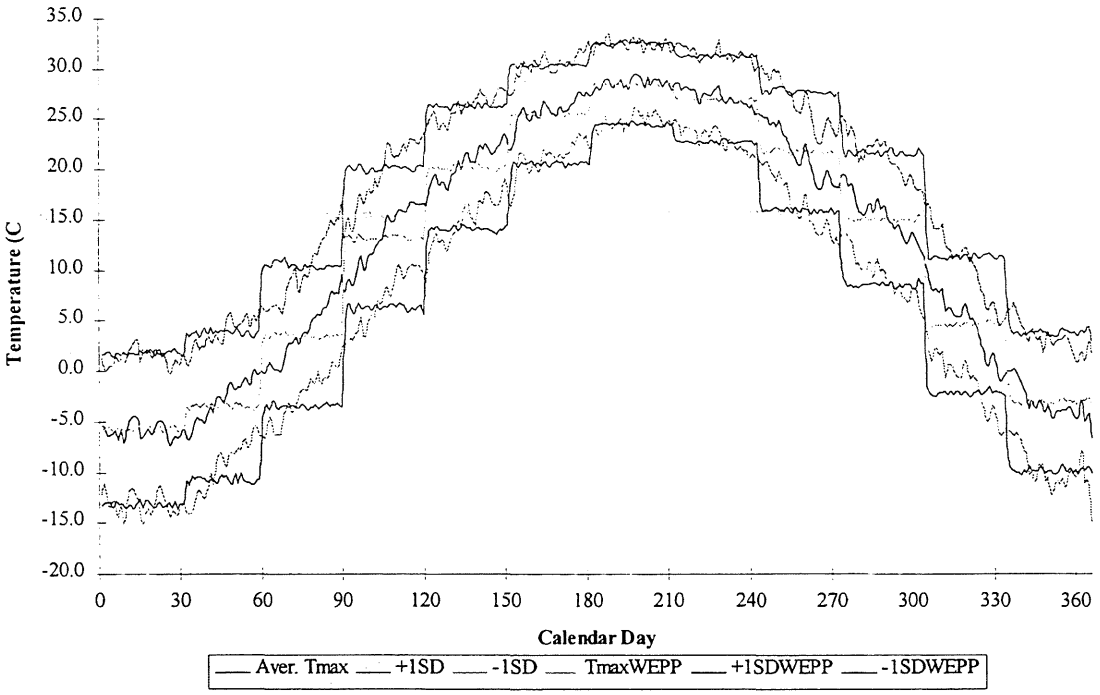

Figure 14. Observed Average Daily Maximum Temperature, Minneapolis, Minnesota

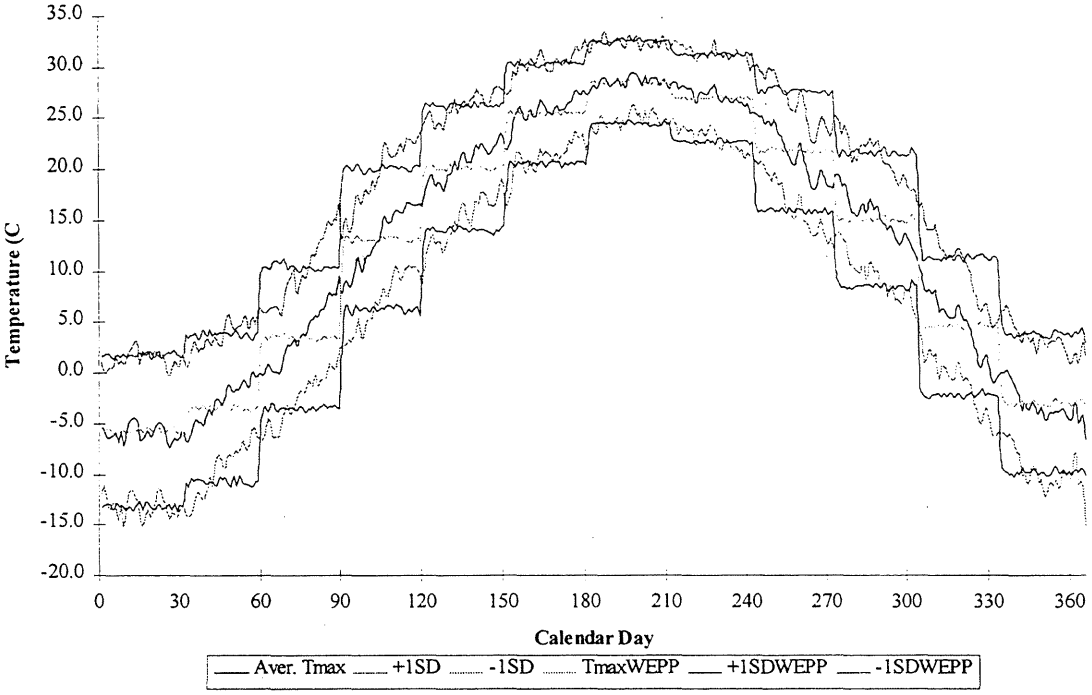

Figure 15. Observed Average Daily Maximum Temperature, Minneapolis, Minnesota.

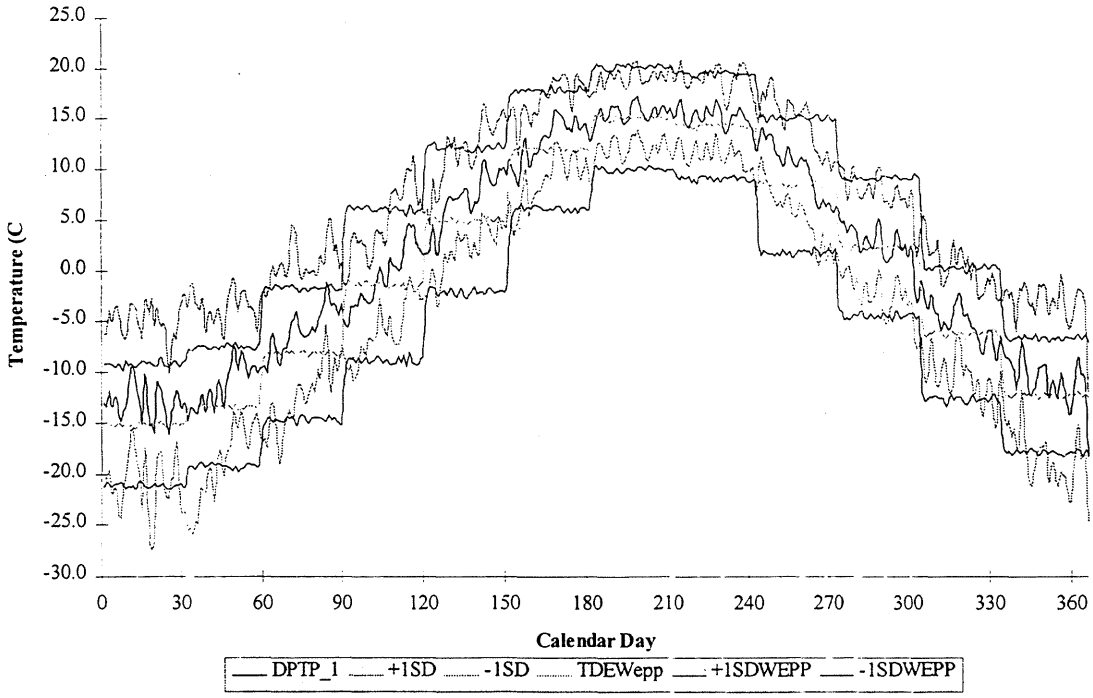

Figure 16. Observed Average Daily Dew-Point Temperature, Minneapolis, Minnesota.

With the possible exception of dew-point temperature, the predicted and observed values shown in Figures 14 through 16 are very good. This is not surprising because the predictive values obtained by Equation 85 should maintain the mean and standard deviation of the observed data set. Differences between predicted and observed statistics for the dew-point temperature probably indicate that the WEPP parameters were derived form a different set of observed values.

Table 3. Means and Standard Deviations for Minneapolis, Minnesota.

	Observed Data °C		**WEPP Data °C**	
	Mean	**Stdev**	**Mean**	**Stdev**
Maximum Temp.	12.42	12.34	12.30	12.10
Minimum Temp.	1.95	11.38	1.30	11.63
Dew-Point Temp.	1.46	10.40	0.11	10.58

Quartiles represent a better test of the simulation accuracy because they are not inherently preserved by the mathematical form of Equation 85. These statistics can be used to access possible differences in the shape of the probability density functions (pdf) corresponding to predicted and observed values. A dimensionless measure is obtained by dividing the 25, 50, and 75 percentiles by observed yearly average value. The dimensionless quartiles for maximum, minimum, and dew-point temperatures for five sites are shown in Figures 17, 18, and 19. Since the trendline is nearly a one to one relationship, the distribution curves of the predicted values are similar to those obtained from the observed data set.

Skew coefficients can also be used to compare the shape of the predicted and observed pdfs. Because it is based on a cubed difference between values and the mean, it is more sensitive to extreme events. If the observed data have similar skew coefficients as those simulated, it is likely that the pdfs are of similar shape and therefore supports the use of the model for extreme events. The skew coefficients obtained from the WEPP model are plotted as a function of observed values for all five sites in Figure 20. The skew coefficients are small and are in good agreement with each other. These results are consistent with those obtained with the quartile analysis. They support the use of Equation 85 to simulate temperature data.

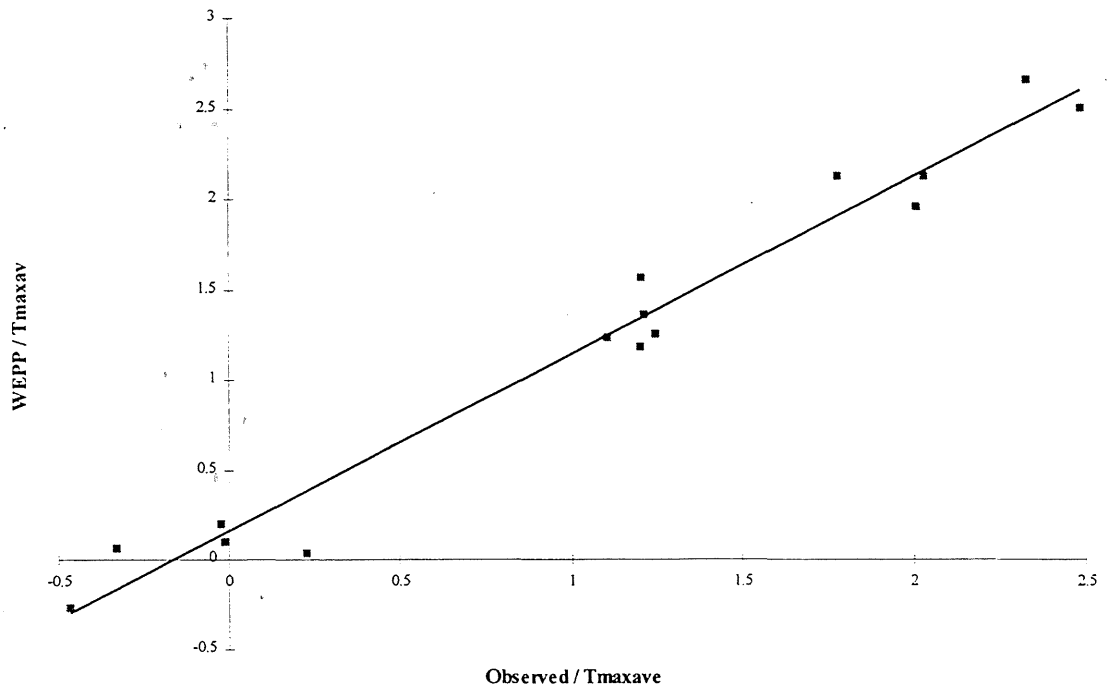

Figure 17. Maximum Temperatures for Quartiles of 0.25, 0.5, and 0.75

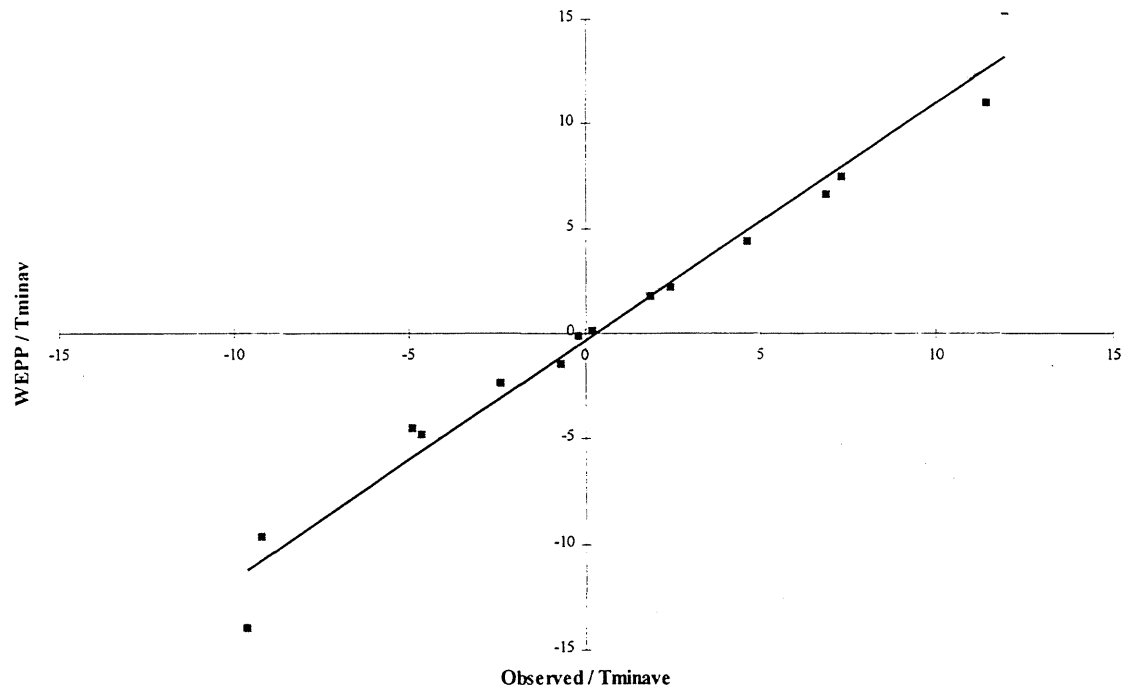

Figure 18. Minimum Temperatures for Quartiles of 0.25, 0.5, and 0.75.

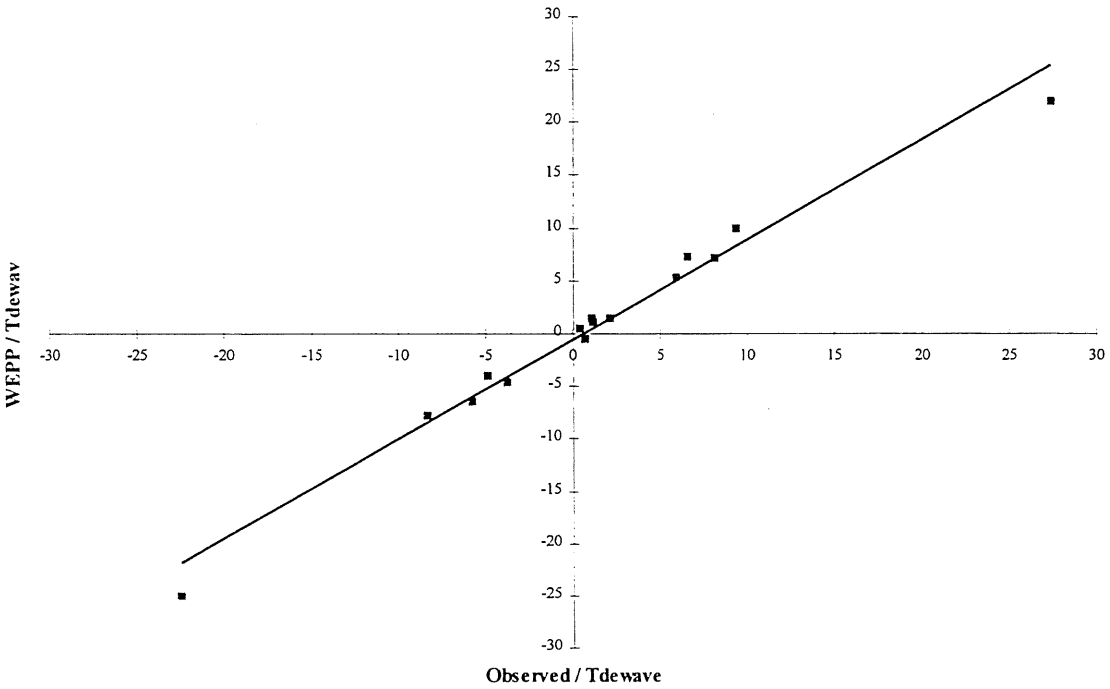

Figure 19. Dew-Point Temperatures for Quartiles of 0.25, 0.5, and 0.75.

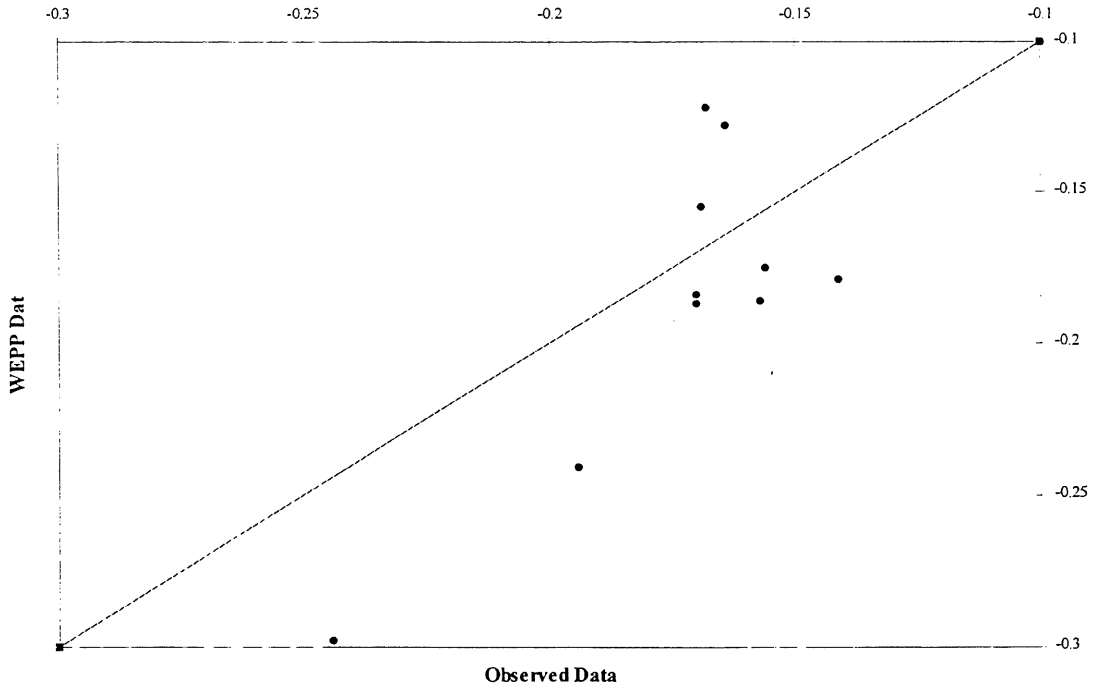

Figure 20. Skew Coefficients for Yearly Maximum, Minimum, and Dew-Point Temperatures.

Precipitation Weather Variables

The WEPP daily precipitation model is a combination of methods used in both the SWRRB and EPIC models. It is based on a two-state Markov chain using transitional probabilities for wet and dry days (Arnolds et al., 1990). Monthly probabilities are used in WEPP and are available at numerous sites in the United States. A random number is then used to determine whether a day is wet or dry.

For a wet day the precipitation depth is calculated using the following approximation to the gamma distribution:

$$z_g = \frac{2}{C_s}\left(1 + \frac{C_s u}{6} - \frac{C_s^2}{36}\right)^3 - \frac{2}{C_s} \tag{86a}$$

and

$$P = \bar{x} + z_g s \tag{86b}$$

where P is the rainfall depth, u is the standard normal variate, $\bar{x}$ is the mean, s is the standard deviation, and C_s is the skew coefficient. For each month the mean, standard deviation, and skew coefficient are calculated. If the temperature is below or equal to zero degrees Celsius, the precipitation is taken as snow; otherwise, it is rain.

The first step in distributing the total precipitation depth is to determine the duration of the storm. The method in WEPP is based on the algorithm of Arnold et al. (1990) in the SWRRB model. Arnold et al. assumed that daily storm duration is exponentially related to mean monthly duration. The following equation then determines the storm duration:

$$D = \frac{9.214}{-\ln(1 - rl)} \tag{87}$$

where D is the event duration in hours, and rl is a dimensionless parameter from a gamma distribution of the half-hour monthly average precipitation amounts. Peak storm intensity used in the WEPP weather generator is based on the algorithm of Arnold and Williams (1989). Peak storm intensity is defined as

$$rp = -2P\ln(1 - rl) \tag{88}$$

where rp is the peak storm intensity, and P is the total storm amount. The rl term is as previously defined.

The WEPP model uses a double exponential function proposed by Arnold and Williams (1989) to distribute storm depths. In comparison to the simple triangle distribution, the double exponential function allows more characteristics of the storm to be incorporated into the pattern.

The WEPP weather generator is evaluated by comparing the depth-duration frequencies (DDF) from its rainfall pattern with the DDF values obtained from the observed data sets. The DDF values of the observed data are also compared to those

of TP-40 (Herschfield, 1961)/HYDRO-35 (Frederick et al., 1997). The observed and WEPP data sets are analyzed to find the largest 0.25, 0.5, 1, 2, 3, 6, 12, 24 hour rainfall depths for each year. Extreme value type I statistics are used to determine the rainfall depths for the 2, 10, 25, and 100 year return periods. The extreme value type I statistic is widely used to represent rainfall depth duration frequency studies (Haan, 1977). The rainfall depths are adjusted for the differences between annual and partial duration series. A factor of 1.136 and 1.0101 for the 2-year and 10-year return periods, respectively, are used to adjust annual series to partial duration series (Haan, 1977). The adjustment factor for return periods greater than 10 years is near unity.

In Figure 21, the observed depth-duration frequencies curves for Rochester, Minnesota are compared to those obtained using HYDRO-35 / TP-40. As shown by Figure 21, the observed and TP-40 / HYDRO-35 values are fairly close for the 1-hour and 24-hour durations, but the observed values are noticeably different for the other durations. The observed depths for the 15 minute and 30 minute are less reliable because of the limited observations of the data set. Differences in other durations likely reflect the limitations of the United States Weather Bureau chart for determining depths for the 2, 3, 6, and 12 hour durations. The observed site specific data are more reliable than the generalized graphs used in TP-40 and HYDRO-35.

The DDF curves obtained from the observed and WEPP data sets are shown in Figure 22. The 24-hour values are fairly close but the predicted depths for the other durations are less accurate.

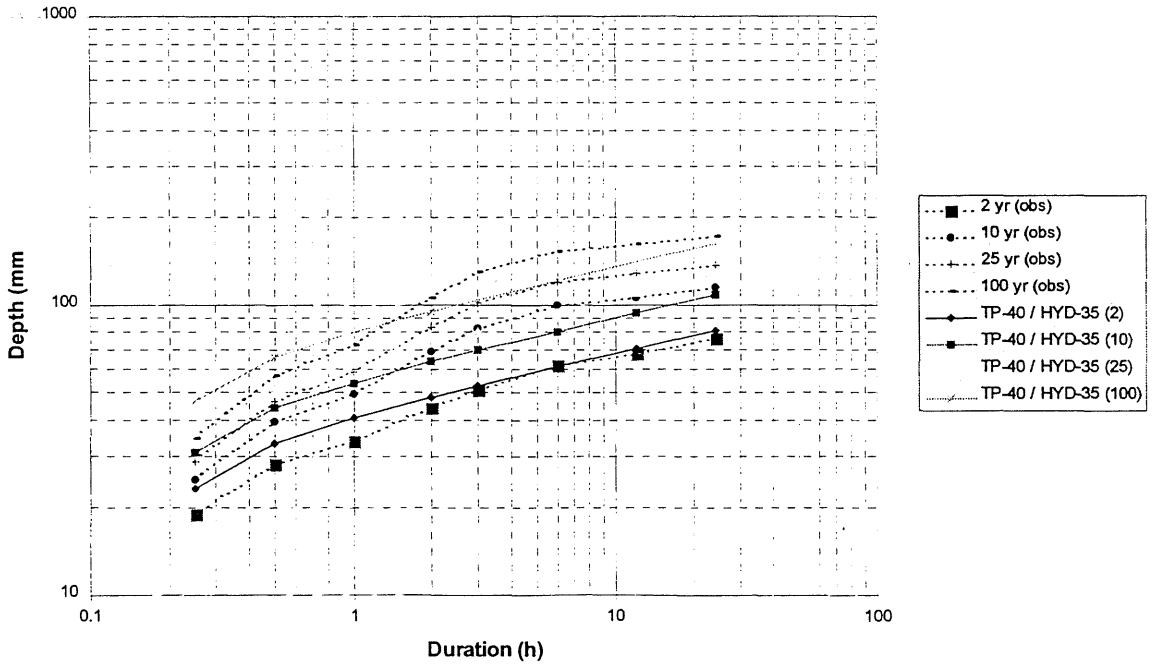

Figure 21. Observed data, TP-40 / HYDRO-35 DDF Values for Rochester, Minnesota.

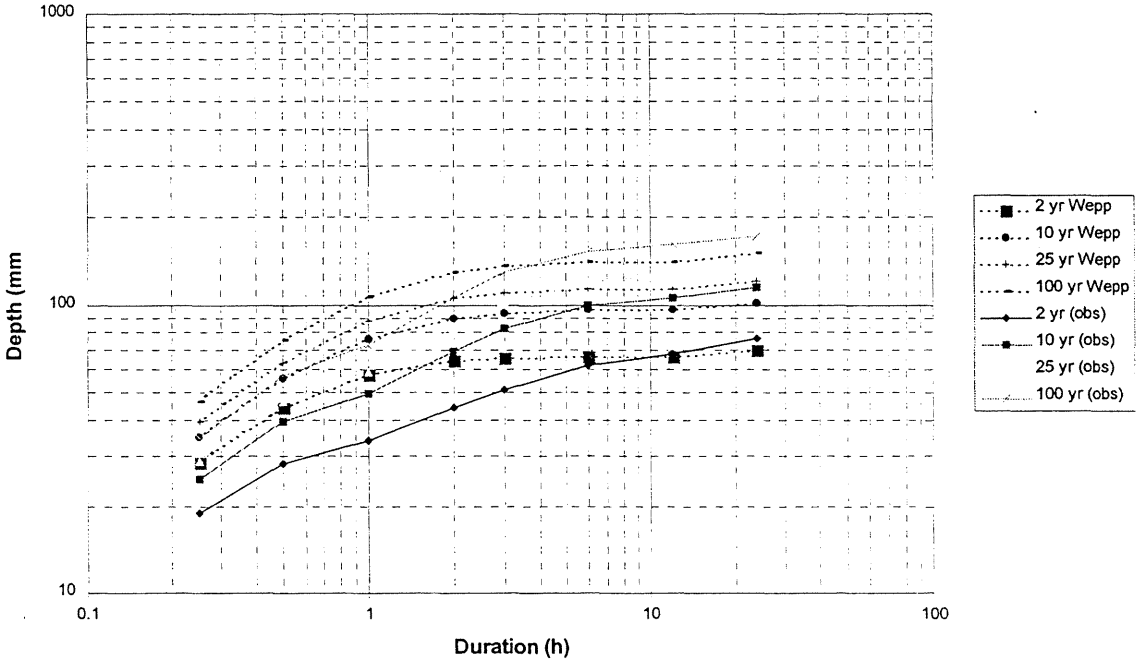

Figure 22. Observed data and WEPP DDF Values for Rochester, Minnesota.

An alternative of representing the result of Figure 22 is to compare directly the return periods for the data set. For the extreme value type I distribution, the depth for a given return period (T) is defined as

$$x = w + \frac{-\ln[-\ln(1-1/T)]}{q} \tag{89a}$$

and the return period for a given depth as

$$T = \frac{1}{1 - \exp(-\exp(-q(x-w)))} \tag{89b}$$

where q and w are statistics that can be easily be calculated from data. Different values are obtained for the observed and WEPP data sets. For the observed data set, the depth is computed for different return periods using Equation 89a. The return period of WEPP data set corresponding to this depth is then computed using Equation 89b. The results of these steps are shown in Figures 23, 24, and 25 for the 15-minute, 1-hour and 24-hour durations, respectively. All figures are for Duluth, Minnesota.

For depths corresponding to a duration of 24-hours, the return periods of WEPP are in agreement with observed values. For a duration of 15 minutes, WEPP severely underpredicts the return period. For example, the observed depth corresponding to a 50 year return period has only a 8 year return period using the WEPP data. These results suggest that the WEPP model is reasonably accurate in the predicting daily precipitation depth. Alternative algorithms are, however, needed to define the rainfall hyetograph.

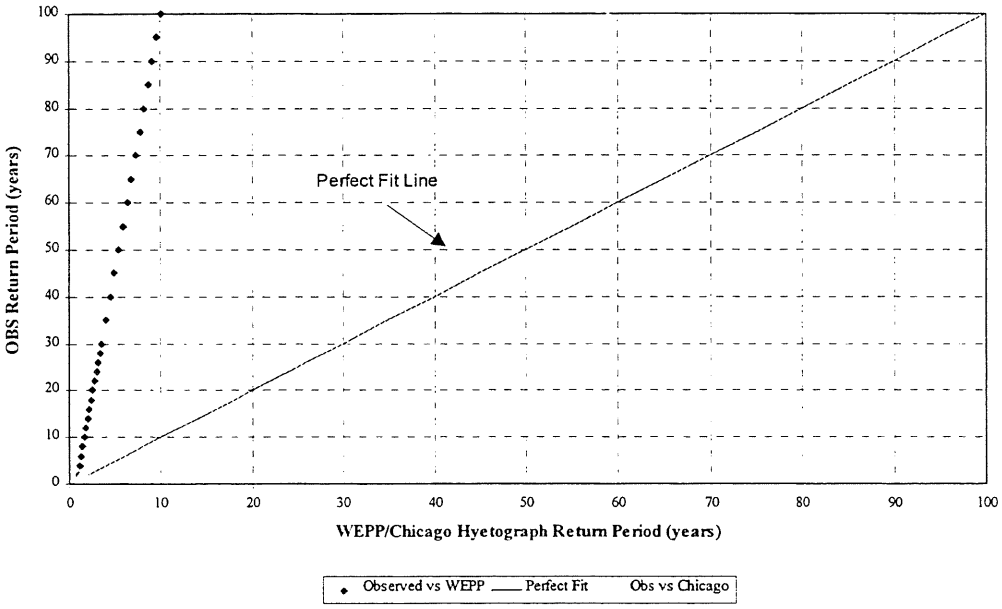

Figure 23. WEPP vs Observed Data for Return Periods of 15 Minute Duration.

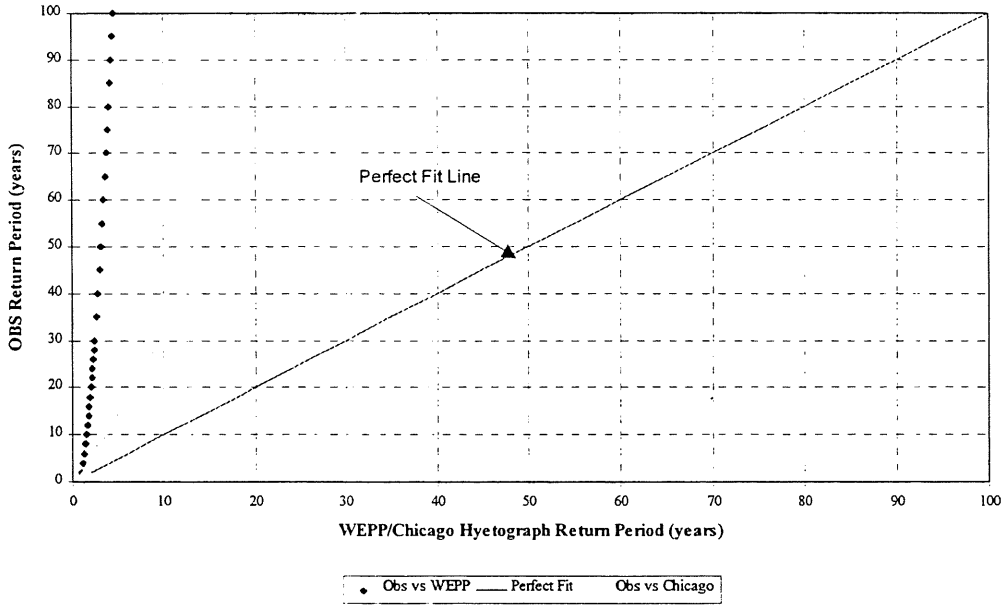

Figure 24. WEPP vs Observed Data for Return Periods of 1-hour Duration.

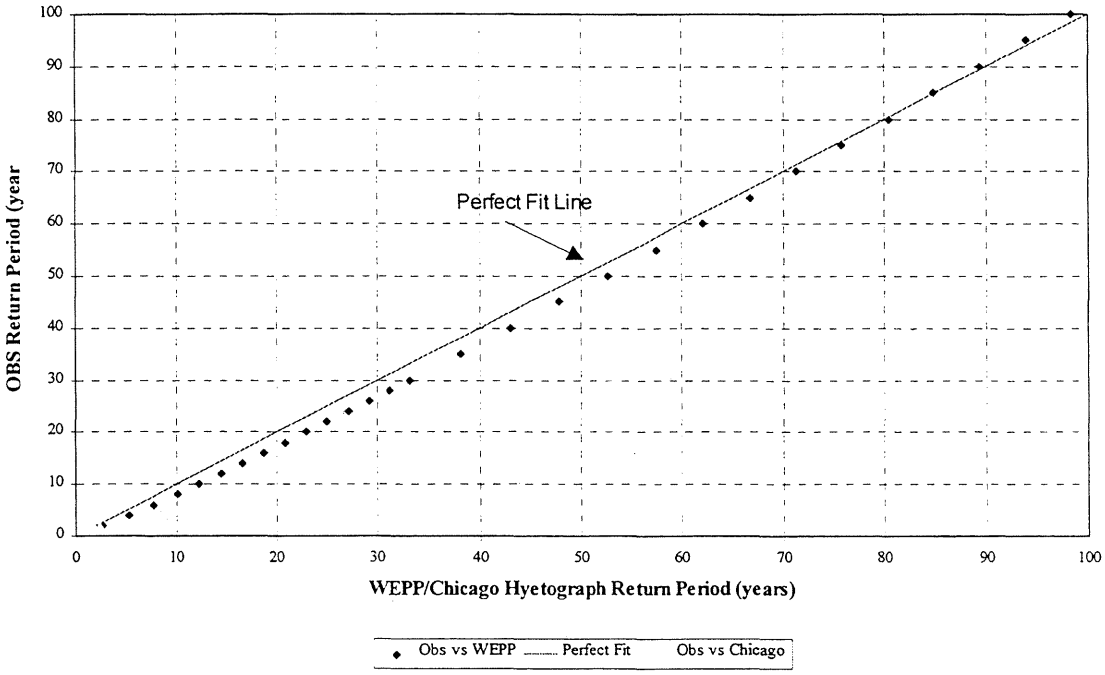

Figure 25. WEPP vs Observed Data for Return Periods of 24-hour Duration.

Snowmelt

Modeling approach

The algorithm for modeling snowmelt of the WEPP model was tested using snow depth and snow density measurements throughout the winters of 1993-94 and 1994-95 at a research site in South Central Minnesota. Meteorologic data measured at the site included solar radiation, net radiation, air temperature, wind speed, relative humidity, and precipitation.

The WEPP model predicts snowmelt on a daily basis using the following equation:

$$M = [0.00254R(1-0.01F)-0.84(1-N_c)(1.0-0.01F)+0.008F) + 0.0268v_2(1-0.008F)(0.18T_x+1.40T_d) + (T_x+T_m)(0.0225+0.248P_d)](0.0254) \quad (90)$$

where M is the snowmelt (m), R is the estimated radiation on a sloping surface expressed in langleys (L), F is the forest cover (%), T_x is the daily maximum temperature (°C), N_c is the estimated cloud cover (dec %), v_2 is the mean daily wind speed measured at a height of 2 m (m s^{-1}), T_d is the dewpoint temperature (°C), and P_d is the mean daily precipitation (m). The first term in the above equation is multiplied by the quantity $(0.36T_x+1)$ when $-3°C \leq T_x < 0°C$.

Incoming solar radiation was cumulated during the day. The mean daily dew point temperature was calculated using mean daily air temperature and mean daily relative

humidity. Saturated vapor pressure (kPa) at a given temperature was calculated using the following equation.

$$e^{\circ} = \exp\left[\frac{16.78T - 116.9}{T + 237.3}\right] \tag{91}$$

The estimated cloud cover was obtained from the following equation used in the WEPP model

$$N_c = \frac{\left(1 - \frac{R_m}{R_c}\right)}{0.7} \tag{92}$$

For the term R_m, which was defined as the mean measured daily solar radiation, the total daily measured solar radiation was used. The term R_c, defined as the potential clear sky radiation on a horizontal surface (L), was calculated using the assumption that the solar constant equaled 117.5 (MJ m^{-2} d^{-1}) and that 30% of the extraterrestrial solar radiation R_A was reflected by the Earth's atmosphere on a clear day. Extraterrestrial solar radiation (MJ m^{-2} d^{-1}) on a horizontal surface is given as

$$R_A = 117.5\left[h_s \sin\lambda \sin\delta + \cos\lambda \cos\delta \sin(h_s)\right]/\pi \tag{93}$$

where λ is latitude in radians and δ is solar declination in radians calculated

$$\delta = \sin^{-1}\{0.39785 \sin[4.869 + 0.0172J + 0.03345 \sin(6.224 + 0.0172J)]\} \tag{94}$$

where J is the day of the year and h_s is the half daylength given by

$$h_s = \cos^{-1}(-\tan\delta \tan\lambda) \tag{95}$$

By using these expressions for R_A, the potential clear sky radiation on a horizontal surface was calculated as

$$R_c = 0.7 R_A \tag{96}$$

In the WEPP subroutine, snowmelt uses the estimated radiation on a sloping surface. In order to test the equation at various locations, the measured radiation was adjusted for different slopes using

$$R = R_H \frac{\cos(I)}{\sin(\Phi)} \tag{97}$$

where R_H is the measured or observed radiation of the horizontal surface, I is the solar incidence angle, and ϕ is the solar altitude or elevation angle, related to the zenith angle θ as

$$\Phi = \frac{\pi}{2} - \theta \tag{98}$$

and the zenith angle is calculated from

$$\theta = \cos^{-1}\left[\sin\lambda \sin\delta + \cos\lambda \cos\delta \cos 0.2618\,(t - t_o)\right] \tag{99}$$

where t_o is the time to solar noon and t is the time of day (for this study the adjustment to the measured horizontal radiation for sloping conditions was calculated at solar noon). The time to solar noon was calculated from

$$t_o = 12 - LC - ET \quad (100)$$

where *LC* is the longitude correction which is +4 minutes, or +1/15 hour for each degree the location is east of the standard meridian and -1/15 hour for each degree west of the standard meridian. The solar incidence angle*(I)* is defined as

$$I = \cos^{-1}\{\sin(\omega)\cos(\Phi)\cos(a-(a_s+\pi)) + \cos(\omega)\sin(\Phi)\} \quad (101)$$

where ω is the land slope in radians, a_z is the azimuth angle (radians), and a_s is the aspect (radians) where a north facing slope is at an aspect of 0°.

The azimuth angle (a_z) is defined as

$$a_z = \sin^{-1}[-\frac{\cos\delta}{\cos\Phi}\sin[\pi(t-t_o)/12]] \quad (102)$$

Accuracy of snowmelt algorithm

There were two thawing periods of interest in 1994. The first thaw started on day 2/15 and continued until day 2/20; the second thaw started on day 2/29. On day 2/22 the site received approximately 20 cm of snow. The depth varied at the site depending upon drifting and topographic position.

The predicted and observed depths for the east-facing field and the west-facing wooded areas are shown in Figures 26 and 27. For both thawing periods, the snowmelt predicted by WEPP was substantially smaller than that observed. For example, the snow had completely melted 10 days earlier than that predicted by the WEPP equations for the second thaw period.

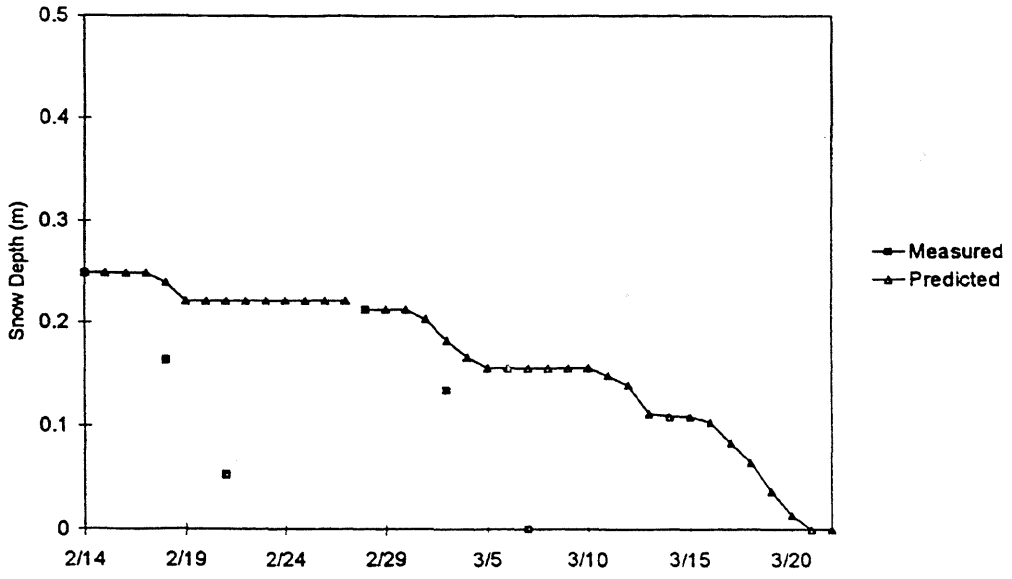

Figure 26. Predicted and Observed Snow Depths for 1994, East Facing Field.

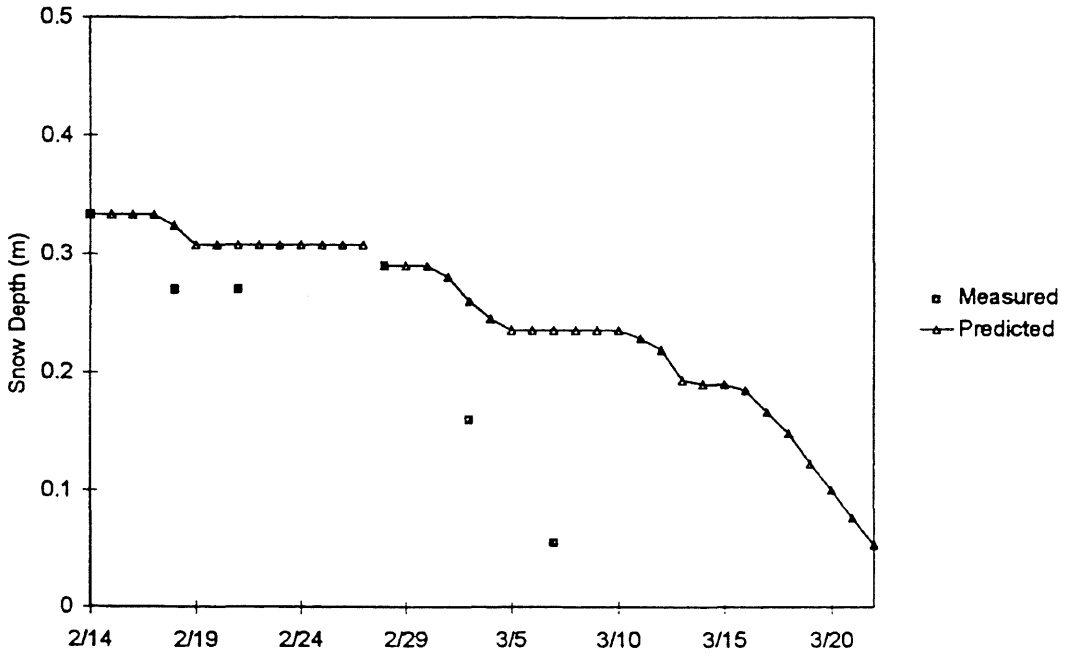

Figure 27. Predicted and Observed Snow Depths for 1994, West Facing Field.

There were also two thaw periods of interest in 1995. The first thaw was a slow melt starting on day 2/11 and continued through 3/10. Measured solar radiation was low during and air temperatures fluctuated from below freezing at night to above freezing during parts of the day. The second thaw period begins with approximately 15 cm of snow on days 3/6 and 3/7. The air temperature rose dramatically rose on 3/10 resulting in rapid snow melt.

The predicted and observed snow depths for the east-facing field and a north-facing slope are shown in Figures 28 and 29. For the first thaw, the WEPP equation once again underpredicted snow melt. It predicted melting on only two of the days during this period and the predicted melt was less than three centimeters for the whole time period. The measured snow completely melted at every location except the north facing wooded slope. For the second thaw, the predicted snow depth was in good agreement with observed values.

Runoff

Introduction

The accuracy of the WEPP model to predict runoff depth was evaluated for three sites in Minnesota: Lamberton, Easton, and St. James. The Lamberton data set was gathered in October, 1993 and the Easton data set in the summer of 1995 as part of other research projects under the supervision of the senior author. The runoff data for the St. James site were obtained as part of the LCMR project by Dr. E. Calvin Alexander and Ms. Sue Magdalene of the Department of Geology and Geophysics of

the University of Minnesota. The Lamberton experiment was conducted on erosion plots using a rainfall simulator at a constant intensity (Wilson et al. 1994; Leaf, 1994). The Easton site uses erosion plots as well, but the observed runoff is from natural rainfall (Brooks et al , 1994; Brown et al, 1994).

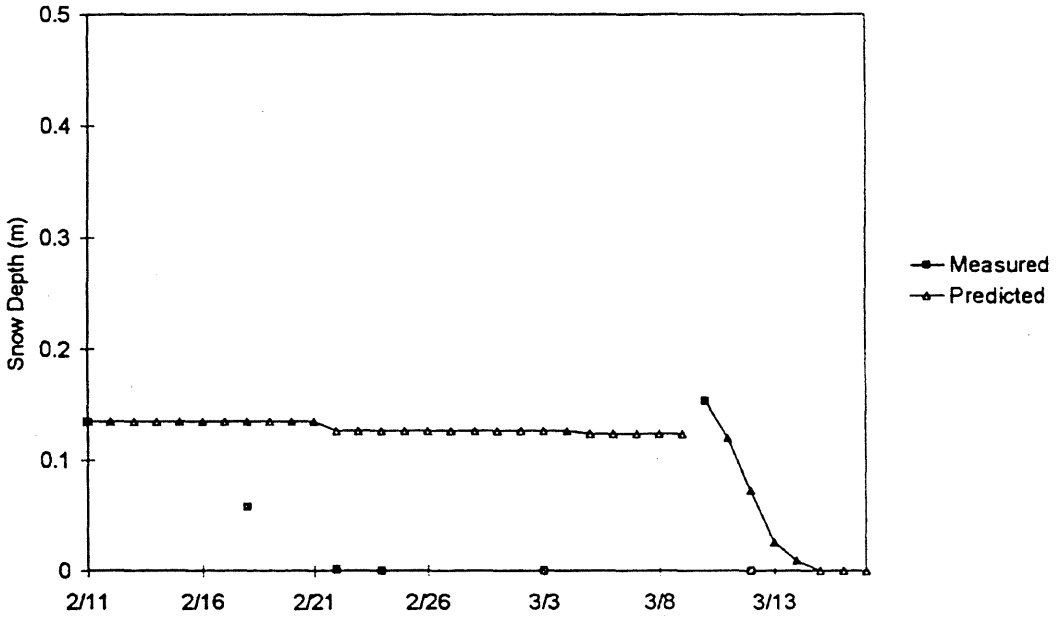

Figure 28. Predicted and Observed Snow Depths for 1995, East Facing Field.

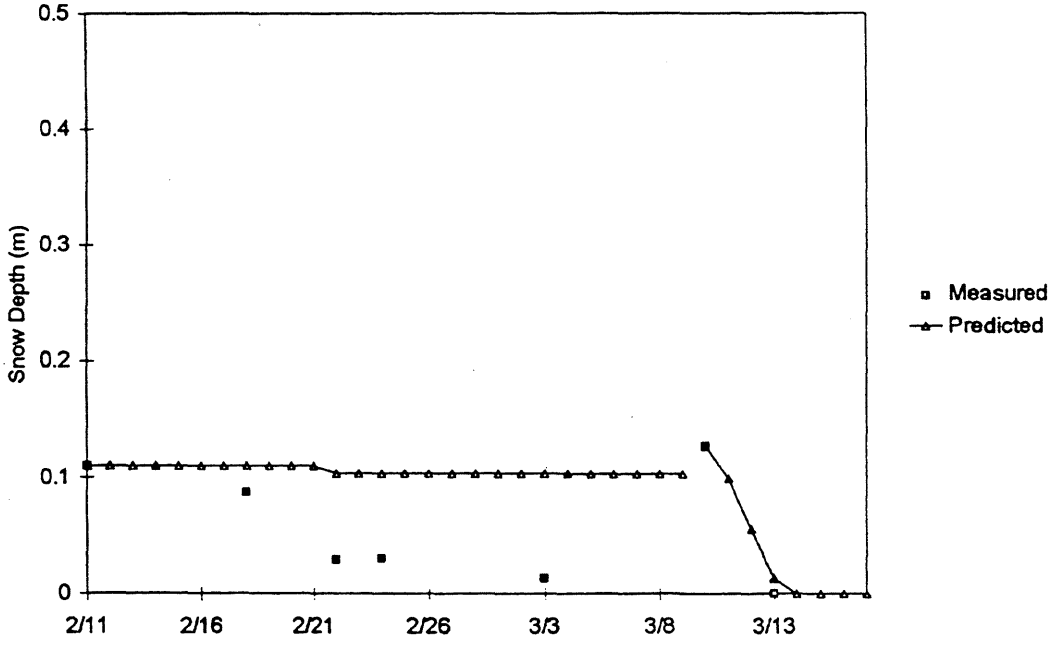

Figure 29. Predicted and Observed Snow Depths for 1995, North Facing Site.

The WEPP model requires four input files to run. They are climate, soil, slope, and management data files. The WEPP model may be used for single storms or continuous mode and for a single hillslope profile or for a small watershed (limited in size to 642 ac). The climate files were built using meteorologic data collected from the sites. Storm information was entered in breakpoint format to run the WEPP model in single storm mode. Soil, slope and management information from the sites were built into a WEPP files (Oduro, 1996).

The model sensitivity to estimated input parameters was determined using a sensitivity analysis. This analysis suggested that runoff was more sensitive to changes in effective hydraulic conductivity than to initial saturation. This was evident both at Lamberton and Easton. At Lamberton, the trend of runoff to increase with increasing with initial saturation and decrease with increasing effective hydraulic conductivity was observed. This simple trend was not observed with the complex time-varying rainfall pattern at Easton.

The following statistics are used in this subsection to assess model accuracy:

$$SSResid = \sum_{i=1}^{n} (O_i - P_i)^2 \tag{103a}$$

$$SSTo = \sum_{i=1}^{n} (O_i - \bar{O})^2 \tag{103b}$$

$$R^2 = 1 - \frac{SSResid}{SSTo} \tag{103c}$$

$$MD = \frac{1}{n} \sum_{i=1}^{n} (O_i - P_i) \tag{103d}$$

$$s_e = \sqrt{\frac{SSResid}{n-2}} \tag{103e}$$

where O_i and P_i are the predicted and observed values, respectively, SSResid is the sum of squared differences between predicted and observed values, SSTo is the total sum of squares, R^2 is the coefficient of determination for the perfect fit line, MD is the mean difference, and s_e is the standard deviation from the perfect fit line.

Lamberton site

The runoff values are predicted using three different estimates of effective conductivity: Time Invariant, Time Variant and WEPP Estimated. The predicted runoff depths results for these effective hydraulic conductivity values are summarized in Figures 30 through 31. The time variant and WEPP estimated effective hydraulic conductivity values are approximately twice as large as the time invariant value.

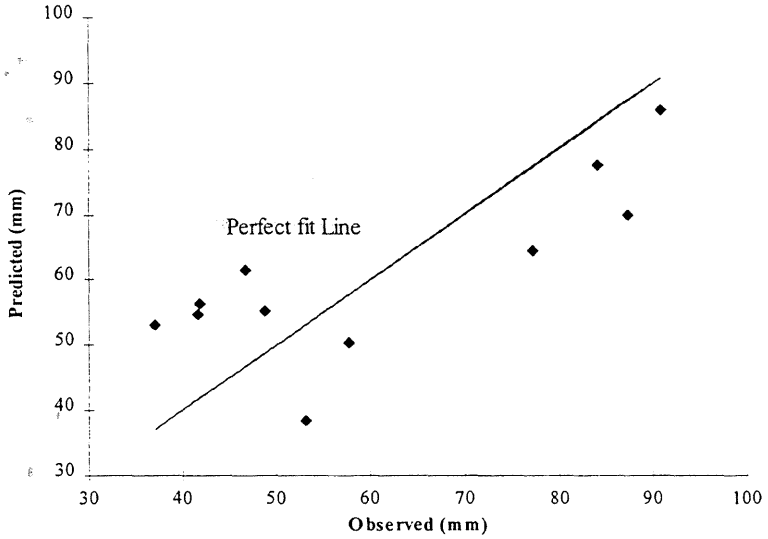

Figure 30. Predicted and Observed Runoff Depths Using Time Invariant Method.

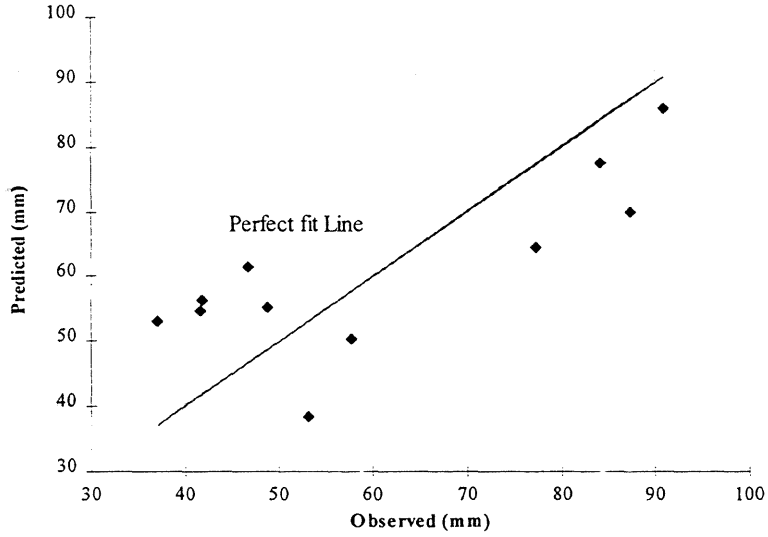

Figure 31. Predicted and Observed Runoff Depths Using Time Variant Method.

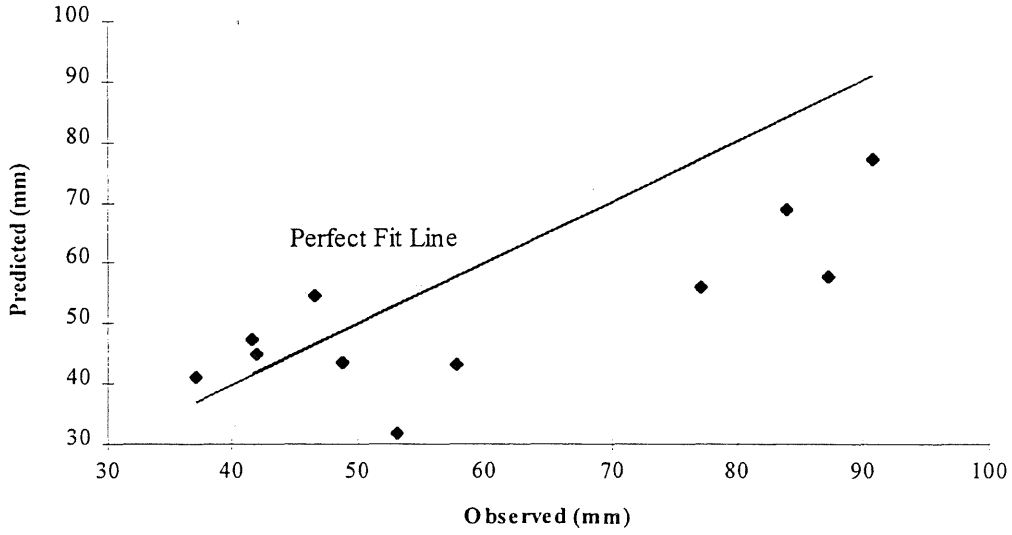

Figure 32. Predicted and Observed Runoff Depth Using WEPP Estimated Method.

The time invariant results for predicted runoff depth correspond to a coefficient of determination (R^2) and mean difference (MD) between predicted and observed values of 0.59 and -0.11 respectively. The negative value of MD indicates that the average predicted runoff depth is greater than observed. The estimated standard deviation of deviation around the one-to-one line is 13.8.

The WEPP model estimates effective hydraulic conductivity internally using the time variant equations. There are slight differences between the hand-calculated values (Oduro, 1996) and those estimated by WEPP. The time variant runoff depths correspond to a R^2 and MD of 0.34 and 9.77 respectively. Runoff depth is underpredicted as indicated by the positive MD value. The estimated standard deviation is 17.4, which indicate a greater spread than the predicted values using the time invariant effective hydraulic conductivity. The results obtained using the WEPP estimated effective hydraulic conductivity are similar to those obtained using the hand-calculated time variant values.

Greater insight into predicted and observed trends can be obtained by examining the results for individual runs shown in Figure 33. For example, runoff depths using the time invariant effective hydraulic conductivity is underpredicted for one of four steep slope plots, and five of seven moderate/flat slope plots. In contrast, WEPP results obtained using the time variant effective hydraulic conductivity value underpredict runoff depths for three of the four steep slope plots, and for five of the seven moderate/flat slope plots. The predicted runoff depths are better represented by the time invariant effective hydraulic conductivity at the Lamberton site. The time invariant effective hydraulic conductivity gives the highest coefficient of determination ($R^2 = 0.59$), the smallest absolute difference (MD = -0.11), and the smallest variation about the perfect fit line ($s_e = 13.75$).

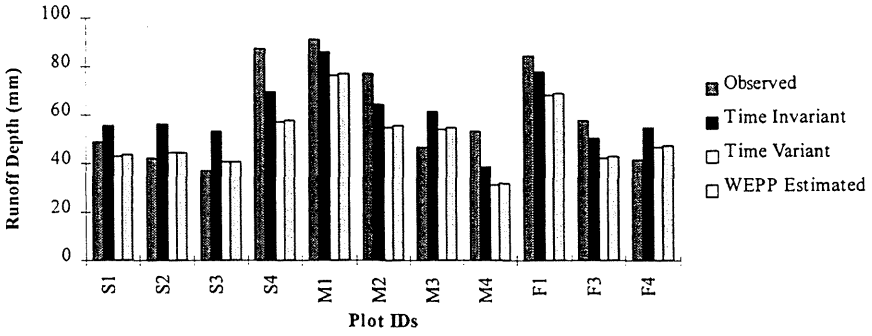

Figure 33. Observed and Predicted Runoff Depths for Lamberton.

Easton site

Predicted and observed runoff values for the Easton site are summarized in Figures 34 and 35. The hand-computed time variant values and the internally computed WEPP values are appreciably different for some storms. Differences are greater than those obtained at Lamberton. The WEPP estimated effective hydraulic conductivity increased gradually from the beginning of the season, peaked, and then were reduced after the plot was weeded. The trend in the manually computed time variant effective hydraulic conductivity values was more closely tied to the storm depth.

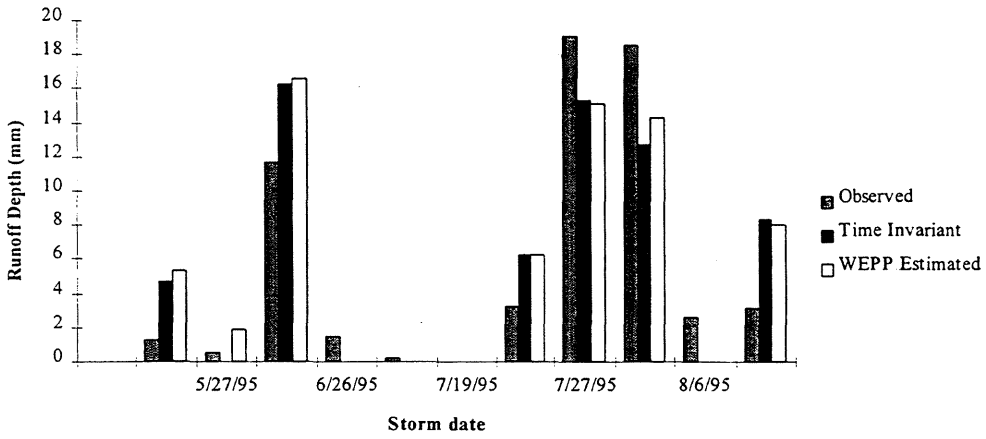

Figure 34. Observed and Predicted Runoff Depths by Storms for Easton.

For the time variant effective hydraulic conductivity, the values of R^2 and MD are 0.76 and 0.34 respectively. The estimated standard deviation s_e is 3.73. The R^2 and s_e for the predicted runoff depth using the WEPP estimated effective hydraulic conductivity are similar to those of the manually computed value. The MD was -0.08, which is smaller than the value obtained with the WEPP estimated (MD = 0.34) in absolute terms. The negative value means that predicted average runoff depth is greater than

the average observed value. Overall, the WEPP estimated effective hydraulic conductivity values result in better runoff depth prediction than the manually computed values.

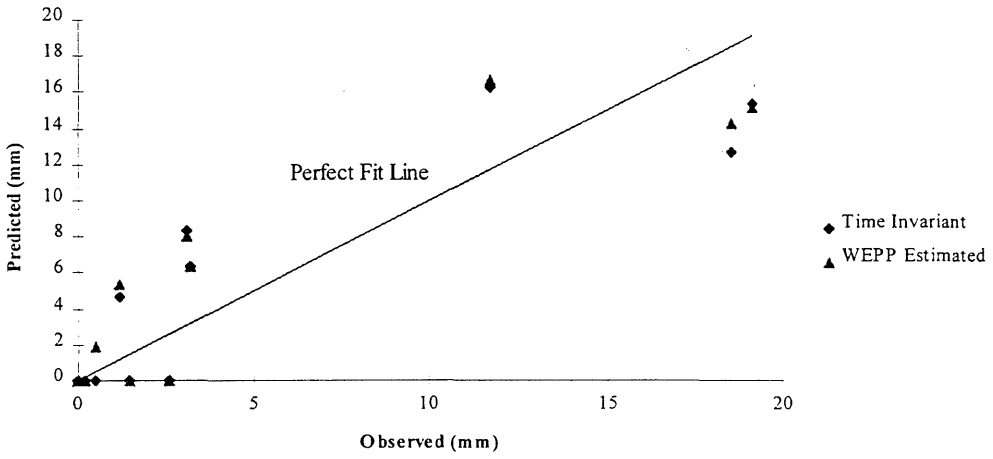

Figure 34. Summary of Predicted and Observed Runoff Depth at Easton.

St. James site

Similar to the Lamberton and Easton sites, the runoff depths for the St. James site were predicted for individual storms. To find the initial conditions at the beginning of each storm, the continuous mode was used for the year. The outputs from the continuous model run are used as input parameters for the single storm simulations. Frost, thaw, and snow depth were set equal to zero since the storms occurred in May and July when none of these are a factor. Since the St. James site is part of the LCMR project, more information is provided on the procedures to estimate the input parameters.

The site was modeled using hillslope option of WEPP. Slopes are broken into segments called overland flow elements (OFE's). On a hillslope, each OFE is an area of homogeneous soils, cropping, and management. The model requires the following inputs: the number of OFE's, the slope's aspect from north, the slope's width, each OFE's slope, each OFE's length, and each OFE's percent of the slope (Flanagan and Livingston, 1995).

The Watonwan County District Conservationist, Terrence Kelly, surveyed the St. James site in September 1993. Dr. E. Calvin Alexander and Sue Magdalene of the University of Minnesota Geology and Geophysics Department drew the contour map (Magdalene and Alexander, 1993). Figure 35 shows the topographic map. The dashed line outlines the drainage area. The arrows with circled numbers are the slopes entered into WEPP. The black circle is the location of the surface tile inlet.

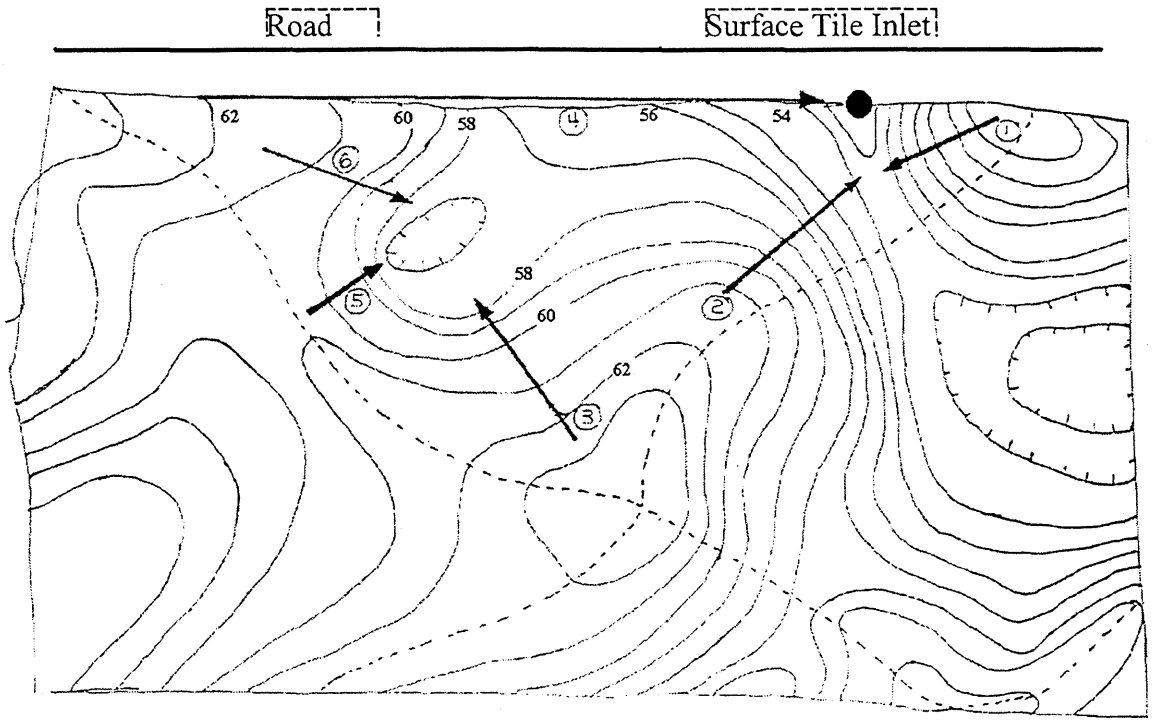

Figure 35. St. James Topographic Map with Slopes.

For each slope length, the area was determined and digitized. To find the slope width, the area was divided by the length. The fourteen soil parameters used to simulate runoff were estimated from site measurements and recommended values in the WEPP manual. Although single storm simulations are used to compare predicted and observed runoff depths, the continuous model was used to find the initial parameters for the single storm runs. Only the initial saturation and effective conductivity need to be estimated for the single storm. The other parameters remain unchanged. The initial saturation is calculated from the total soil water, soil depth, and porosity. The soil depth is known and the total soil water and porosity can be taken from the continuous simulation results.

The effective conductivity can be estimated four different ways: time variant, time invariant using the tillage operations equations, time invariant using the curve number equation, and WEPP internal calculations. WEPP developers (Flanagan and Livingston, 1995) and Oduro (1996) recommend using the time variant method to predict effective conductivity. This method is used in this study.

The WEPP values were used for the plant growth section and residue input files. The operation, initial conditions, surface effects, drainage, and management sections used known values from the site. For the plant growth section, WEPP allows a user to enter detailed information regarding plant growth or use one of WEPP's detailed plant growth files. The latter option was selected because of limited plant growth information for the site. The surface effects and operation sections were almost all known or easily estimated from the operation date, implement used, operation depth,

and type of tillage. The St. James site has patterned subsurface drain tile and reasonable estimates of the depth to tile drain, drain tile diameter, and the drain tile spacing could be made. The drainage coefficient of 0.0127 m/day (0.5 in/day) was assumed (Soil Conservation Service, 1971). The management section requires harvest date, plant date, row width, and residue management. The row width is known from the equipment used and the farmer's notes of practices were used to estimate other values.

Four storms in 1993 are used to evaluate the accuracy of the WEPP model to predict runoff depths. The rainfall depths and storm durations are given in Table 4 and the rainfall patterns are shown in Figure 36. These storms were selected because they caused relatively large runoff depths. The May 1, 1993 storm had a steady rainfall while the storms of July 17, 1993 and July 27, 1993 have their greatest intensities at the beginning of the storm. The storm of July 3, 1993 has its greatest intensities at the end of the storm.

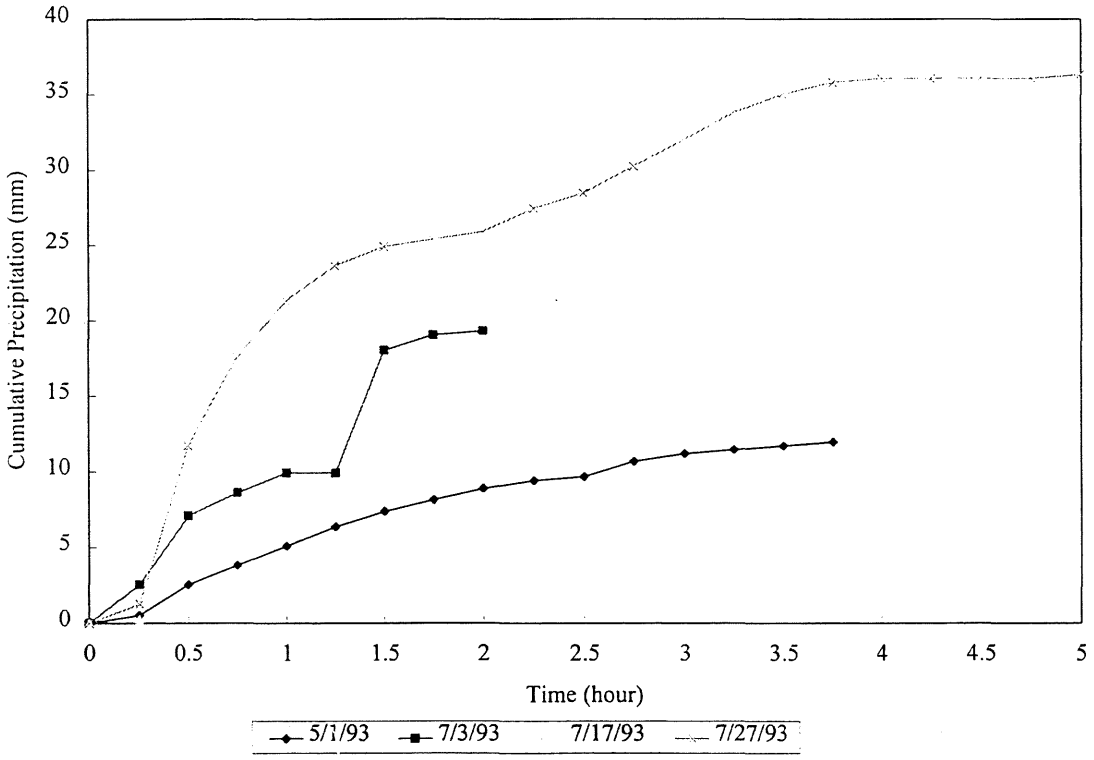

Figure 36. Rainfall Distribution of the Storms

The WEPP predicted runoff depths for the four storms are also shown in Table 4. Predicted and observed runoff depths are shown in Figure 37. Predicted WEPP values were obtained using the time variant effective conductivity method previously mentioned.

The WEPP model overpredicts runoff depths for two events and underpredicts runoff for other two events. For the storm of July 27, 1993, the predictive accuracy was quite good. Table 4 also shows the abstraction values. The observed percent abstraction ranges from 78.8 to 97.2 % and WEPP's percent abstraction ranges between 81.1 to 100%. For the storm of July 27, 1993, the abstraction percentage is quite good with less than a two percent difference. Overall, the abstraction percentages are reasonable.

Table 4. Observed and Predicted Runoff Depths

			Percent Abstractions		Runoff Depth (mm)		
	Rain (mm)	Duration (hr)	Observed	WEPP	Observed[1]	WEPP[1]	Curve Number
5/1/93	11.94	3.75	78.7	100.0	2.545	0.004	0.000
7/3/93	19.30	2	90.3	99.0	1.877	0.201	0.077
7/17/93	36.07	3	90.0	81.1	3.606	6.817	3.630
7/27/93	36.32	5	97.2	95.9	0.999	1.491	3.717

[1]The road runoff depth was calculated using the SCS Curve Number Method.

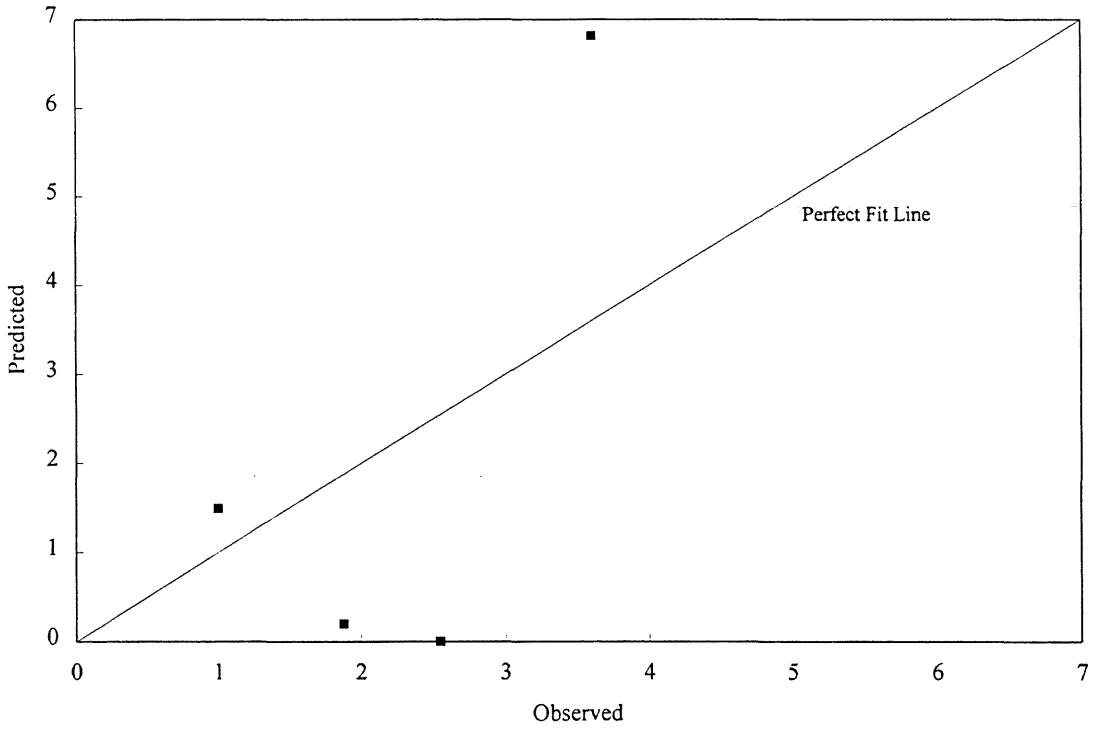

Figure 38. Observed and Predicted Runoff Depths

The Soil Conservation Service Curve Number method for determining runoff depth was used for comparison purposes. According to the old National Engineering Handbook Chapter 4 (Soil Conservation Service), the antecedent moisture content (AMC) is one. For AMC I, there was no runoff. There are efforts to underway to

redefine AMC guidelines. Results obtained using AMC II conditions are shown in Table 4.

For the storm of July 17, 1993, the Curve Number method predicts the runoff depth quite well, but for the other three storms the Curve Number method does not predict the runoff depth very well. The Curve Number method underpredicts for two storms and overpredicts for one storm. WEPP and the Curve Number method both underpredicts the May 1, 1993 and July 3, 1993 storms and overpredicts for the July 27, 1993 storm.

Erosion

Predicted sediment load of the WEPP model are compared to those observed from field runs conducted at Lamberton, Minnesota. The erosion data were collected from the same set of experiment previously used to evaluate runoff accuracy. The primary factor in the experimental design was to obtain a range of uniform slopes for similar soils. Experiments were conducted using a flat slope of 0 to 3%, a moderate slope of 3 to 6% and a steep slope of 6 to 9%. Two different land uses, disturbed and undisturbed, were also considered. The soil is a Ves loam/clay loam.

For each of the three slopes, four erosion plots were used for a total of twelve plots. Ten of these plots were rototilled and raked to create a uniform surface condition for comparison among slopes. Rows and other cross-slope features were obliterated by the rototilling and raking of the plots. The other two plots were clipped and raked bare.

A rotating boom rainfall simulator, similar to that designed by Swanson (1979), was used to produce runoff events. The rotating boom sprays a relatively uniform, circular rainfall pattern of 50 ft diameter with the kinetic energy approximately equal to that of natural rainfall. Erosion and runoff values are obtained from two rectangular plots with an approximate width of 8 ft and length of 32 ft located on both sides of the simulator.

The sensitivity of predicted sediment load of WEPP was evaluated for the Lamberton site. Since deposition is possible, rigorous theoretical relationships for the relative sensitivity coefficient are difficult to derive. Sediment load increases with increasing interrill and rill erodibilities and decreases with increasing critical shear stress. The sediment load response to interrill and rill erodibilities and critical shear stress is affected by slope and surface condition.

The predicted and observed sediment loads for each plot are shown in Figure 39 and summarized in Figure 40 for the Time Variant estimate of conductivity. The WEPP model overpredicted sediment load at Lamberton. Since the runoff depth was underpredicted, the predicted errors in sediment load would have been even greater had the runoff depths been predicted correctly. The R^2 and MD for sediment load predictions using the time variant effective hydraulic conductivity are 0.61 and -0.54

for R^2 and MD, respectively. The s_e value is 2.52 tons/ac.

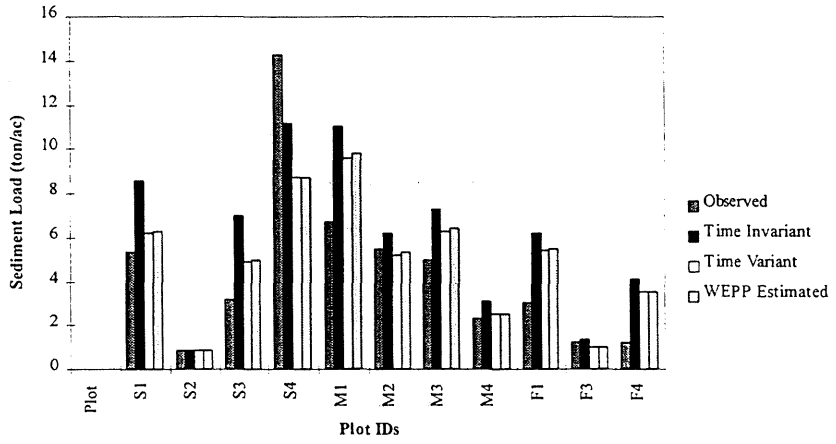

Figure 39. Predicted and Observed Sediment Load for Each Plot.

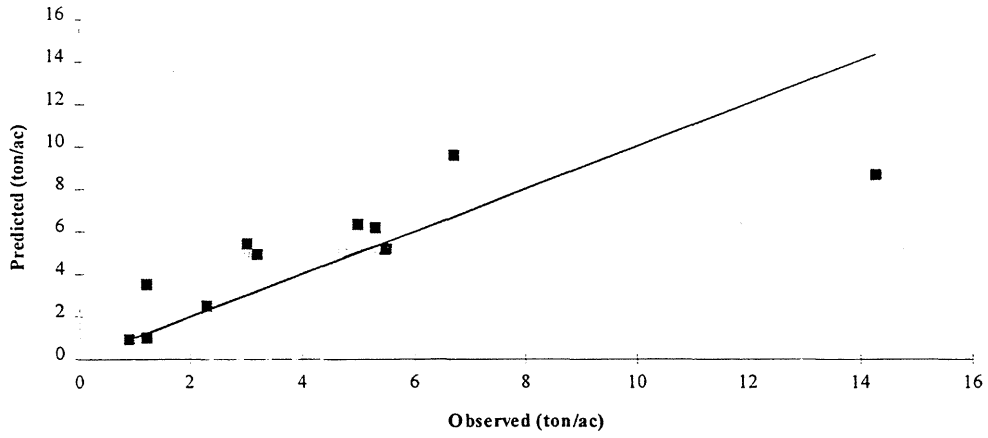

Figure 40. Observed and Predicted Sediment Loads Using Time Variant Conductivity.

The WEPP model is a continuous simulation model intended for the prediction of erosion. To isolate the erosion component from possible errors in predicted runoff, the WEPP model is calibrated so that predicted and observed runoff depths are equal. The effective hydraulic conductivity is adjusted to obtain the observed runoff depth. Figure 41 shows the sediment load predicted at Lamberton when predicted depths match observed values. As expected, the WEPP model overpredicted sediment load. The R^2, MD, and s_e are 0.61,-1.95, and 2.59, respectively.

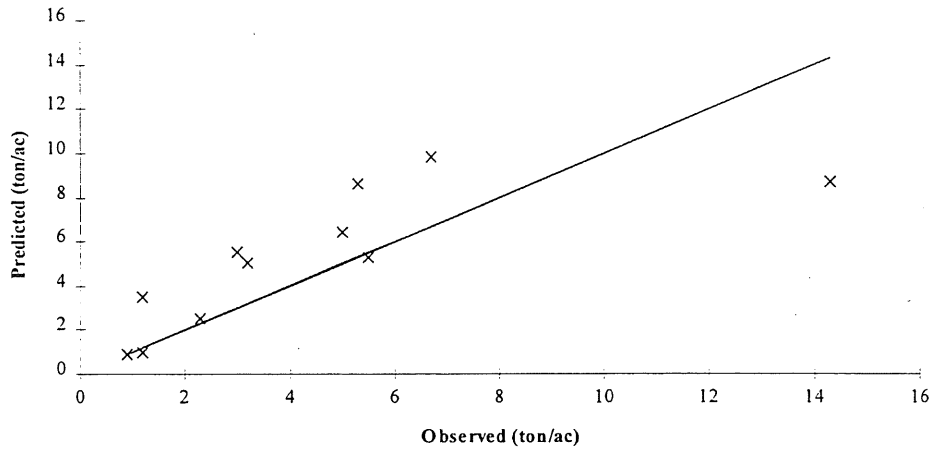

Figure 41. Observed and Predicted Sediment Loads Using Observed Runoff Depths.

Applications of the DROPLETS Model

Introduction

Simulation models are tools that can be used to evaluate the impact of management practices on the hydrologic and sedimentologic response of watersheds. Because Minnesota weather is highly variable from year to year, it is risky to use one or two years of experimental data to draw conclusions about the typical (or long-term average) response of a basin. Physically-based models, such as DROPLETS, can simulate many years of data. Another major benefit of simulation is that it is relatively simple to evaluate different management practices. The collection of experimental data is very expensive. Simulation provides a realistic approach for evaluating the impact of numerous management scenarios practices over a reasonably long time period.

To illustrate the usefulness of the DROPLETS model, the two different management scenarios are considered: (1) the impact of upland tillage practices on the sediment load to the inlet and (2) the effectiveness of a grass buffer zone around the surface tile inlet. Both scenarios are evaluated for the Rollins East Experimental Site using a minimum of 200 years of simulation. This research site is located near Vernon Center in south-central Minnesota.

There are numerous erosion events that occur within a 200 year time period. The likelihood or frequency of events of given magnitude is an extremely useful representation. If interest lies in the *number* of events, the following relative frequency definition is useful

$$rf(\Delta x) = \frac{\text{Number of Observations in } \Delta x}{\text{Total Number of Observations}} \quad (104a)$$

where $rf(\Delta x)$ is the relative frequency of the number of observations within a class of Δx. The corresponding cumulative distribution is defined as

$$F(x) = \frac{\text{Number of Observations less than x}}{\text{Total Number of Observations}} \quad (104b)$$

where f(x) is the cumulative distribution.

An alternative, and often more useful, representation of the data is a measure of the frequency of *sediment mass*. The fraction of sediment mass is defined as

$$mf(\Delta x) = \frac{\text{Mass in } \Delta x}{\text{Total Mass}} \quad (105a)$$

where $mf(\Delta x)$ is the fraction of the total mass that had events within the class of Δx. The cumulative mass distribution is defined as

$$Mf(x) = \frac{\text{Cumulative Mass less than x}}{\text{Total Mass Conventional Tillage}} \quad (105b)$$

where Mf(x) is the cumulative fraction of mass of events with sediment loads less than x compared to the total mass of the conventional tillage. Conventional tillage has been selected as the standard for comparison purposes.

Impact of Tillage Practices

The impact of tillage practices was evaluated using conventional tillage and no-till operations. Details of the conventional and no-till operations are given in Tables 5 and 6, respectively. Both tillage operations were evaluated using four hundred years of simulated weather data.

Table 5. Conventional Tillage Operations

Date	Corn tillage operations	Date	Soybeans tillage operations
4/15	Disk, tandem-finishing 7-9" spacing	4/15	Disk, tandem-finishing 7-9" spacing
4/25	Disk, tandem-finishing 7-9" spacing	5/5	Disk, tandem-finishing 7-9" spacing
5/1	Planter, double disk openers	5/10	Planter, double disk openers
6/1	Cultivator, row, multiple sweeps per row	6/10	Cultivator, row, multiple sweeps per row
6/15	Cultivator, row, multiple sweeps per row	6/25	Cultivator, row, multiple sweeps per row
11/1	Moldboard plow, 8"	11/1	Chisel plow with coulters and twisted points or shovels

Table 6. No-till Operations.

Date	Corn tillage operations	Date	Soybean tillage operation
5/1	Planter, no-till with ripple coulters	5/10	Drill, no-till in flat residues-smooth coulters
6/1	Anhydrous applicator		

The conventional tillage and no-till simulations require input parameters for the WEPP model, hillslope version. Input parameters for climate, slope, soil, and management are needed for these simulations. The weather variables were obtained using the stochastic weather generator for North Mankato. North Mankato is the closest weather station to Vernon Center that can be simulated with the WEPP model. Four hundred years of climate data were created.

The parameters for the slope file was measured from a detailed topographic map of the site. The topographic map was surveyed by the University of Minnesota's Department of Biosystems and Agricultural Engineering. The parameters for the soil file was obtained from recommended WEPP manual values and site specific soil information provided by the University of Minnesota's Department of Soil, Water, and Climate. The parameters for the management files were obtained from WEPP's management files for a corn and soybean rotation with medium fertilization.

The relative frequency of events, $rf(\Delta x)$, for different classes for the conventional tillage and no-till operations is shown in Figures 42 and 43, respectively. The majority of the erosion events have relatively small sediment loads for both tillage operations. More than 70% of the events are less than 0.25 tons/acre for the conventional tillage operation, and more than 90% of the events are less than 0.25 tons/acre for the no-till operation. There are very few events for the no-till operation with sediment loads exceeding 0.5 tons/acre.

Although the number of events provides useful insights, the fraction of total mass for different events is of greater interest. Few events with large sediment loads may still be important for the sediment budget for the site. The mass fraction defined by Equation 105a for conventional tillage and no-till is shown in Figures 44 and 45, respectively. For conventional tillage, the fraction of the total mass corresponding to events less than 0.25 tons/acre is still the largest component, but represents less than 12% of the total load. There is a considerable fraction of the total load for relatively rare events of 2-to-3 tons/acre. For no-till, the fraction of the total mass corresponding to events less than 0.25 tons/acre is greater than 70%.

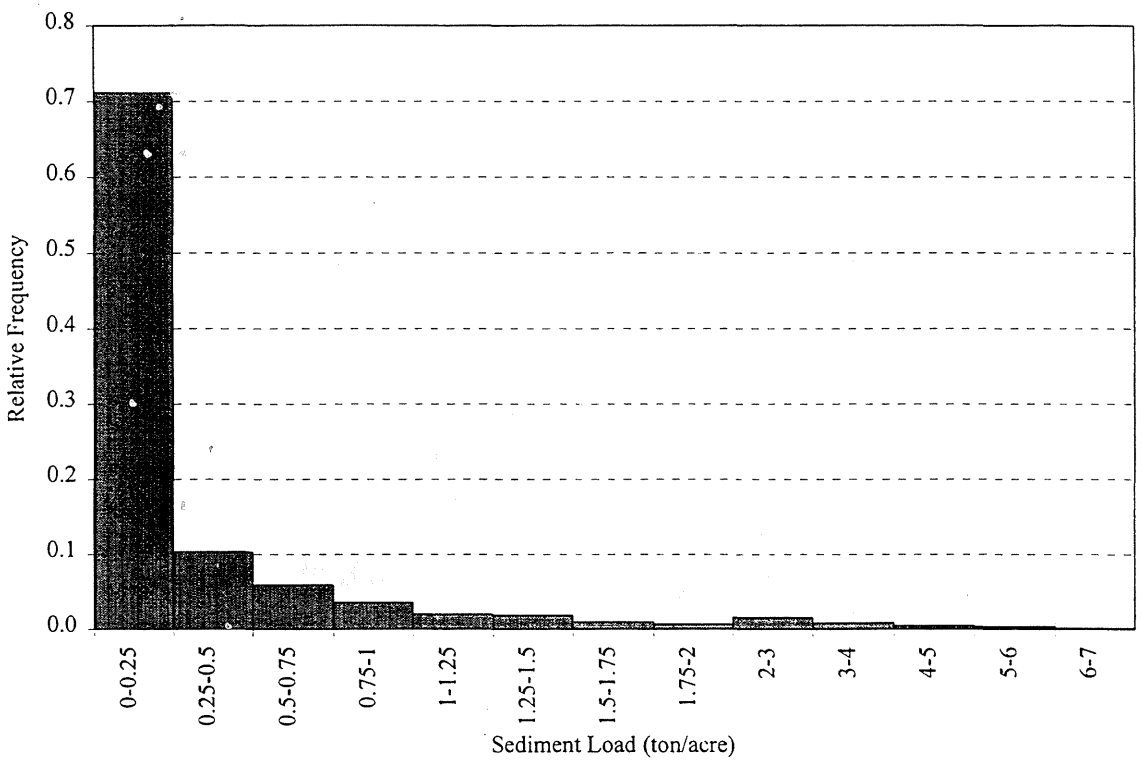

Figure 42. Relative Frequency for Conventional Tillage.

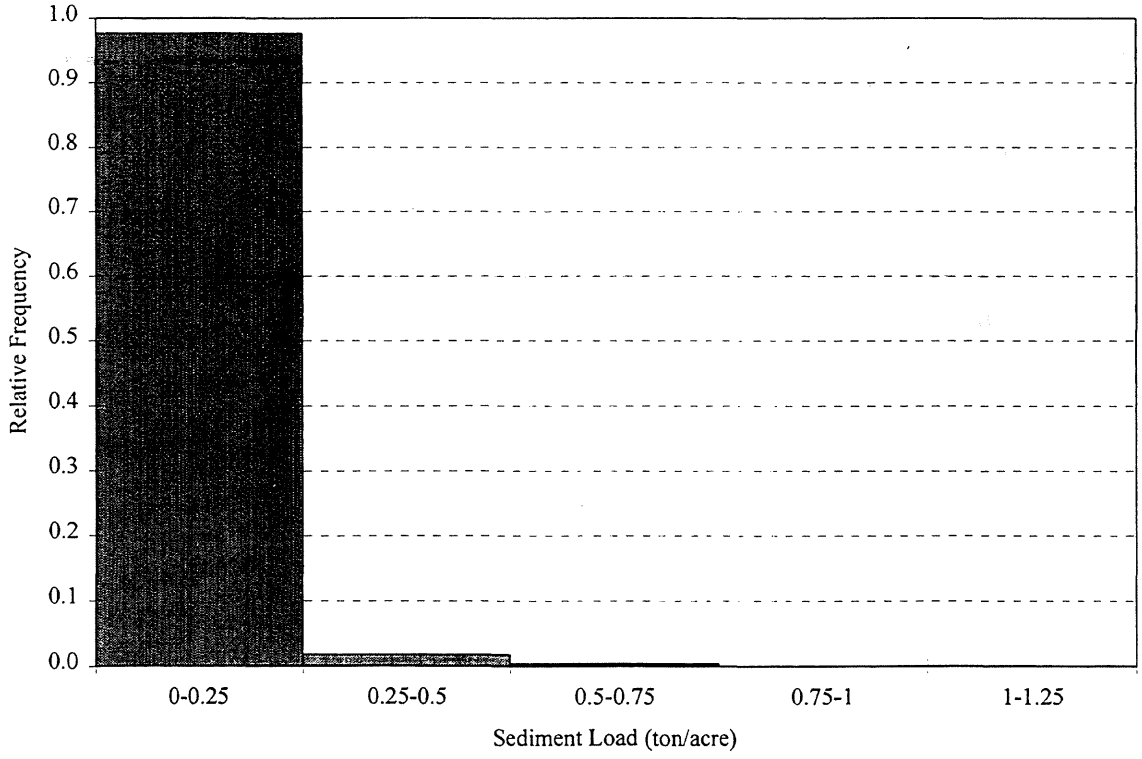

Figure 43. Relative Frequency for No-Till.

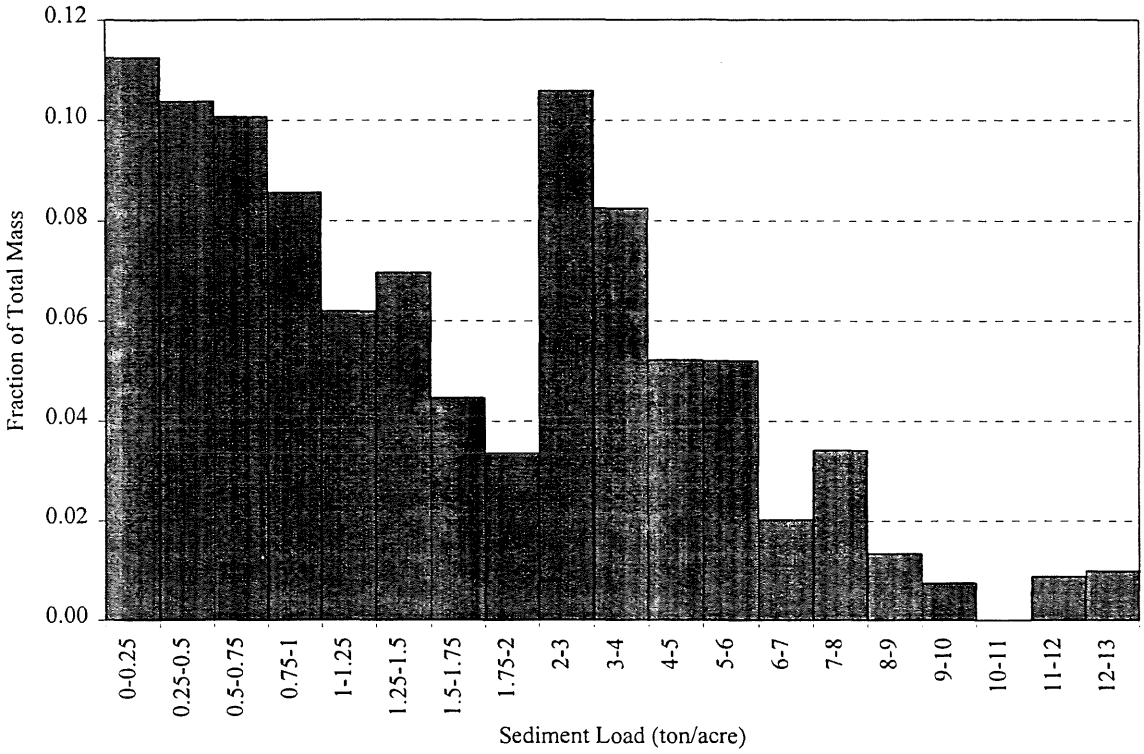

Figure 44. Fraction of Total Mass for Conventional Tillage.

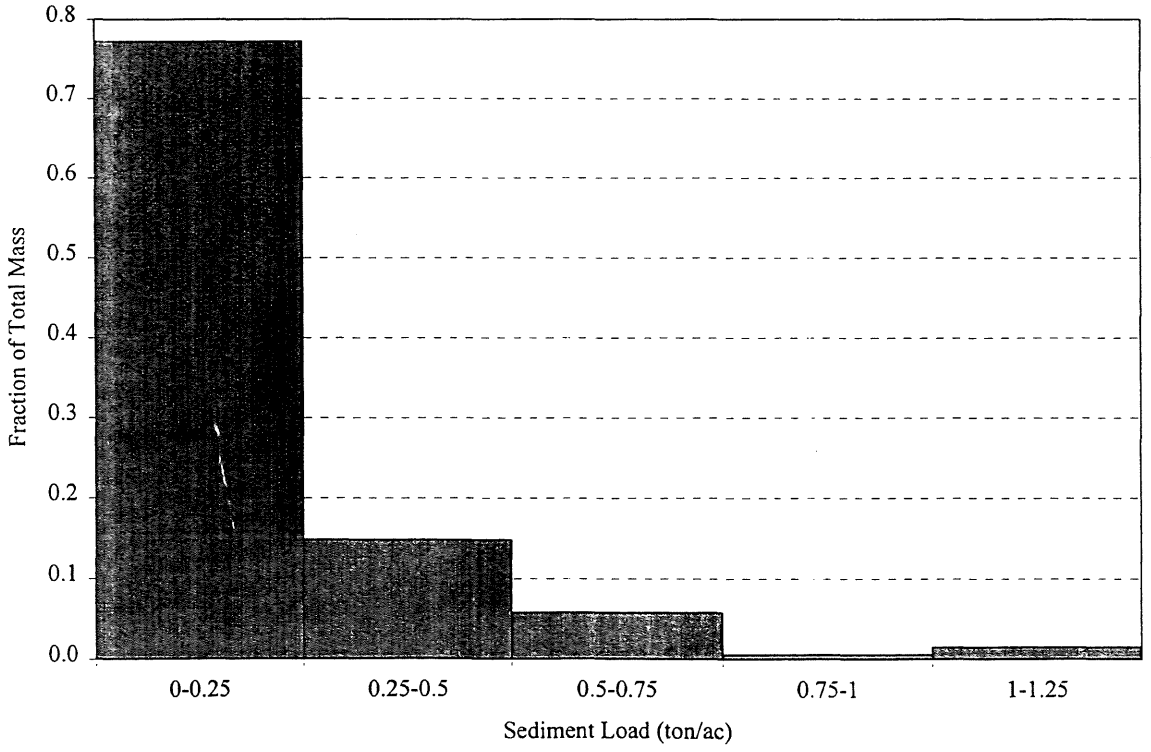

Figure 45. Fraction of Total Mass for No-Till.

A summary of the simulated results for conventional tillage and no-till is given in Table 7. The runoff depth, average annual sediment load, and median sediment load for conventional tillage are 2.7 inches, 3.55 tons/acre, and 0.071 tons/acre, respectively. The corresponding values for the no-till are 1.7 inches, 0.41 tons/acre, and 0.014 tons/acre, respectively. The conventional tillage operation clearly has a larger runoff depth, greater average annual sediment load, and a higher median sediment load than the no-till operation. No-till reduces the annual runoff depth by 35.5 percent, the average annual sediment load by 88.5 percent, and the median sediment load by 80.6 percent. If the fraction of sediment deposited at the inlet is equal for conventional and no-till operations, the reduction in sediment load by changing tillage practices is approximately 85%.

Table 7. Summary of Conventional Tillage and No-Till Results.

	Conventional	No-Till	%Difference
Annual Runoff Depth (inches)	2.7	1.7	-80.6%
Average Annual Sediment Load (tons/acre)	3.6	0.41	-85.5%
Median Sediment Load (tons/acre)	0.071	0.014	-80.6%

For comparison purposes, it is useful to compare the tillage results to the T value. The Natural Resources Conservation Service (NRCS) recommends a T of 3 tons/acre for the Guckeen soil type, which is the predominate soil type. The conventional tillage sediment load is slightly greater than the NRCS recommended value. The WEPP value includes possible deposition.

Effectiveness of Vegetative Filter

Surrounding the surface tile inlet by a grass buffer area is a management practice that is used to reduce the sediment load leaving the field. The effectiveness of this practice was evaluated for the Rollins East Experimental Site. A schematic of the grass buffer area is shown in Figure 46. A terrace located immediately south of the inlet limits flow from this direction.

The grass buffer is a 60 feet by 30 feet rectangular area. These dimensions correspond to current practices in the Minnesota River Basin (personal communication, 1997, Mr. Tim Larson, Minnesota Pollution Control Agency). The parameters of the grass correspond to those of a perennial rye: a grass height of 4.5 inches, a spacing of grass stems of 0.66 inches, a Manning's n of 0.0124, and a grass stiffness of 0.7 N/m^2. The land slope is taken as 1.2 percent. The soil type is a Guckeen silty clay loam, which corresponds to a low infiltration rate. It was assumed that the initial depth of sediment in the filter was zero and that the grass continues to grow with time so the buffer does not become filled with sediment. It was also assumed that potential water ponding for major events had a negligible impact on the trapping of the buffer area.

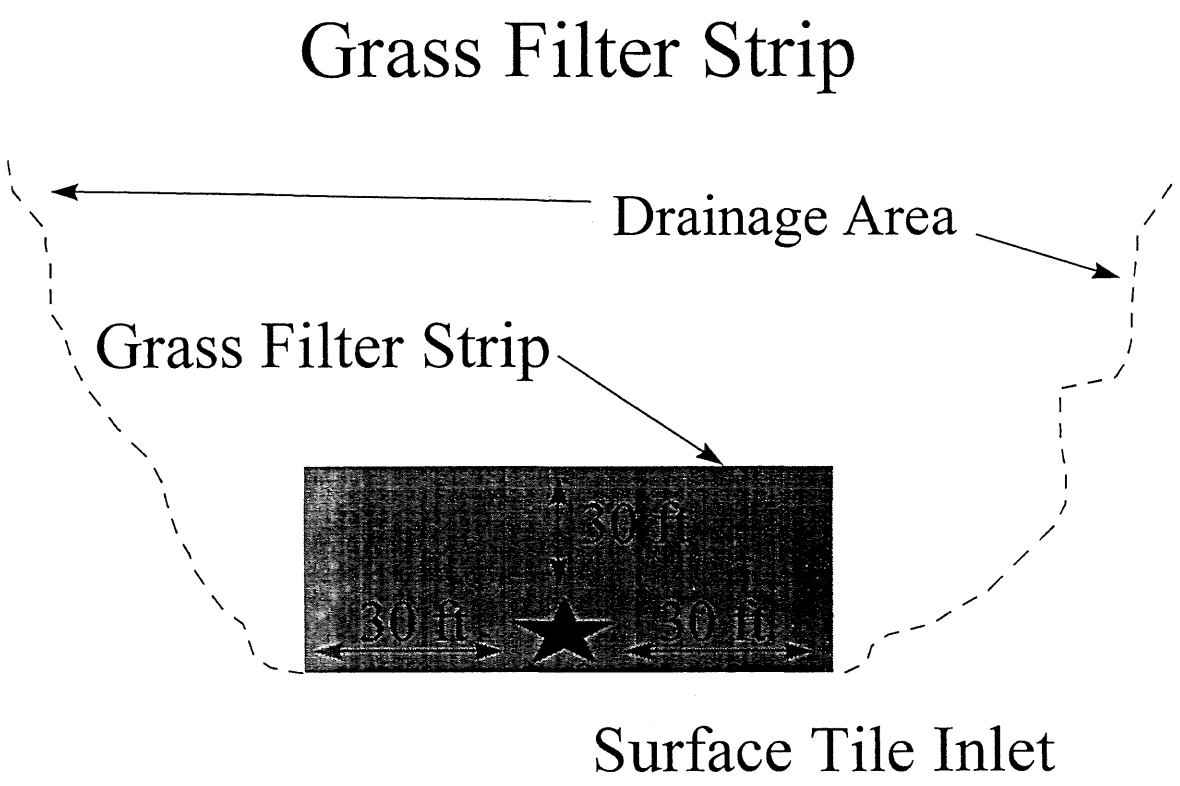

Figure 46. Schematic of Grass Buffer Area.

Runoff and sediment loads to the buffer area are determined using two-hundred years of simulation assuming conventional tillage on the watershed. As previously discussed, the WEPP input and output files are converted into a data file for GRASSF using SPA97.

For upland conventional tillage operations, the relative frequency of events for different classes with a grass buffer is shown in Figure 47. These values correspond to the sediment load leaving the site. Once again, the majority of the erosion events have relatively small sediment loads. More than 80% of the events are less than 0.25 tons/acre for the conventional tillage operation.

The grass filter has an average trap efficiency of 56 percent. The median trap efficiency trap efficiency is 59 percent. GRASSF predicts that the grass filter will trapping more than one half of the sediment entering it.

The relative effectiveness of no-till versus grass buffer can be examined using cumulative distribution (Equation 105a) shown in Figure 48 and cumulative mass distribution (Equation 105b) shown in Figure 49. No additional deposition of sediment is assumed at the inlet from possible ponding.

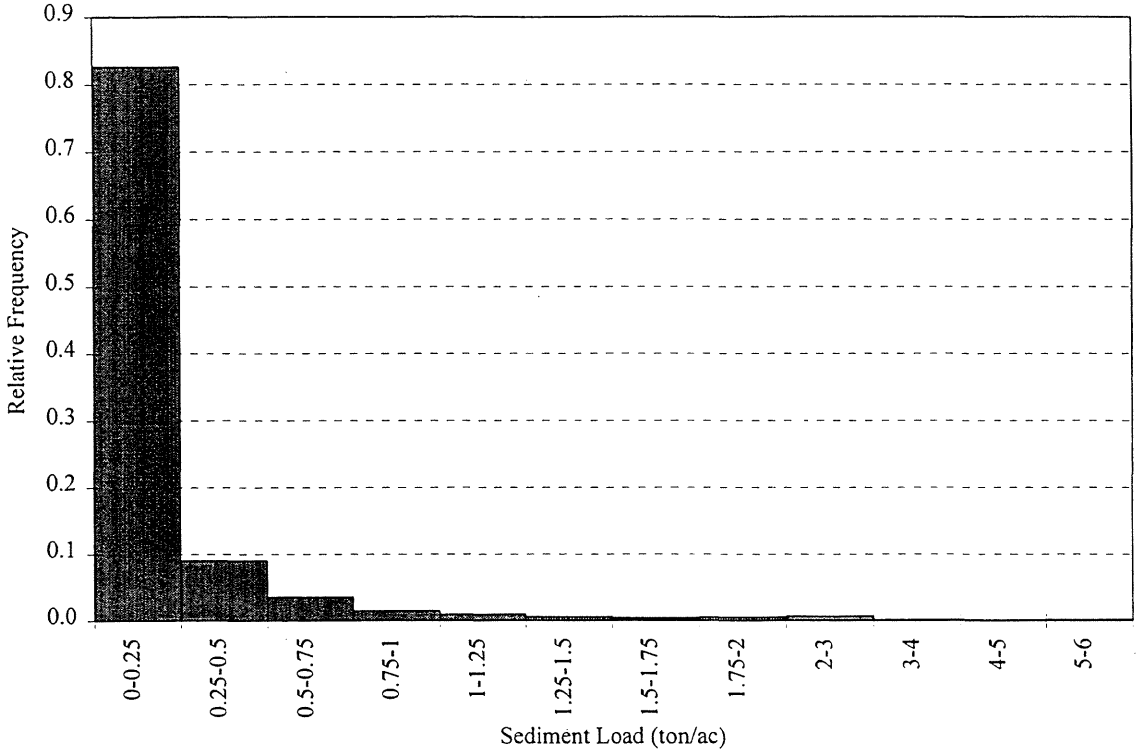

Figure 47. Relative Frequency of Conventional Tillage with Grass Buffer.

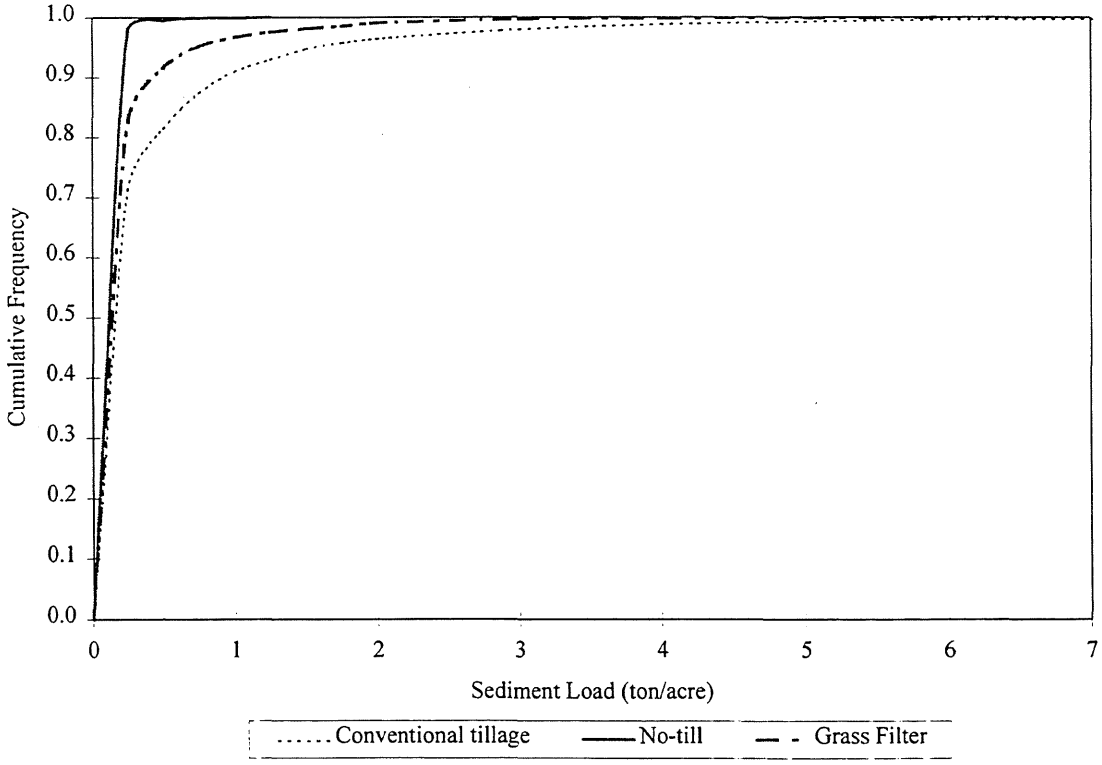

Figure 48. Cumulative Distribution of Alternative Management Practices.

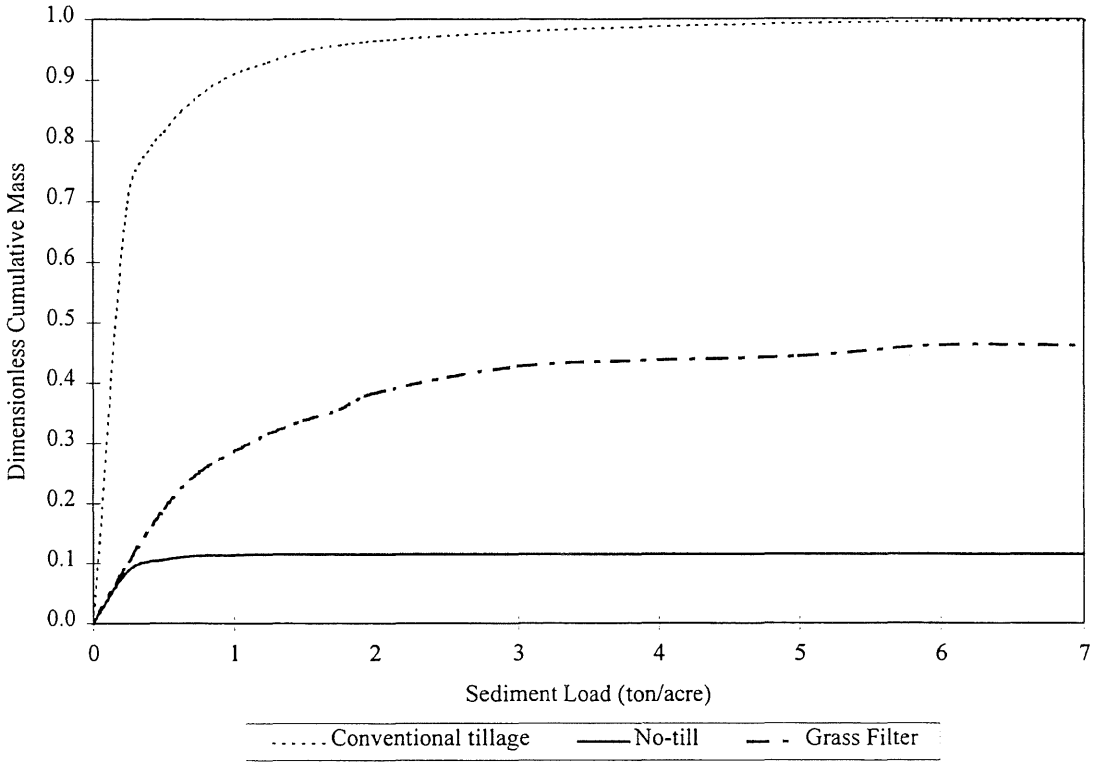

Figure 49. Cumulative Mass Distribution of Alternative Management Practices.

As shown by Figure 48, no-till operations has a greater fraction of small events than the grass buffer practice. As shown by Figure 49, the no-till is the most effective management practice to reduce sediment load. In comparison to conventional tillage, the no-till operation reduced sediment load by approximately 85%. The grass buffer reduced sediment load of conventional tillage by approximately 55%.

Summary and Conclusions

A suite of routines, collectively referred to as the DROPLETS (**D**rainage **R**esponse **O**f **P**othole **L**andscapes and the **E**rosion and **T**ransport of **S**ediment) Model, to assess the hydrologic and sedimentologic impact of surface tile inlets are described. Important components are: (1) the Water Erosion and Prediction Project (WEPP) model to simulate the hydrology and sedimentologic response of the upland watershed of surface inlets, (2) interface routines to extract information from WEPP output files, (3) the BASIN routine to simulate the trapping of sediment at the inlet by ponded water, (4) the GRASSF routine to simulate the trapping of sediment by a vegetative filter, (5) the routine to simulate the hydraulic response of a series of surface tile inlets, and (6) the routine to simulate the flow from subsurface tile lines. The long-term is link these routines/algorithms into a single comprehensive model.

The project evaluated the accuracy of the WEPP model for Minnesota conditions. The climate, snowmelt, runoff and erosion components were evaluated using observed

data. The snowmelt routines typically underpredicted the snowmelt. The climate component predicted quite well the observed statistical characteristics of non-precipitation parameters. The predicted hyetographs, however, resulted in return periods of rainfall depths for durations less than 24 hours that do not correspond to those observed. The runoff depths were predicted accurately for some events and poorly for other events. Since none of the parameters were calibrated to the site condition, the predicted accuracy is better than expected. The erosion component was evaluated for nearly bare plots. The predicted values of the WEPP model are in good agreement with observed values, considering that there was no calibration of erosion parameters.

Two different management scenarios, the impact of upland tillage practices on the sediment load to the inlet and the effectiveness of a grass buffer zone around the surface tile inlet, are analyzed using the DROPLETS routines. Both scenarios are evaluated for the Rollins East Experimental Site using a minimum of 200 years of simulation. The no-till operations were more effective in reducing the sediment load. In comparison to conventional tillage, the no-till operation reduced sediment load by approximately 85%. The grass buffer reduced sediment load of conventional tillage by approximately 55%.

References

Addiscott, T., J. Smith, and N. Bradbury. 1995. Critical Evaluation of Models and their parameters. Journal of Environmental Quality 24: 803-807.

Arnold, J.G. and J.R. Williams. 1989. Stochastic generation of internal storm structure. Transactions of the ASAE 32(1):161-166.

Arnold, J.G., J.R. Williams, A.D. Nicks and N.B. Sammons. 1990. SWRRB A Basin Scale Simulation Model for Soil and Water Resources Management. Texas A&M University Press, College Station pp. 19-23.

Baffaut, C., M.A. Nearing, and A.D.Nicks. 1996. Impact of CLIGEN parameters on WEPP-predicted average annual soil loss. Transactions of the ASAE 39(2):447-457.

Barfield, B. J. and J. C. Hayes. 1980. Modeling sediment filtration by vegetative filters. American Society of Civil Engineers Watershed Management Symposium, Boise, ID.

Barfield, B.J. and R.C. Warner. 1981 Applied Hydrology and Sedimentology for Disturbed Areas. Oklahoma State University. Stillwater, Oklahoma.

Brooks, E.S., J.L. Nieber, and B.N. Wilson. 1994. The Spatial and Temporal Variability of Soil Water and a Frozen Soil Layer in a Heterogeneous Landscape. Presentation made at 1994 Winter Meeting of the ASAE. Paper No. 942569. ASAE, 2950 Niles Road, St. Joseph, MI 49085.

Brown, J.W., B.N.Wilson, J.L.Nieber, B.Hansen, E.Brooks, M. Sanda. 1994. Field Instrumentation of a Depression Focused Recharge Site. Presentation made at 1994 Winter Meeting of the ASAE. Paper No. 942161. ASAE, 2950 Niles Road, St. Joseph, MI 49085.

DeBoer, D. W. and H. P. Johnson. 1971. Simulation of runoff from depression characterized watersheds. Transactions of the ASAE 14(4):615-620.

Einstein, H. A. 1950. The bed-load function for sediment transportation in open channel flows. U.S. Dept. Ag. Tech. Bull., 126:29-42.

Frederick, R.H., V.A. Myers, and E.P. Auciello. 1977. Five-to-60-Minute Precipitation Frequency for the eastern and Central United States. National Oceanic and Atmospheric Administration Technical Memorandum NWS HYDRO-35, United States Department of Commerce, Washington D.C.

Flanagan D.C. and M.A. Nearing (eds) 1995. Hillslope Profile and Watershed Model Documentation. NSERL Report NO. 10. West Lafayette.

Flanagan D.C. and S. J. Livingston (eds) 1995. WEPP User Summary. NSERL Report NO. 11. West Lafayette.

Haan, C.T. and H.P. Johnson. 1967. Geometrical Properties of Depresions in North-Central Iowa. Iowa State Journal of Science.42(2):149-160.

Haan, C. T. and H. P. Johnson. 1968a. Hydraulic model of runoff from depressional areas; Part I. General considerations. Transactions ASAE 11(3):364-367.

Haan, C. T. and H. P. Johnson. 1968b. Hydraulic model of runoff from depressional areas; Part II. Development of the model. Transactions ASAE 11(3):368-373.

Haan, C.T. Statistical Methods in Hydrology. Iowa State University Press, 1977.

Haan, C.T., B. Allred, D.E. Storm, G. Sabbagh and S. Prabhu. 1993. Evaluation of Hydrologic/Water Quality Models: A Statistical Procedure. Presentation made at the 1993 International Winter Meeting of the ASAE. Paper No. 932505. ASAE, 2950 Niles Road, St. Joseph, MI 49085.

Hayes, J. C. 1979. Evaluation of design procedures for vegetal filtration of sediment from flowing water. Unpublished Ph.D., University of Kentucky, Lexington.

Hershfield, D.M. 1961. Rainfall Frequency Atlas of the United States. Technical Paper 40, United States Department of Commerce. Waether Bureau. Washington D.C.

Kirkham, D. 1958. Seepage of Steady Rainfall through Soil into Drains. Transactions, American Geophysical Union 39(5):892-908.

Kirkham, D. 1964. Physical Artifices and Formulas for Approximating Water Table Fall in Tile-Drained Land. Soil Science Society of American Proceedings 28(4) Sept./Oct.

Leaf, R.B. 1994. Development and Evaluation of a Microrelief meter for Field Analyses. MS Thesis: University of Minnesota.

Magdalene, S. And E.C. Alexander, Jr. 1993. Minnesota River Assessment Project. Interim Report on Merle Anderson Farm Study Site.

Moore, I. D. and C. L. Larson. 1979. Effects of drainage projects on surface runoff from small depressional watersheds in the north central region. Water Resources Research Center, University of Minnesota Graduate School. WRRC Bulletin 99.

Moore, I.D. and C.L. Larson. 1980. Hydrologic Impact of Draining Small Depressional Watersheds. Journal of Irrigation and Drainage. Proceedings of the ASCE 106(IR4):345-363.

Nearing,M.A., G.R. Foster, L.J. Lane, and S.C. Finckner. 1989. A Process-based soil

erosion model for USDA-Water Erosion Prediction Project Technology. Transactions of the ASAE 32(5): 1587-93.

Nicks, A. D., V. L. Lopes, M. A. Nearing, and L. J. Lane. 1995. WEPP Modeling Techniques. USDA-ARS, National Soil Erosion Laboratory, West Lafayette, Indiana.

Oduro, P. 1996. An Evaluation of the Water Erosion Prediction Project Model. MS Thesis. University of Minnesota.

Tokoz, S. and D. Kirkham. 1971. Steady Darinage of Layered Soils: 1, Theory. Journal of the Irrigation and Drainage Division, Proceedings of American Society of Civil Engineers, March, 1971:1-17

Tollner, E. W., B. J. Barfield, C. T. Haan, and T. Y. Kao. 1976. Suspended sediment filtration capacity of simulated vegetation. Transactions of the ASAE 19(4):678-682.

Tollner, E. W., B. J. Barfield, and J. C. Hayes. 1982. Sedimentology of erect vegetal filters. Proceedings of. American Society of Civil Engineers, Journal of Hydraulic Division.

Swanson, N.P. 1979. Field plot rainfall simulation (Rotating-boom rainfallsimulator). Proceeding of the Rainfall Simulator Workshop, USDA-ARSAgricultural Reviews and Manuals, pp. 166-169.

United States. Department of Agriculture. Soil Conservation Service. 1971. Hydrology Guide for Minnesota. St. Paul, Minnesota.

United States. Department of Agriculture. Soil Conservation Service. 1978. Soil Survey of Blue Earth County, Minnesota. Washington D.C.

Wilson, B. N., B. J. Barfield, and I. D. Moore. 1982. A hydrology and sedimentology watershed model. Part I: Modeling techniques. University of Kentucky, Department of Agricultural Engineering, Special Publication, Lexington.

Wilson, B. N., B. J. Barfield, and D. G. Colliver. 1984. Modeling the performance of sediment detention ponds, 2, The BASIN model based on advection-diffusion and reactor mixing concepts, Tech. Rep. Inst. for Min. and Miner. Res., Univ. of Ky., Lexington. IMMR 84/122,210.

Wilson, B. M. and B. J. Barfield. 1985. Modeling sediment detention ponds using reactor theory and advection-diffusion concepts. Water Resources Research 21(4):523-532.

Wilson, B.N., R.B. Leaf, B.J. Hansen, J.W. Brown, and D.E. Storm. 1994. Observed Surface Flow Paths from Field Erosion Plots. Presentation made at 1994 International Summer Meeting of the ASAE. Paper No. 942049. ASAE, 950 Niles Road, St. Joseph, MI 49085.

Appendix A: SPA97 User's Guide

Purpose: SPA97 converts Water Erosion Predication Project (WEPP) input and output files into an input file for GRASSF and BASIN.

Need: SPA97.exe, READ97.exe, SED97.exe, and COND97.exe.

Warning: SPA97 does not work for a single year.

Installation

These folders need to be created:
c:\wepp\dist\output\event
c:\wepp\dist\output\summary
c:\wepp\dist\output\soils

CopySPA97.exe, READ97.exe, SED97.exe, and COND97.exe in the c:\wepp\dist\ directory.

WEPP and SPA97 file names need to be less than eight characters. In the WEPP hillslope building menu, there are three columns. The first column has general information about the simulation. The second column contains the input file names and two output options. These output options are 'graphics' and 'summary'. The graphics output should have a 'no' next to it. The summary has the ability to produce 5 summary outputs: annual-abbreviated, detailed-abbreviated, event-by-event-annual, event-by-event-detailed, and monthly. To run SPA97, run WEPP's summary as event-by-event-detailed. The third column has 'plotting', 'event', 'summary', 'OFE', 'winter', 'yield', 'water', 'crop', and 'soil'. Only the 'summary', 'OFE', and 'soil' should have yes' next to them. The others should have no' next to them.

The WEPP output files need to be moved from c:\wepp\output to c:\wepp\dist\output.

Table 1. Location of WEPP files and SPA97 files

Name & Extension	WEPP output files	SPA97 input files
filename.ofo	c:\wepp\output\event	c:\wepp\dist\output\event
filename.sum	c:\wepp\output\summary	c:\wepp\dist\output\summary
filename.soi	c:\wepp\output\soils	c:\wepp\dist\output\soils

Executing SPA97

1. In DOS, type 'cd wepp' (change directory to wepp)
2. Type 'spa97' (run SPA97)

Enter WEPP file name with no extention.

3. Type in the file name

```
Accessing WEPP file address.
The WEPP file addresses for (filename) have been obtained.
```

4. After the file address has been completed, the following screen will appear. Follow the directions given.

```
Accessing WEPP file address.
The WEPP file addresses for (filename) have been obtained.

Hit Any Key to Continue.
```

5. The program will read in the sediment data and create filename.sed.

```
Reading Sediment Information:
Dy: __ Mo: __ Yr: __ Load: __ kg/m
```

6. After the sediment file is created, the following screen will appear. Follow the directions.

```
Reading Sediment Information:
Dy: __ Mo: __ Yr: __ Load: __ kg/m

Sediment Data Conversion is Complete
Hit Any Key to Continue.
```

7. The program will reduce the WEPP files into the file: filename.dat.

```
Reducing WEPP output to one file.
Dy: __ Mo: __ Yr: __ K: __ Qp: __
```

8. After data reduction is completed, the next screen will appear. Follow the directions.

```
Reducing WEPP output to one file.
Dy: __ Mo: __ Yr: __ K: __ Qp: __

Data Reduction is complete.
Hit Any Key to Continue.
```

9. The program will be completely finished. Follow the directions to return to DOS.

```
Reducing WEPP output to one file.
Dy: __ Mo: __ Yr: __ K: __ Qp: __

Data Reduction is complete.
Hit Any Key to Continue.

The process is complete.
```

Hit any key to exit.

SPA97 will return you to DOS. The output files are located in the c:\wepp\dist\ directory. The two output files are filename.sed and filename.dat.

Appendix B: GRASSF User's Guide

Purpose: To model sediment trapped by a grass filter strip.

Files needed:
Gin.dat
Gobs.dat
Gpart.dat
Grass.dat
Grass.std
Grass1.chr
Grass2.chr
Grass3.chr
Gtin.dat
Gtobs.dat
Gtpart.dat
Oem08
Oem10
Wgrass.std
Wgrass.exe

Input parameters

Screen 1

General Input Parameters	
Description of Input	Exit here or <Esc>
Total number of events:	
Bulk Specific Gravity of Deposited Sediment:	1.25
Kinematic viscosity:	0.0096
Initial Depth of Sediment in Zone D:	0
Load-flow-rate exponent:	1.50
Watershed area (acres):	
Width of watershed (meters):	
Path of input/output files:	
Grass characteristics:	Grass1.chr
Output file name:	filename.out
WEPP file name:	filename.dat
Plotting filename:	filename.plt
Run identification:	

Screen 2

Grass Characteristics for Segment 1	
Description of Input	Exit here or <Esc>
Manning's roughness coefficient:	
Grass height (in):	
Total length of the filter (ft):	
Spacing between grass elements (in):	
Bed slope of the filter (%):	
Filter width:	
Infiltration rate (in/hr):	
Grass stiffness:	

Descriptions of Input Parameters

The bulk specific gravity of deposited sediment must be entered to calculate the advancement of the deposition wedge and to accumulate the depth of deposited sediment in the last zone of the filter (Zone D). Bulk specific gravities for different sediment compositions are given in Table 1. GRASSF assumes that only particles greater than 37 microns are trapped in the deposition wedge.

Table 1. Specific Gravity of Submerged Sediment for Imhoff Cone Test

Sediment Composition		Submerged Specific Gravity (SBSG)
100 % > 50 microns		1.56
Coarse:	80% > 50microns 10 microns < 15% < 50 microns 5% < 10 microns	1.49
Medium Fine:	40 % > 50microns 10 microns < 35% < 50 microns 25 % < 10 microns	1.35
Fine:	10 % > 50microns 10 microns < 60 % < 50 microns 30 % < 10 microns	1.18
100 % < 50 microns		1.12

Kinematic viscosity is the ratio of absolute viscosity to mass density. The absolute viscosity is the fluid's ability to resist shear.

The initial depth variable (Zone D) is entered to aid in simulating the performance of the filter for a runoff event that occured before the grass has been able to completely recover from the previous event. GRASSF was originally developed assuming the bedload is eventually trapped by stools and indentation of the filter.

Table 5 contains Manning's roughness coefficient.

Grass height, filter length, slope, and filter width are input parameters that depend on the construction and maintenance plans. Grass height must be enters in inches, filter length and width in feet, and slope in percent.

Table 4 contains average spacing between grass stems (inches).

GRASSF assumes that the filter is at its steady-state infiltration rate when the sediment laden flow reaches the filter. A rough estimate of steady-state infiltration rate is given in Table 2. Local Natural Resources Conservation Service, formerly known as Soil Conservation, SCS, (NRCS) offices can be consulted for more detailed information. Infiltration rate must be entered in inches per hour.

Table 2. Steady-State Infiltration Rates

Soil Group	Infiltration Rate (in/hr)
A	> 0.30
B	0.15-0.30
C	0.05-0.15
D	0-0.05

Soil Group A - deep sand, deep loess, aggregated silts
Soil Group B - shallow loess and sandy loams
Soil Group C - clay loams, shallow sandy loams, soil usually high in clay
Soil Group D - soil of high swelling point, heavy plastic clays

Grass stiffness factors, MEI, for different vegetative types are given in Table 5 in the appendix. MEI values are used to estimate when the grass becomes prone to bending. At this point, the filter is no longer effective.

Table 3. Lower limit, Upper Limit, and Default Values for Input Parameter

Input Parameter	Lower limit	Upper limit	Default value
Bulk specific gravity of deposited sediment	0.5	3.0	1.25
Initial depth, Zone D	0.0	0.8	0.0
Manning's n	0.003	0.017	None
Average grass spacing	0.1	3.0	None
Infiltration rate	0.0	4.0	None
Grass stiffness factor (MEI)	0.002	250	None

Description of Output Parameters

Results from a grass filter design are shown below in Table 6. An overall trap efficiency of 81.4 percent was obtained. The peak settleable solids concentration is 117 ml/ℓ. The performance of the grass filter may be improved by increasing the filter width and/or using a check dam prior to the filter to reduce the sediment load entering the filter.

Table 4. Spacing and Manning's n for Different Grass Species (Hayes et al.,1978)

Grass	Spacing (in.)	Manning's n	Description of Grass Condition
Rye	0.67	.0121	good stand; fairly well established, grown for 3 months in greenhouse, cut once
Rye	0.65	.0127	good stand; fairly well established, grown for 3 months in greenhouse, cut once
Fescue	0.56	.0161	very dense; well established sod-like condition, grown for 15 months in greenhouse, repeatedly cut
Fescue	0.59	.0096	dense; well established, grown for 5 months in greenhouse, repeatedly cut
Fescue	0.67	.0141	good stand; well established, grown for 5 months in greenhouse, cut two times
Sorghum	0.86	.0054	about 11.8 inches tall, somewhat thin compared to fescue and ryegrass, 2 months old
Sorghum	0.61	.0086	dense; spacing limited plant growth, 15.7 inches tall, 3 months old, had many dead leaves
Sorghum	0.59	.0071	dense; close spacing limited plant growth, 11.8 inches tall, 2 months, beginning to die
Sorghum	0.51	.0088	very dense; very think density for sorghum, competition limited growth, 2 months old, 9.8 inches tall
Sorghum	0.96	.0117	fair stand; sparse thickness, 4 months old, 21.7 inches tall, still growing well when tested

Table 5. Grass Stiffness Factors

Retardance Class	Cover type	Cover Condition	Calibrated stiffness MEI (N/m^2)
A	Weeping lovegrass	Excellent stand, tall (average 30 in.)	200
A/B	Kikuyu Grass	Excellent stand (average 16.5 in.)	47
	Kudzu Grass	Very dense growth, uncut	---
	Bermudagrass	Good stand, tall (average 12 in.)	17
	Native grass mixture (little bluestem, blue grama, and other long and short mid-west grasses)	Good stand, unmowed	20
	Weeping lovegrass	Good stand, tall (average 24 in.)	30
B	Lespedeza sericea	Good stand, not woody, tall (average 20 in.)	10
	Alfalfa	Good stand, uncut, (average 11 in.)	4
	Weeping lovegrass	Good stand, mowed, (average 13 in.)	6
	Kudzu	Dense growth, uncut	---
	Blue grama	Good stand, uncut (average 13 in.)	8
	Dallas	Uncut (average 30 in.)	20
B/C	Crabgrass	Fair stand, uncut (10-48 in.)	
	Bermudagrass	Good stand, mowed, (average 6 in.)	2.0
	Common lespedeza	Good stand, uncut, (average 11 in.)	3.0
	Grass-legume mixture-summer (orchard grass, redtop, Italian ryegrass, and common lespedeza)	Good stand, uncut, (average 4-5 in.)	
	Centipedgrass	Very dense cover (average 6 in.)	2.0
	Kentucky bluegrass	Good stand, headed (6 to 12 in.)	
	Bermudagrass	Good stand, cut to 64 mm	0.15
	Common lespedeza	Excellent stand, uncut (4.5 in)	0.10
	Buffalograss	Good stand, uncut (3 to 6 in.)	0.16
D	Grass-legume mixture-fall, spring (orchard grass, redtop, Italian ryegrass, and common lespedeza)	Good stand, uncut (4 to 5 in.)	0.7
	Lespedeza sericea	After cutting to 2 in., very good stand	0.005
	Kentucky bluegrass	Cut to 3 in.	0.10
	Bermudagrass	Good stand, cut to 1.5 in. height	0.03
	Bermudagrass	Burned stubble	

Table 6. Grass Filter Summary Table

Specific gravity of sediment	=	2.5
Bulk specific gravity	=	1.25
Viscosity	=	.0090 cm2/sec
Critical prone velocity	=	.8122 ft/s
Peak flow depth	=	.16 in
Filter travel time	=	.1000 hr
Filter infiltration rate	=	.1389 cfs
Total filtration rate	=	.1007 acre-ft
Wedge location	=	36.37 feet
Sediment depth, Zone D	=	.5397 inch
Outflow runoff volume	=	.11 acre-ft
Peak discharge rate	=	2.58 cfs
Peak effluent concentration	=	364571.75 mg/ℓ
Peak settleable concentration	=	117.7713 ml/ℓ
Peak settleable concentration	=	147214.16 mg/ℓ
Total mass discharged	=	81.45 percent
Overall trap efficiency of all segments	=	81.45

References

Hayes, J. C., B. J. Barfield, and R. I. Barnhisel. 1978. Evaluation of Grass Characteristics Related to Sediment Filtration. Transactions of ASAE.

Warner, R.C., B.N. Wilson, B.J. Barfield, D.S. Logsdon, and P.J. Nebgen. 1984. A Hydrology and Sedimentology Watershed Model. Part II: Users' Manual. University of Kentucky, Lexington, Kentucky.

Wilson, B.N., B.J. Barfield, and I.D. Moore. 1984 A Hydrology and Sedimentology Watershed Model. Part I. Modeling Techniques Techniques. University of Kentucky, Lexington, Kentucky.

Appendix C: BASIN User's Guide

Purpose: To model the trap efficiency of a detention basin.

Caution: The author recommends knowledge of numerical methods and sediment transport theory to successfully use this model.

Need:
Oem08
Oem10
Rollin.vel
Rollin1.dat
Rollin1.pnd
Rollin1.stg
Wbasin.std
Wbasin.vcw
Wbasin.wepp
Wbasin.wsp
Wbasin.exe
Wbasin.std

Preparing Input Files

The user needs to create the following files for their site. Examples of these files are provided with the program. Copy and rename the file to the user's preference the following files. The file input parameters can be changed once executing the program.
filename.vel
filename.pnd
filename.wep

The stage-discharge and stage-area curves needs to be changed in the filename.stg. The stage is entered in centimeters, the discharge in liters per second, and the area is entered in meters.

The users is strongly recommended not to change the filename.dif. Copy and rename the file to the user's preference.

List of screens

Screen 1

General Input Parameters	
Description of Input Parameters	Exit here of <Esc>
Number of cstrs:	1
Number of discharge levels:	5
Number of nodes:	18
Numerical time step (hr):	0.002778
Kinematic viscosity (cm2/s):	0.00879
Bed specific gravity:	1.40
Imhoff cone sg:	1.20
Stokes largest diameter (mm):	0.030
Time step for debugging (hr):	200.00
Path of input/output files:	
Filename of velocity input:	filename.vel
Basin geometry filename:	filename.pnd
Output filename:	filename.out
Watershed information filename:	filename.wep
Run identification:	

Screen 2 (filename.vel)

Velocity Related Input Parameters	
Description of Input Parameters	Exit here of <Esc>
Number of velocity segments:	5
Wilson dimensionless scour parameter:	0.0000020
Einstein dimensionless parameter:	0.143
Normalized deviation of turbulent lift:	2.0
Hiding particle factor:	1.00
Irregular lift coefficient:	1.00
Einstein bed coefficient:	1.00
Bed roughness parameter (mm):	0.0500
Log-velocity constant: 8.50	
Height of approximately uniform velocity:	0.00
Initial bottom velocity ratio:	2.00
Initial time for h1:	1.00
Time for h2 = h1:	2.00

Screen 3 (filename.wep

WEPP Default Values	
Description of Input Parameters	Exit here of <Esc>
Number of total inflow events:	
Load-flow-rate:	1.5
Watershed area (ac):	
Width of watershed (meters):	
Filename of WEPP data:	filename.dat
Spreadsheet filename:	filename.plt
Detailed output (0-no, 1-yes):	1
Store for spreadsheet (0-no, 1-yes):	0
View screen plots (0-no, 1-yes):	0

Screen 4 (filename.pnd)

Basin Related Input Parameters	
Description of Input Parameters	Exit here of <Esc>
Percent of inflow volume to halt routing:	98.0
Number of stage points:	
Number or cross sections:	
Subscript of spillway elevation:	
Subscript of initial water level:	
Dead space (%):	5
Permanent pool level (l):	0
Distance between cross sections (m):	
Inlet bed scour stage:	70.88
Filename of diffusion/particle adjustments:	rollin.dif
Filename of stage-area values:	filename.stg

Description for input parameters

The number of cstrs is the number of reactors the basin is divided into to determine how much sediment is being deposited.

The number of discharge levels is 5 and the number of nodes is 18. The time step is 0.002778 hours. The kinematic viscosity is 0.00879 cm2/sec. The bed specific gravity is 1.40. The Stokes largest diameter is 0.030 mm. The time step for debugging is 200 hr. The author recommends these values are not changed. The Imhoff cone specific gravity can be determined from the Table 1.

Table 1. Specific Gravity of Submerged Sediment for Imhoff Cone Test

Sediment Composition		Submerged Specific Gravity (SBSG)
100 % > 50 microns		1.56
Coarse:	80% > 50microns 10 microns < 15% < 50 microns 5% < 10 microns	1.49
Medium Fine:	40 % > 50microns 10 microns < 35% < 50 microns 25 % < 10 microns	1.35
Fine:	10 % > 50microns 10 microns < 60 % < 50 microns 30 % < 10 microns	1.18
100 % < 50 microns		1.12

The Velocity Related Input Parameters, which is the filename.vel, should not be changed until you have considerable experience with BASIN.

The WEPP Default Values, which is the filename.wep, should be changed to the site specific information. The number of events is site specific. The watershed area is in acres. The width of the watershed is in meters. The load-flow-rate exponents should be 1.50 and no changed.

The Basin Related Input Parameters is filename.pnd. The number of stage points, number of cross sections, subscript of spillway elevation, subscript of initial water level, permanent pool volume, and distance between cross section should be entered for the specific site. The precent inflow volume to halt routing, dead space, and inlet bead scour stage should not be changed.